Nucleosome dynamics resolved with single-pair fluorescence resonance energy transfer spectroscopy

Koopmans, W.J.A.

Nucleosome Dynamics Resolved with Single-Pair Fluorescence Resonance Energy Transfer Spectroscopy

Proefschrift

ter verkrijging van

de graad van Doctor aan de Universiteit Leiden,

op gezag van Rector Magnificus prof. mr. P. F. van der Heijden,

volgens besluit van het College voor Promoties

te verdedigen op donderdag 18 juni 2009

klokke 10:00 uur

door

Wiepke Jelle Anthonie Koopmans

geboren te Papendrecht

in 1980

Promotiecommissie

Promotor:	prof. dr. T. Schmidt
Co-promotor:	dr. ir. J. van Noort
Referent:	dr. A. N. Kapanidis (Oxford University, United Kingdom)
Overige leden:	prof. dr. J. Brouwer
	prof. dr. M. Orrit
	dr. ir. E. J. G. Peterman (Vrije Universiteit, Amsterdam)
	prof. dr. J. M. van Ruitenbeek
	prof. dr. H. Schiessel
	prof. dr. C. Wyman (Erasmus Universiteit, Rotterdam)

Cover illustration: nucleosome crystal structure adapted from protein database *1kx5*, Davey *et al.* (2002)

Casimir PhD Series, Delft-Leiden, 2009-03

ISBN 978-90-8593-051-8

An electronic version of this thesis can be found at https://openaccess.leidenuniv.nl

Dit werk maakt deel uit van het onderzoekprogramma van de Stichting voor Fundamenteel Onderzoek der Materie (FOM), die financieel wordt gesteund door de Nederlandse Organisatie voor Wetenschappelijk Onderzoek (NWO).

Contents

Chapter 1

Introduction

The work described in this thesis addresses an intriguing question at the heart of many processes that govern life: how is accessibility to the genetic information in the DNA achieved in its very tightly folded context? This chapter introduces the main subjects in this study: the nucleosome and single-pair FRET spectroscopy. It concludes with an outline of the scope of this thesis.

1.1 The nucleosome

Eukaryotic DNA is organized in arrays of nucleosomes. The hereditary information in the human genome is encoded in more than 3 billion base pairs (bp), equivalent to 1 m of DNA. Somatic cells contain two copies of the complete genome, distributed over 46 chromosomes. If not condensed, the DNA in a chromosome would form a swollen coil of ~100 μm in diameter [1]; yet all the DNA is stored in the nucleus, which is only about 5 μm in size! The challenging task of packaging eukaryotic DNA to make it fit in the nucleus is achieved by specialized proteins that bind and fold the DNA in higher and higher levels of condensation, as schematically depicted in figure 1.1.a. The resulting DNA-protein complex is termed chromatin. In the hierarchy of chromatin, condensation ranges from 10^5-fold linear compaction in the mitotic chromosome down to 5-fold compaction in the fundamental repeating unit of DNA organization, a structure called the nucleosome.

A detailed description of the structure of the nucleosome can be obtained from high-resolution X-ray crystal structures [2, 3], as shown in figure 1.1.b. The nucleosome core particle consists of 147 bp of DNA wrapped around a histone octamer protein core in 1.7 left-handed superhelical turns. The histone octamer core has a modular design: it is composed of a $(H3\text{-}H4)_2$ tetramer at the center, and two H2A-H2B dimers at the ends of the DNA path. DNA binding

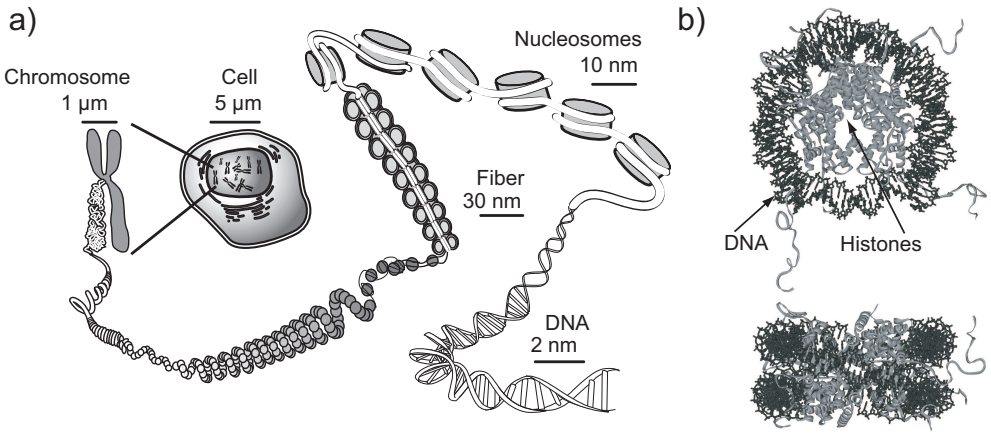

Figure 1.1: Eukaryotic DNA is organized in arrays of nucleosomes. a) DNA in the nucleus is compacted in chromatin, of which the nucleosome is the basic unit. Arrays of nucleosomes form higher-order structures, ultimately giving rise to the highly condensed mitotic chromosome. b) Top view and side view of a high resolution crystal structure (*1kx5* [2]) of the nucleosome core particle. The nucleosome core particle consists of ~50 nm of DNA wrapped in 1.7 turns around a histone octamer protein core.

occurs primarily to the DNA backbone facing the histone core: electrostatic interactions and hydrogen bonds form contacts every 10 bp when the DNA minor groove faces inwards. This lack of sequence specificity ensures that almost any DNA can be incorporated in a nucleosome. Nucleosome core particles are separated from each other by 10-50 bp linker DNA, forming a "beads-on-a-string" chain. In this array nucleosomes interact with neighboring nucleosomes, resulting in higher-order structure to achieve more DNA compaction.

The nucleosome is a remarkable structure, for several reasons:

- The stiffness of DNA is characterized by a persistence length of 50 nm, which means that DNA is essentially straight on that length scale. Yet one persistence length of DNA is wrapped in nearly two full turns in the nucleosome, effectively making it a loaded spring [1].

- Nucleosomes favor particular sequences over others, even though most histone-DNA interactions are not sequence specific. This presumably reflects the ability of particular sequence motifs to more easily accommodate the bending and twisting required for wrapping DNA along the histone octamer perimeter [4]. It has been proposed that this sequence dependence acts as a nucleosome positioning code, that drive nucleosomes to strategic positions in regulatory processes [5].

- The nucleosome has a pronounced charge distribution, with a highly negatively charged

DNA chain that repels itself, and positively charged lysine and arginine groups on the histones. Nucleosome structure is sensitive to salt conditions [6] and to modifications of the charge distribution (e.g. by acetylation of lysine groups [7]).

- Flexible, unstructured histone tails protrude from the core and are exposed. Covalent modifications to residues on these tails, such as phosphorylation and methylation, play a crucial role in regulating nucleosome structure. This may reveal a “histone code" that regulates the genetic information [8].

It is of vital importance that nucleosomes reconcile two conflicting demands: nucleosomes have to package DNA, but also have to ensure that the encoded information in the DNA can be accessed at appropriate times. This leads to the complex and exciting interplay of nucleosome structure and function described in the above.

Nucleosome dynamics are the key for understanding gene regulation. All transactions on DNA in the nucleus take place on nucleosome substrates. The nucleosome is intimately involved in transcription control, and therefore lies at the heart of gene regulation. For example, histones serve as general gene repressors [9], because DNA wrapped in nucleosomes is sterically occluded from enzymes in the transcription machinery. Chromatin structure has to be substantially remodeled to accommodate transcription of the DNA to mRNA. Therefore, in order to understand physical aspects of gene regulation, it is of key importance to understand the conformational dynamics and structural plasticity of nucleosomes that underlie accessibility to the wrapped DNA.

Several mechanisms that ensure nucleosome accessibility have been identified (reviewed for example by Luger [10] or Flaus and Owen-Hughes [11, 12]). These mechanisms can be divided into two broad classes: i) Actively driven accessibility to nucleosomal DNA is catalyzed by chromatin remodelling enzymes, large protein machines that change the position, structure or composition of nucleosomes. In doing so, they consume energy in the form of ATP [12, 13]. ii) Spontaneous accessibility does not require ATP, but relies on intrinsic conformational changes, such as thermal repositioning [14], histone dimer exchange [15], and transient site-exposure by DNA binding and rebinding at the nucleosome ends, in a process termed breathing [16, 17](schematically depicted in figure 1.2.a-c). How these different mechanisms are coupled to each other and how they are employed in transcription, repair, and replication is an intriguing and important question. For example, unwrapping of nucleosomal DNA by breathing may be captured by a site-specific DNA-binding protein, that in turn recruits a remodeling factor to a particular nucleosome [18]. However, many details of the underlying conformational changes in these mechanisms remain to be resolved. For example, little is known about the kinetics of processes such as DNA breathing. Also, the large number

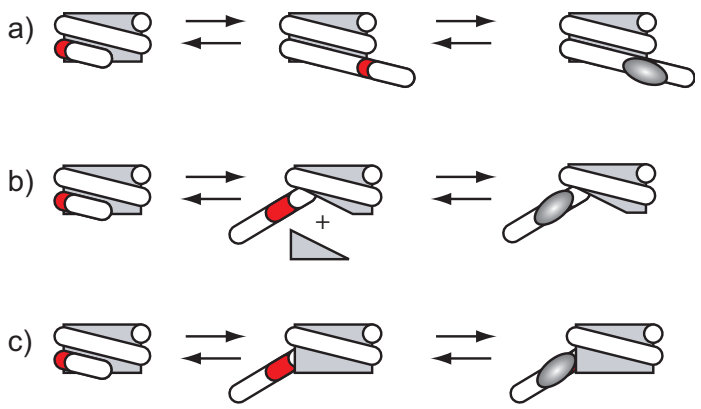

Figure 1.2: Mechanisms for spontaneous enzyme accessibility of nucleosomal DNA. a) Thermal repositioning. b) H2A-H2B dimer exchange. c) Site exposure by DNA breathing from the nucleosome ends. Each mechanism exposes a previously occluded stretch of DNA. In this way, regulatory proteins (dark gray) may bind their recognition site (red) in the nucleosomal DNA.

of DNA-histone contacts raise the questions which bonds are broken in what order for achieving DNA accessibility. Finally, each mechanism probably involves a wealth of closely related intermediate states, and a subtle free energy landscape which is difficult to probe experimentally. Yet for a complete understanding of regulated DNA accessibility at any given site, it is necessary to understand the structure of the underlying chromatin at molecular detail [10].

1.2 Single-pair Fluorescence Resonance Energy Transfer Spectroscopy

FRET is a sensitive tool for studying conformational changes in bio-molecules. Fluorescence (or Förster) Resonance Energy Transfer (FRET) is a process in which excitation energy from a donor fluorophore is transferred non-radiatively to an acceptor molecule via an induced dipole-induced dipole interaction [19]. The efficiency of energy transfer, E, is given by

$$E = \frac{1}{1 + \left(\frac{R}{R_0}\right)^6}, \tag{1.1}$$

where R is the distance between donor and acceptor and R_0 is the Förster radius, at which 50% energy transfer occurs (typically 5 nm). Because of this strong distance dependence, FRET can be applied as a molecular ruler in the 2-8 nm range [20]: a small change in distance is converted to a shift in fluorescence emission which can easily be detected. The dimensions

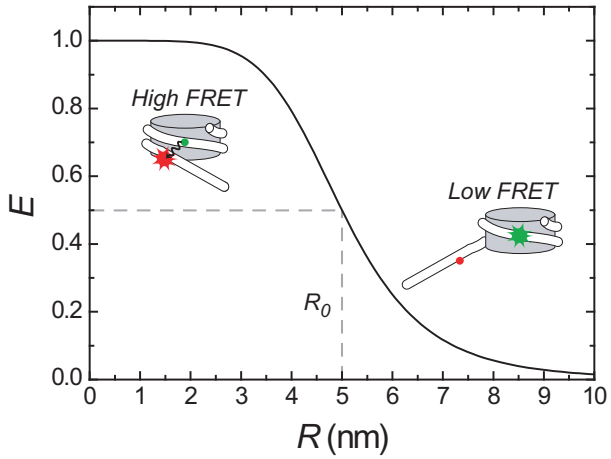

Figure 1.3: FRET as a molecular ruler for detecting conformational changes in the nucleosome. A wrapped nucleosome with a FRET pair at a strategic location brings the fluorophores in close proximity, resulting in efficient energy transfer. A transiently unwrapped nucleosome, as a result of DNA breathing for example, temporarily shows a loss in FRET.

of many biologically relevant structures, such as the Holliday junction or the nucleosome, are accessible by FRET. Furthermore, specific fluorescence labeling of strategic sites on DNA or proteins is possible in many instances. Therefore, FRET is a technique well-suited to studying conformational changes in bio-molecules [21] that govern life at its molecular basis, such as nucleosome dynamics (see figure 1.3).

spFRET spectroscopy reveals the conformational distribution and dynamics of single molecules. In bulk FRET experiments, the fluorescence emission of an ensemble of molecules is recorded, yielding an ensemble-averaged FRET efficiency of the system under study. Information about the conformational heterogeneity or kinetic processes that occur in the ensemble is lost in this way. This information can be obtained with single-pair FRET (spFRET) spectroscopy, in which FRET is applied at the single-molecule level. This was first demonstrated over a decade ago by Ha *et al.* [22]. Using spFRET, the conformational distribution can be reconstructed from the FRET footprint of many individual molecules, and conformational dynamics can be monitored by following a single molecule in time.

To detect the fluorescence of a single pair of fluorophores, it is crucial to collect as many photons as possible. This is a challenging task, which can only be achieved at an acceptable signal to noise ratio because of recent technical advances that resulted in superior quality microscope objectives, photostable fluorophores, optimized fluorescence emission filters, and

sensitive single-photon avalanche photodiodes and multiplication gain CCD cameras. Two detection schemes are frequently employed in spFRET experiments [23]: widefield TIRF microscopy on molecules immobilized to a surface, and confocal microscopy on molecules that freely diffuse in solution. Surface immobilization provides an extended observation time, limited only by photobleaching (a light-induced reaction that results in irreversible loss of the fluorescent state of a fluorophore). Immobilization therefore is a great tool for studying slow processes that occur on timescales longer than 10 ms. A drawback of this method is that the surface may interact with the molecule of interest, so that great care must be taken to employ an optimized immobilization scheme. In-solution experiments do no suffer from these surface-induced artifacts. In this case, the observation time is limited by diffusion through the confocal spot, which is typically on the order of 1 ms. Hence this detection scheme is better suitable for following fast processes or obtaining snapshots of the conformational distribution. Both detection schemes have been successfully employed to unravel subtle conformational changes in a variety of bio-molecules, such as DNA [24, 25], RNA [26] and DNA-protein interactions [27].

Conceptually, spFRET is a versatile, simple and elegant tool in molecular biophysics. Great care has to be taken to interpret spFRET data correctly, though. For example, it is not straightforward to convert a FRET efficiency to an accurate value for distance [28]. Also, photochemical processes that strongly affect the fluorescence emission of the dyes, such as photoblinking and photobleaching, interfere with fluctuations in FRET due to conformational changes. A more advanced alternating laser excitation scheme (ALEX), that simultaneously reports on the FRET efficiency and label stoichiometry [29, 30], is needed to filter out all blinking and bleaching events. Finally, immobilization and dilution to the picomolar concentration needed to resolve single molecules may induce artifacts. In this thesis, I describe how we addressed these issues and how we were able to use spFRET as a sensitive reporter on nucleosome conformation and dynamics.

1.3 Scope of this thesis

This thesis reports experimental work on nucleosome structure and dynamics, using spFRET as a reporter of nucleosome conformation at the single-molecule level. Each chapter was written as a separate research article focusing on specific aspects of nucleosome conformational changes and the experimental methodology used to study these.

Chapter 2 is the materials and methods section of this thesis. It gives a detailed overview of the procedures that were established to reconstitute nucleosomes with a FRET pair exactly at the desired location, and how to analyze them with ensemble and single-molecule techniques. We describe the microscope setups that were constructed to perform experiments on immobilized nucleosomes and on nucleosomes in solution, and present example data.

Chapter 3 describes spFRET experiments on immobilized nucleosomes, that resolve DNA breathing in individual nucleosomes. Immobilization results in dissociation of a large fraction of the nucleosomes, which are excluded from further data-analysis. We report how photoblinking interferes with determination of breathing kinetics, and how this issue is resolved using alternating excitation and a special triplet quencher. We observe that most of the properly immobilized, non-blinking nucleosomes show stable FRET on timescales between 0.01-10 s, while 3% show dynamics with a dwell time of 120 ms that we attribute to conformational changes in the nucleosome. Our findings illustrate not only the merits but also typical caveats encountered in single-molecule FRET studies on complex biological systems.

Chapter 4 further explores the issue of nucleosome immobilization. We report on various nucleosome immobilization strategies, such as single point attachment to polyethylene glycol or bovine serum albumin coated surfaces, and confinement in porous agarose or polyacrylamide gels. We compared the immobilization specificity and structural integrity of immobilized nucleosomes. A crosslinked star polyethylene glycol coating performed best with respect to tethering specificity and nucleosome integrity, and enabled us for the first time to reproduce bulk nucleosome unwrapping kinetics in single nucleosomes without immobilization artifacts.

Chapter 5 reports on spFRET experiments on diffusing nucleosomes, either in free solution or after PAGE separation. We combined spFRET and alternating excitation with a correlation analysis on selected bursts of fluorescence, to resolve a variety of progressively unwrapped nucleosome conformations. The experiments reveal that nucleosomes are considerably unwrapped, but yet remains stably associated. Our findings quantify the delicate interplay between accessibility and condensation in nucleosomes using a powerful combination of single-molecule fluorescence techniques and gel electrophoresis to resolve the resulting conformational heterogeneity.

Bibliography

[1] Schiessel, H. The physics of chromatin. *J. Phys.: Condens Matter* **15**, R699–R774 (2003).

[2] Davey, C., Sargent, D., Luger, K., Maeder, A., and Richmond, T. Solvent mediated interactions in the structure of the nucleosome core particle at 1.9 Å resolution. *J. Mol. Biol.* **319**, 1097–1113 (2002).

[3] Luger, K., Mader, A., Richmond, R., Sargent, D., and Richmond, T. Crystal structure of the nucleosome core particle at 2.8 Å resolution. *Nature* **389**, 251–260 (1997).

[4] Widom, J. Role of DNA sequence in nucleosome stability and dynamics. *Q. Rev. Biophys.* **34**, 269–324 (2001).

[5] Segal, E., Fondufe-Mittendorf, Y., Chen, L., Thastroem, A., Field, Y., Moore, I. K., Wang, J.-P. Z., and Widom, J. A genomic code for nucleosome positioning. *Nature* **442**, 772–778 (2006).

[6] Yager, T., Mcmurray, C., and Vanholde, K. Salt-Induced Release of DNA from Nucleosome Core Particles. *Biochemistry* **28**, 2271–2281 (1989).

[7] Brower-Toland, B., Wacker, D., Fulbright, R., Lis, J., Kraus, W., and Wang, M. Specific contributions of histone tails and their acetylation to the mechanical stability of nucleosomes. *J. Mol. Biol.* **346**, 135–146 (2005).

[8] Jenuwein, T. and Allis, C. D. Translating the Histone Code. *Science* **293**, 1074–1080 (2001).

[9] Kornberg, R. and Lorch, Y. Twenty-five years of the nucleosome, fundamental particle of the eukaryote chromosome. *Cell* **98**, 285–294 (1999).

[10] Luger, K. Dynamic nucleosomes. *Chromosome Res.* **14**, 5–16 (2006).

[11] Flaus, A. and Owen-Hughes, T. Mechanisms for nucleosome mobilization. *Biopolymers* **68**, 563–578 (2003).

[12] Flaus, A. and Owen-Hughes, T. Mechanisms for ATP-dependent chromatin remodelling: farewell to the tuna-can octamer? *Curr. Opin. Genet. Dev.* **14**, 165–173 (2004).

[13] Saha, A., Wittmeyer, J., and Cairns, B. Chromatin remodelling: the industrial revolution of DNA around histones. *Nat. Rev. Mol. Cell Biol.* **7**, 437–447 (2006).

[14] Flaus, A. and Owen-Hughes, T. Dynamic properties of nucleosomes during thermal and ATP-driven mobilization. *Mol. Cell. Biol.* **23**, 7767–7779 (2003).

[15] Kimura, H. and Cook, P. Kinetics of core histones in living human cells: Little exchange of H3 and H4 and some rapid exchange of H2B. *J. Cell Biol.* **153**, 1341–1353 (2001).

[16] Polach, K. and Widom, J. Mechanism of Protein Access to Specific DNA-Sequences in Chromatin - A Dynamic Equilibrium-Model for Gene-Regulation. *J. Mol. Biol.* **254**, 130–149 (1995).

[17] Anderson, J., Thåström, A., and Widom, J. Spontaneous access of proteins to buried nucleosomal DNA target sites occurs via a mechanism that is distinct from nucleosome translocation. *Mol. Cell. Biol.* **22**, 7147–7157 (2002).

[18] Li, G. and Widom, J. Nucleosomes facilitate their own invasion. *Nat. Struct. Mol. Biol.* **11**, 763–769 (2004).

[19] Förster, T. Delocalized excitation and excitation transfer. In Modern Quantum Chemistry, Sinanoglu, O., editor, 93–137. Academic Press, New York (1965).

[20] Stryer, L. and Haugland, R. Energy Transfer - a Spectroscopic Ruler. *Proc. Natl. Acad. Sci. U.S.A.* **58**, 719–726 (1967).

[21] Clegg, R. M. Fluorescence resonance energy transfer. *Curr. Opin. Biotechnol.* **6**, 103–110 (1995).

[22] Ha, T., Enderle, T., Ogletree, D., Chemla, D., Selvin, P., and Weiss, S. Probing the interaction between two single molecules: fluorescence resonance energy transfer between a single donor and a single acceptor. *Proc. Natl. Acad. Sci. U.S.A.* **93**, 6264–6268 (1996).

[23] Rasnik, I., Mckinney, S., and Ha, T. Surfaces and orientations: Much to FRET about? *Acc. Chem. Res.* **38**, 542–548 (2005).

[24] Mckinney, S., Freeman, A., Lilley, D., and Ha, T. Observing spontaneous branch migration of holliday junctions one step at a time. *Proc. Natl. Acad. Sci. U.S.A.* **102**, 5715–5720 (2005).

[25] Deniz, A., Dahan, M., Grunwell, J., Ha, T., Faulhaber, A., Chemla, D., Weiss, S., and Schultz, P. Single-pair fluorescence resonance energy transfer on freely diffusing molecules: Observation of Förster distance dependence and subpopulations. *Proc. Natl. Acad. Sci. U.S.A.* **96**, 3670–3675 (1999).

[26] Zhuang, X., Bartley, L., Babcock, H., Russell, R., Ha, T., Herschlag, D., and Chu, S. A single-molecule study of RNA catalysis and folding. *Science* **288**, 2048–2051 (2000).

[27] Ha, T., Rasnik, I., Cheng, W., Babcock, H., Gauss, G., Lohman, T., and Chu, S. Initiation and re-initiation of DNA unwinding by the Escherichia coli Rep helicase. *Nature* **419**, 638–641 (2002).

[28] Lee, N., Kapanidis, A., Wang, Y., Michalet, X., Mukhopadhyay, J., Ebright, R., and Weiss, S. Accurate FRET measurements within single diffusing biomolecules using alternating-laser excitation. *Biophys. J.* **88**, 2939–2953 (2005).

[29] Kapanidis, A., Lee, N., Laurence, T., Doose, S., Margeat, E., and Weiss, S. Fluorescence-aided molecule sorting: Analysis of structure and interactions by alternating-laser excitation of single molecules. *Proc. Natl. Acad. Sci. U.S.A.* **101**, 8936–8941 (2004).

[30] Sabanayagam, C., Eid, J., and Meller, A. Long time scale blinking kinetics of cyanine fluorophores conjugated to DNA and its effect on Förster resonance energy transfer. *J. Chem. Phys.* **123**, – (2005).

Chapter 2

Engineering Mononucleosomes for Single-Pair FRET Experiments[1]

Abstract In DNA nanotechnology, DNA is used as a structural material, rather than as an information carrier. The structural organization of the DNA itself determines accessibility to its underlying information content *in vivo*. Nucleosomes form the basic level of DNA compaction in eukaryotic nuclei. Nucleosomes sterically hinder enzymes that must bind the nucleosomal DNA, and hence play an important role in gene regulation. In order to understand how accessibility to nucleosomal DNA is regulated, it is necessary to resolve the molecular mechanisms underlying conformational changes in the nucleosome. Exploiting bottom-up control, we designed and constructed nucleosomes with fluorescent labels at strategically chosen locations to study nucleosome structure and dynamics in molecular detail with single-pair Fluorescence Resonance Energy Transfer (spFRET) microscopy. Using widefield total internal reflection fluorescence (TIRF) microscopy on immobilized molecules, we observed and quantified DNA breathing dynamics on individual nucleosomes. Alternatively, fluorescence microscopy on freely diffusing molecules in a confocal detection volume allows a fast characterization of nucleosome conformational distributions.

[1]Part of this chapter is to appear as a contribution to protocols in DNA nanotechnology (ed. G. Zuccheri & B. Samori) in the Methods in Molecular Biology series, Humana Press

2.1 Introduction

DNA nanotechnology uses DNA molecules as smart building blocks for construction at the nanoscale [1]. It exploits the unique molecular recognition properties of DNA to direct the self-assembly of new nanostructures and devices with bottom-up control. A major goal of DNA nanotechnology is to use DNA as a scaffold to structure other molecules (e.g. proteins or electronic components), relying on its chemical stability, rigidity, and predictable structure [2]. To date, DNA has been successfully used to create a variety of complex 2D and 3D architectures, ranging from cubes [3] and tetrahedrons [4] to elaborate world-maps [5]. For this purpose, DNA is used as a structural material, rather than as an information carrier.

At a higher level, it is the structural organization of the DNA itself that determines accessibility to its underlying information content *in vivo*. The basic unit of DNA organization in eukaryotic nuclei is the nucleosome. A nucleosome core particle consists of 50 nm of DNA wrapped in nearly two turns around a histone-octamer core [6]. Arrays of nucleosomes can fold into fibers, which in turn can condense into higher-order structures. Since nucleosomes sterically hinder enzymes that bind the nucleosomal DNA, they play an important role in gene regulation. To understand the mechanisms underlying gene regulation, it is essential to resolve the structural and dynamic properties of nucleosomes in detail [7].

We use a bottom-up approach similar to DNA nanotechnology to study DNA organization in the nucleosome using single-pair Fluorescence Resonance Energy Transfer (spFRET) microscopy [8, 9]. We designed and chose individual DNA and histone components exactly such that DNA folding can be studied at any desired location in the nucleosome.

Nucleosomes are assembled on a DNA template through a salt dialysis reconstitution with purified core histones [10]. The fluorescently labeled DNA template contains a strong nucleosome positioning element [11], so that nucleosomes are exactly positioned at a specific location on the DNA. This level of control ensures that the fluorescent labels in the DNA are incorporated at the desired location in the nucleosome, resulting in efficient FRET. Further modifications of the DNA allow specific immobilization of the nucleosomes to a surface. The FRET efficiency of individual nucleosomes can be monitored in detail with single-molecule fluorescence microscopy. For these experiments, nucleosomes are diluted to single-molecule concentrations in optimized buffer conditions. Widefield total internal reflection fluorescence (TIRF) microscopy on immobilized molecules allows the monitoring of individual nucleosomes for tens of seconds to minutes, revealing their dynamic behavior in time [8, 9]. Alternatively, fluorescence microscopy on freely diffusing molecules in a femtoliter confocal detection volume allows a fast characterization of nucleosome conformational distributions [12, 13].

2.2 Materials

2.2.1 DNA preparation and purification

1. Template DNA containing the 601 nucleosome positioning sequence.
2. HPLC grade fluorescently labeled forward and reverse primer (IBA GmbH) dissolved at 50 µM in 1X TE (10 mM Tris.HCl pH 8, 1 mM EDTA). Store in aliquots at -20 °C.
3. FastStart PCR kit (Roche) with thermostable hot start polymerase (5 U/µl), nucleotide mix (10 mM of each dNTP), and 10X reaction buffer. Store at -20 °C.
4. Thin-walled PCR tubes (Eppendorf).
5. QIAquick PCR purification kit, or QIAquick Gel Extraction kit (Qiagen).

2.2.2 Mononucleosome reconstitution

1. TE dialysis buffer: 50X stock solution (500 mM Tris.HCl pH 8, 50 mM EDTA).
2. 5 M NaCl stock solution.
3. 5-20 µM recombinant histone octamers in 1X TE, 2 M NaCl, and 5 mM 2-mercapto-ethanol; 2 µM mixed sequence competitor DNA (~147 bp) in 1X TE, 2 M NaCl, or
4. 3-10 µM micrococcal nuclease digested nucleosome core particles.
5. Dialysis tubes: Slide-A-Lyzer MINI dialysis units (10K MWCO, Pierce).

2.2.3 Polyacrylamide Gel Electrophoresis (PAGE)

1. Running buffer: 5X TB (450 mM Tris, 450 mM Boric Acid). Store at room temperature.
2. 40% acrylamide:bisacrylamide solution (29:1, Bio-Rad) (this is a neurotoxin when unpolymerized, so avoid exposure). Store at 4 °C.
3. N,N,N,N'-Tetramethyl-ethylenediamine (TEMED, Bio-Rad).
4. Ammonium persulfate (APS): 10% solution in water (*see* **Note 1**), stored in aliquots at -20 °C.
5. Loading buffer (6X): 10 mM Tris.HCl pH 8, 60 mM EDTA, 60% glycerol.

2.2.4 Single-molecule FRET measurements

Cover slide preparation

1. Microscope cover slips (24 x 60 mm # 1.5, Menzel).
2. Cleaning agents: RBS-50 detergent (Fluka), 96% AR grade ethanol (Biosolve).
3. Poly-D-lysine (Sigma) dissolved at 0.1 mg/ml in water, and stored at 4 °C.
4. NCO star PEGs (kind gift of Dr. Groll, RWTH Aachen, *see* **Note 2**).
5. Tetrahydrofuran (THF) (Sigma)
6. Biocytin (Sigma) dissolved at 1 mg/ml in water, and stored at -20 °C.

Single-molecule imaging

1. T50 buffer (*see* **Note 3**): 10 mM Tris.HCl (pH 8), 50 mM NaCl.
2. Oxygen scavenger system: Catalase (Fluka) stored at 4 °C, glucose oxidase (Sigma) stored at -20 °C.
3. β-D-glucose (Sigma).
4. Triplet quencher (trolox): tetramethylchroman-2-carboxylic acid (Sigma).
5. Sodium hydroxide solution (120 mM NaOH)
6. 100X bovine serum albumin (BSA) solution: 10 mg/ml in T50.
7. 10 mM Tris.HCl (pH 8).
8. Neutravidin (Pierce), dissolved at 5 mg/ml in water and 10% glycerol, stored in aliquots at -80 °C.
9. CoverWell perfusion chamber gaskets (Invitrogen).

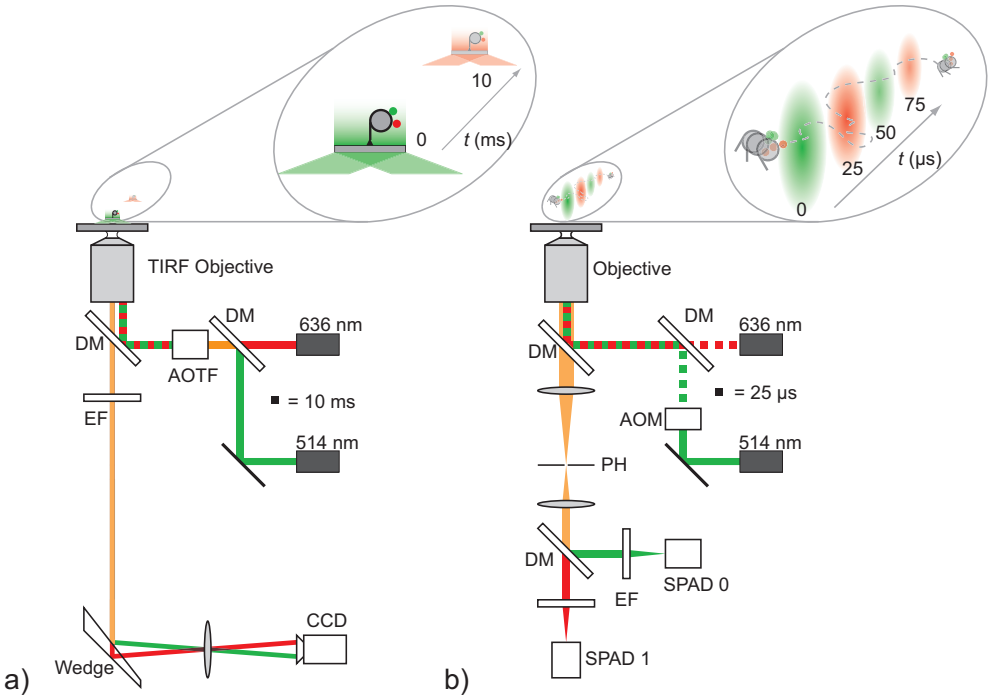

Figure 2.1: Single-pair FRET microscopes. a) Widefield TIRF microscope. DM, dichroic mirror; AOTF, Acousto Optical Tunable Filter; EF, Emission Filter; CCD, Charge Coupled Device. The combined lasers are alternated (green and red boxes) at 20-100 Hz with an AOTF that is synchronized with the CCD camera. TIR excitation is achieved by displacing the excitation beams relative to the optical axis. The resulting fluorescence (orange) from immobilized molecules is collected by the objective, and filtered through an emission filter. Donor (green) and acceptor (red) fluorescence are simultaneously imaged on separate areas of the CCD chip using a dichroic mirror wedge. b) Fluorescence microscope with confocal geometry. AOM, Acousto Optical Modulator; PH, Pinhole; SPAD, Single-Photon Avalanche Diode. The lasers are alternated at 20 kHz by analog modulation either directly (636 nm laser) or with an AOM (515 nm laser), synchronized with the 10 MHz clock on the photon counting board. The resulting fluorescence from freely diffusing molecules in the excitation volume is collected by the objective, filtered through an emission filter, and spatially filtered through a pinhole. Donor and acceptor fluorescence are imaged on different SPADs using a dichroic mirror.

2.3 Single-molecule fluorescence microscopes

We used two complementary approaches to image individual nucleosomes using single-molecule fluorescence microscopy, as depicted in figure 2.1.

We imaged nucleosomes tethered to a polymer-coated cover slide with a widefield TIRF microscope. In this configuration, 10-100 molecules can be observed in parallel for seconds or even minutes. It is even possible to perform multiple experiments on an individual molecule, e.g. by varying the buffer conditions while observing a specific molecule. The time resolution is given by the readout time of the CCD camera, typically 10 ms in our experiments. Single-molecule sensitivity is achieved by using an electron multiplication gain CCD with 90% quantum efficiency, an evanescent excitation volume to reduce background fluorescence and a high NA objective that increases the overall photon collection efficiency of the microscope.

Alternatively, we imaged molecules in free solution with a confocal microscope. In this configuration, thousands of molecules can be sampled rapidly to extract the conformational distribution of the sample. Additionally, there is no need for immobilization, which is a potential source of artifacts. The observation time is limited to the diffusion time through the excitation volume, typically a few milliseconds. Single-molecule sensitivity is achieved by using single photon avalanche diodes with >60% quantum efficiency, a pinhole in combination with a diffraction-limited excitation volume to reject background fluorescence, and a high NA objective that increases the overall photon collection efficiency of the microscope.

In both setups, we use Alternating Laser Excitation (ALEX) to monitor the label stoichiometry. This allows us to direct the data analysis to properly folded, doubly labeled molecules, to reject molecules with only a donor or acceptor fluorophore, and to discriminate nucleosome conformational dynamics from photobleaching and photoblinking of the dyes.

2.3.1 Widefield TIRF setup

Immobilized nucleosomes were imaged with a home-built TIRF microscope equipped with a 100X oil-immersion TIRF microscope objective (NA = 1.45, NIKON), as schematically depicted in figure 2.1.a. The 514 nm line of an Ar-ion laser (Coherent) and a 636 nm diode laser (Power Technology) were used as excitation sources. The beams were spatially filtered with a single-mode polarization maintaining fiber (O.Z. Optics) or a pinhole, and were combined with a dichroic mirror (z514bcm). ALEX was achieved through an Acousto Optical Tunable Filter (AOTF, A.A. Opto–Electronics), alternating at 20-100 Hz. The alternating beams were then expanded and focused in the back focal plane of the objective. Both beams were circularly polarized and were displaced parallel to the optical axis of the objective, so that an evanescent excitation field (0.1-1 kW/cm^2) was generated by total internal reflection of the light at the glass-water interface. The fluorescence was collected by the objective and filtered through a

custom-made dual color band pass filter (z514-639m) that rejects scattered laser light, and a long pass filter (OG530, Schott). The fluorescence was further split into a donor and an acceptor channel by a custom-made dichroic wedge mirror (0.5° angle interferometer flat wedge (CVI), with 640dcxr and 640dcspxr coatings) placed in the infinity path of the microscope. A +150 mm achromatic lens projected the separate images on a multiplication gain CCD camera (Cascade 512B, Roper Scientific) operating at a frame rate of 20 to 100 Hz. The microscope was enclosed in light-tight containers, to prevent ambient light from illuminating the CCD. CCD and AOTF were synchronized, so that each captured frame was illuminated either with the 514 nm laser or with the 636 nm laser. Subsequent data-analysis allowed sorting of the images based on excitation and emission wavelength.

2.3.2 Confocal setup

Freely diffusing molecules were imaged in solution with a home-built confocal microscope equipped with a 60X water-immersion microscope objective (NA = 1.2, Olympus), as schematically depicted in figure 2.1.b. A 515 nm diode pumped solid state laser (Cobolt) and a 636 nm diode laser (Power Technology) were used as excitation sources. The lasers were alternated at 20 kHz by analog modulation, either directly (636 nm laser) or with an AOM (515 nm laser; Isomet). The alternation was synchronized with the 10 MHz clock on the TimeHarp 200 photon counting board. The linearly polarized beams were combined with a dichroic mirror (z514bcm) and were spatially filtered with a single mode optical fiber (O.Z. Optics). The beams were collimated with a +45 mm achromatic lens, projected into the objective with a dichroic mirror (z514/640rpc), and focused to a tight spot by the objective, with an intensity of ~1 kW/cm²at the minimal beam waist. The fluorescence was collected by the objective and filtered through a custom-made dual color band pass filter (514/639m), that rejects scattered laser light. The fluorescence emission was imaged with a +150 mm achromatic lens and spatially filtered with a 50 µm pinhole in the image plane. The fluorescence was collimated with a +75 mm achromatic lens and was split into a donor and an acceptor channel by a dichroic mirror (640dcxr). The fluorescence was filtered with emission filters (hq570/100m for the donor channel, hq700/75m for the acceptor channel) to minimize crosstalk, and was imaged on the active area of single photon avalanche photodiodes (SPCM AQR-14, EG&G) with +75 mm achromatic lenses. The photodiodes were enclosed in a light-tight container, to reduce background illumination. The photodiodes were connected to a TimeHarp 200 photon counting board (Picoquant GmbH) through a router. Subsequent data-analysis allowed sorting of the photon arrival times based on excitation and emission wavelength. Unless stated otherwise, all filters and dichroic mirrors were purchased from Chroma; all posts, mounts, mirrors, and lenses were purchased from Thorlabs.

2.4 Methods

To obtain exact positioning of a FRET pair at a specific location in the nucleosome, the use of a nucleosome positioning DNA sequence is necessary. We use the 601 sequence, which has a single dominant position for nucleosome formation [11]. Strategic locations for labeling the DNA can be deduced from a high resolution crystal structure [14]. Donor and acceptor fluorophores are then incorporated in the template DNA through a PCR with fluorescently labeled primers. Long, ~80 base pair (bp), primers are needed to label the DNA at internal positions in the nucleosome.

Mononucleosomes are then assembled on the DNA with a salt dialysis reconstitution [10]. It is important to mix DNA and histone proteins in the right stoichiometry: a too low octamer-to-DNA ratio results in a sub-saturated reconstitution, a too high ratio results in the formation of DNA-histone aggregates. The optimal stoichiometry is found by titrating the DNA with increasing amounts of histone octamers. To prevent formation of aggregates, mixed sequence competitor DNA can be included in the reaction. Nucleosomes will preferentially form on the labeled DNA containing the nucleosome positioning element. Excess histones will bind to the competitor DNA.

Alternatively, an exchange reconstitution is used. Histone octamers are then supplied in the right stoichiometry in the form of micrococcal nuclease digested nucleosome core particles (NCPs). In a reconstitution with a 5-10 fold excess of NCPs over the fluorescently labeled DNA, nucleosomes will first form on the nucleosome positioning DNA. The reconstitution yield in both cases is checked with polyacrylamide gel electrophoresis (PAGE). The FRET efficiency is obtained from a bulk fluorescence emission spectrum.

In order to image single nucleosomes, the concentration should be sufficiently low (10-100 pM). To prevent dilution-driven dissociation [15], nucleosomes are diluted in a buffer containing BSA and 10-100 nM unlabeled nucleosomes. Imaging takes place in a buffer containing an oxygen scavenger system, to prevent photobleaching and -blinking (*see* **Note 4**). Widefield TIRF microscopy is performed on nucleosomes that are immobilized to the microscope cover slide through biotin-neutravidin linkage. In this way, individual nucleosomes can be monitored for tens of seconds to minutes. The cover slide has to be treated with a special starPEG coating to prevent non-specific adsorption of the -sticky- histone proteins to the glass [9]. Alternatively, short bursts of fluorescence from freely diffusing molecules can be used to determine the conformational distribution. With this approach, immobilization to a coated cover slide is not necessary.

2.4.1 Choice of label positions and primer design

1. A good indication for where each base is located in the nucleosome core particle, can be derived from high-resolution nucleosome crystal structures [14]. We mapped out the base-to-base distance for each possible combination of bases on opposite DNA strands, as shown in figure 2.2.a. Bases separated a full nucleosomal turn (~80 bp) are spaced less than 2 nm apart, so that efficient FRET can occur when these locations are labeled with a FRET pair. Note that the average distance between the fluorophores is slightly different than depicted in figure 2.2.a, since they are attached to the bases with a short carbon linker.

2. The forward strand is labeled with a donor fluorophore, the reverse strand with an acceptor. We chose Cy3B as donor and ATTO647N as acceptor, because of the photostability, high extinction coefficients, and high quantum yields of these dyes. The Förster radius is approximately 5.5 nm for this pair.

3. Fluorescent labeling is done with modified bases. Thymine bases are optimal targets for this, since they can easily be replaced with a modified dUTP. Cytosine bases are an alternative; they can be replaced with a modified dCTP. The dyes are attached to the base with a carbon linker, so that the fluorophore can rotate freely. Furthermore, it is important to only label bases that face outward from the nucleosome to prevent interactions of the fluorophores with the histone protein core.

4. The fluorescent labels are inserted in the DNA with labeled single-stranded DNA primers through a PCR reaction. A biotin modification can be applied at one of the 5' ends to allow for immobilization of the DNA to a neutravidin-coated surface. To label the DNA deep inside the nucleosome, long (> 80 bp) primers are needed. It is important to place the label not too close (<5 bp) to the primer end, to prevent stalling of the polymerase reaction. We successfully used the following primers on the 601 nucleosome positioning sequence: forward primer: 5'-TTGGC<u>T</u>GGAGAATCCCGGTGCCGAGGCCGCTCAATTGGTCGTAGACAGCTCTAGCACCGCTTAAACGCACGTACGCGCTG-3', reverse primer 5'-biotin-TTGGACAGGATGTATATATCTGACACGTGCCTGGAGACTAGGGAGTAATCCCCTTGGCGGTTAAAACG<u>C</u>GGGGGACAGC-3'. Label positions are underlined. This set of primers places one label at the nucleosome exit, and the other internally at the nucleosome dyad axis, to monitor DNA unwrapping starting from one nucleosome end. If different label positions are chosen, the same primers can be used to monitor a variety of positions inside the nucleosome.

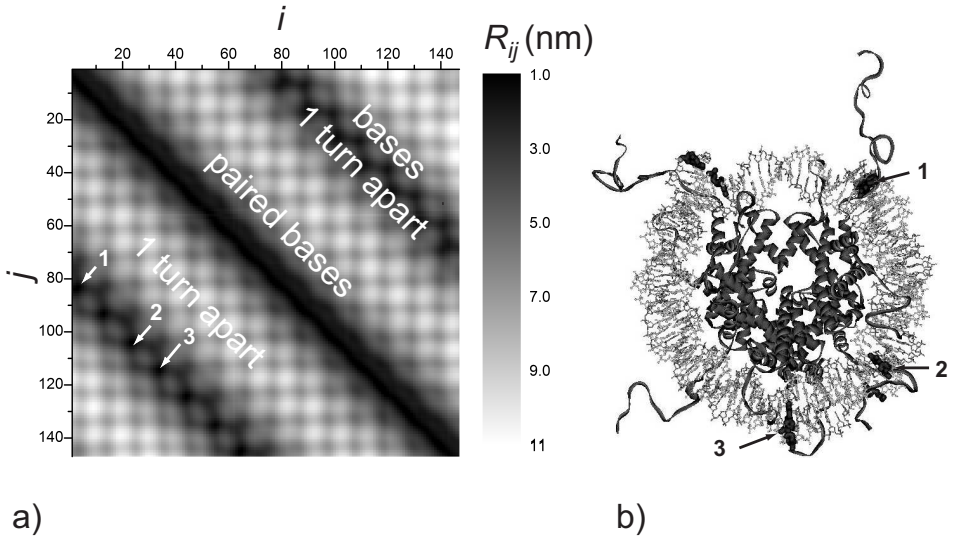

Figure 2.2: Choice of labeling positions. a) Map of the distance R_{ij} between DNA base *i* and base *j* on the complementary strand for crystal structure 1kx5 [14]. The bases come within 2 nm proximity when they are separated by a full nucleosomal turn (~80 bp). When facing outward from the nucleosome, these are ideal locations for placing a FRET pair (e.g. locations 1-3). The diagonal represents paired bases. b) Strategic positions for placing a FRET pair indicating in the nucleosome crystal structure: at the nucleosome exit (1), or reporting on internal sites in the nucleosome (2,3).

2.4.2 DNA preparation and purification

1. In a 0.5 ml PCR tube, mix 5 µl PCR buffer containing $MgCl_2$, 1 µl solution of dNTPs, 1.5 µl fluorescently labeled forward primer, 1.5 µl fluorescently labeled reverse primer, 0.5 µl faststart Taq polymerase, 200 ng template DNA containing the 601 sequence, and water in a total volume of 50 µl.

2. Place the tube in a thermal cycler equipped with a heated lid, such as the Techgene (Techne, Cambridge, UK).

3. Amplify the DNA with 35 cycles of the following two-step PCR cycle: 30 sec denaturation at 95 °C, 1 min annealing and polymerization at 72 °C. The first cycle is preceded by a 5 min initial denaturation step at 95 °C. The last cycle is followed by a final 10 min polymerization step at 72 °C. We use a two-step cycle because of the long, ~80 bp, primers involved.

4. Purify the DNA with a Qiagen PCR purification kit according to the instructions supplied in the manual. We observed that it is difficult to remove all free primer DNA in this way. Alternatively, for a higher degree of purity, analyze the PCR reaction on a 1% agarose gel, excise the desired DNA band, and purify with a Qiagen Gel Extraction kit according to the instructions supplied in the manual.

2.4.3 Mononucleosome reconstitution

Titration with stoichiometric DNA-to-octamer ratios

1. Titrations are carried out by varying the DNA-to-octamer ratio, typically from 1:0.5, 1:1, 1:1.5, 1:2, to 1:2.5, or as high as necessary. We use a minimum reaction volume of 30 µl for the dialysis tubes. The initial salt concentration should be 2 M NaCl, adjusted with a 5 M NaCl solution.

2. In a 1.5 ml centrifuge tube, mix 2 µg of labeled DNA, and 2 µg of unlabeled competitor DNA in 30 µl of 2 M NaCl buffered with 1X TE (pH 8).

3. Add the appropriate amount of histone octamers, and mix.

4. Incubate 30 min on ice.

5. Transfer the sample to a presoaked dialysis tube. Cap the tube and place the tube in floating device in a beaker containing the buffer for the first dialysis step (1X TE with 0.85 M NaCl).

6. Dialyze at 4 °C against 500 ml of 1X TE containing 0.85, 0.65, 0.5, and finally 0 M NaCl for at least 60 min per step. Continuously stir the buffer with a magnetic stirrer at a low speed setting.

7. Recover the contents from the dialysis tube, and analyze with bulk fluorescence spectroscopy and 5% PAGE as described below. An example result is shown in figure 2.3.a. The reconstituted material can be stored at 4 °C for several weeks (*see* **Note 5**). The titration point with the highest reconstitution yield (typically 80%) is subsequently used for single-molecule experiments.

Nucleosome Exchange Reconstitution

1. Exchange reconstitutions are carried out by transferring nucleosome cores from micrococcal nuclease digested nucleosome core particles to the fluorescently labeled DNA containing the 601 sequence. We use a minimum reaction volume of 30 µl for the dialysis tubes. It is important to completely dissociate the nucleosome core particles. Therefore, the initial salt concentration should be 2 M NaCl, adjusted with a 5 M NaCl solution.

2. In a 1.5 ml centrifuge tube, mix 2 µg of labeled DNA, and a 5-fold excess of nucleosome core particles in 30 µl of 2 M NaCl buffered with 1X TE (pH 8).

3. Incubate 30 min on ice.

4. Transfer the sample to a presoaked dialysis tube. Cap the tube and place the tube in floating device in a beaker containing the buffer for the first dialysis step.

5. Dialyze at 4 °C against 500 ml of 1X TE containing 0.85, 0.65, 0.5, and finally 0 M NaCl (for at least 60 min per step). Continuously stir the buffer with a magnetic stirrer at a low speed setting.

6. Recover the contents from the dialysis tube, and analyze with bulk fluorescence spectroscopy and 5% PAGE as described below. The reconstituted material can be stored at 4 °C for several weeks (*see* **Note 5**). The reconstitution yield is typically >90%. An example result is shown in figure 2.3.b.

2.4.4 Polyacrylamide Gel Electrophoresis

1. We use a Amersham Bioscience Hoefer SE 400 vertical gel slab unit (14 cm wide, 14 cm high), with a custom made pump unit for buffer recirculation. Buffer recirculation is necessary to prevent depletion of the low ionic strength running buffer (0.2X TB). Low ionic strengths are needed to prevent dissociation of nucleosomes.

2. The glass plates should be scrubbed clean with a detergent and rinsed extensively with distilled water. Rinse with 70% ethanol and air-dry.

3. Prepare a 1.5 mm thick 5% polyacrylamide gel (29:1 acrylamide:bisacrylamide, 0.2X TB) by mixing 5 ml acrylamide, 1.6 ml 5X TB, 33 ml water. Degas for 10 min and mix with 200 µl APS and 80 µl TEMED to initiate polymerization. Pour the gel, insert the comb, and allow to polymerize for 30 min.

4. Remove the comb and rinse the wells with 0.2X TB buffer. Add 0.2X TB running buffer to the upper and lower chambers of the gel unit.

5. Prerun the gel for at least 60 min at 4 °C at 19 V/cm, while continuously recirculating the buffer.

6. Load 0.2-1 pmol of reconstituted nucleosome core particles in 6 µl 1X loading buffer. The use of dyes such as xylene cyanol and bromophenol blue is not recommended, since their autofluorescence may interfere with the fluorescence from the nucleosomes. To track the migration of DNA in the gel, load the dye in a separate lane of the gel.

7. Run the gel for 75 min at 4 °C at 19 V/cm, while continuously recirculating the buffer.

8. Image the fluorescence with a gel imager such as the Typhoon 9400 (GE). To assess the reconstitution yield, excite the acceptor fluorophore (as shown in figure 2.3.a and b.) since this is a direct reporter of the amount of DNA in each band. To obtain an indication of the FRET efficiency, the donor and acceptor fluorescence should be recorded separately while exciting the donor fluorophore. If the reconstitution yield is known, the FRET efficiency can be further quantified with a bulk fluorescence emission spectrum, as shown in figure 2.3.c. We use the $ratio_A$ method as described in detail by Clegg [16].

2.4.5 Single-molecule FRET measurements

Microscope slide cleaning

1. Place the microscope slides in a rack. Use clean tweezers.

2. Sonicate 15 min in 1% anionic detergent (RBS 50) at 90 °C. Rinse with water.

3. Sonicate 60 min in ethanol. Rinse with water

4. Flame dry slides with a Bunsen burner to remove any remaining traces of organic impurities. Hold the slides with a reverse action tweezers, and gently move the slide through the flame.

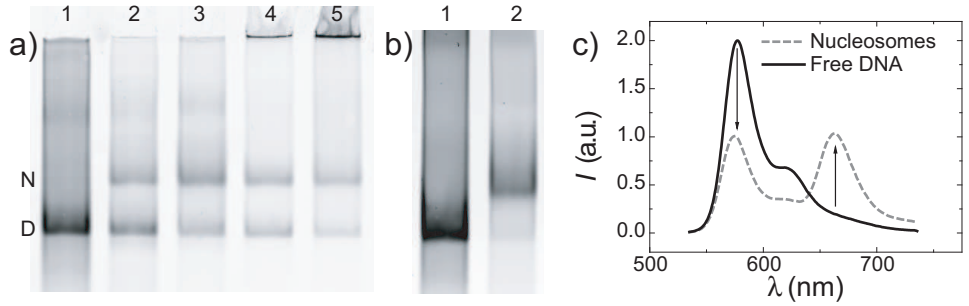

Figure 2.3: Nucleosomes analyzed on 5% PAGE (acceptor fluorescence with excitation at 633 nm) and with bulk fluorescence spectroscopy. a) Octamer titration reconstitution. Lane 1: free DNA, Lane 2-5: DNA:octamer ratios ranging from 1:2 to 1:3.5. All lanes show a band of nucleosomes (N) which migrate slower through the gel than the DNA (D). Lane 4 and 5 show fluorescence in the slots, originating from DNA-histone aggregates due to an excess of histone octamer proteins. b) Exchange reconstitution. Lane 1: free DNA. Lane 2: nucleosome reconstitution. The reconstitution yield in this case is >95%. c) Fluorescence emission spectra of free DNA and reconstituted nucleosomes. Excitation was at 515 nm, the emission was recorded from 535-735 nm. Reconstituted nucleosomes show efficient (>60%) FRET, indicated by the decrease in donor fluorescence around 560 nm, and the increase in acceptor fluorescence at 670 nm.

5. Clean the slides with an UVO ozone cleaning device (Jelight) for at least 60 min to obtain hydrophilic slides without any fluorescent impurities.

Passivation and functionalization

1. Cover the clean slides with 100 µl poly-D-lysine (0.01 mg/ml, Sigma), and incubate for 1 min. This step is needed for amino-functionalization of the slides. Rinse with water and blow dry in a nitrogen stream.

2. Dissolve six-arm NCO PEG stars (MW 12 kDa) in THF at a concentration of 20 mg/ml, and dilute in water to a concentration of 2 mg/ml. This will initiate a crosslinking reaction between the PEGs. Add biocytin (Sigma) to a final concentration of 1 µg/ml to obtain sparse biotinylation.

3. Sterile filtrate the solution through a 0.22 µm syringe filter (Milli-Q) five minutes after mixing, onto the amino-functionalized cover slide.

4. Spincoat the fully covered slide for 45 seconds at 2500 rpm.

5. Incubate the slides at room temperature overnight to complete the crosslinking reaction. Slides can be stored in the dark for up to one week.

Oxygen scavenger system

1. A 1X oxygen scavenger system consists of 0.4-4% glucose, 2.2 µg/ml (2170 U/ml) catalase, 0.92 mg/ml (165 U/ml) glucose oxidase, and 2 mM trolox.

2. Mix 11 µl catalase with 1 ml T50, sterile filtrate with a 0.22 µm syringe filter and centrifuge for 15 min (at 4 °C, 13.2k rpm) in a table-top centrifuge. Take 200 µl of the supernatant.

3. Dissolve 92 mg glucose oxidase in 1 ml T50, sterile filtrate with a 0.22 µm syringe filter and centrifuge for 15 min (at 4 °C, 13.2k rpm) in a table-top centrifuge. Take 200 µl of the supernatant.

4. Mix the catalase and glucose oxidase to obtain a 50X stock solution, and keep on ice. This is more than sufficient for a day of measurements. Further storage is also possible (*see* **Note 6**).

5. Prepare a 40% w/v solution of β-D-glucose and sterile filtrate with a 0.22 µm syringe filter. Store at 4 °C.

6. Dissolve 250 mg trolox in 1 ml 120 mM NaOH (by vortexing and sonicating) to obtain a 100 mM (50X) trolox stock solution. Sterile filtrate with a 0.02 µm syringe filter. Store in aliquots at -80 °C.

Single-pair FRET microscopy with widefield microscopy

1. Assemble a flow channel by placing a CoverWell perfusion chamber gasket on a functionalized slide.

2. Fill the flow chamber with T50 buffer and hydrate the slide for 5 min.

3. Inject a neutravidin solution (0.01-0.1 mg/ml) and incubate for 5 min. Wash excess neutravidin away with 2-3 flow chamber volumes of T50.

4. Dilute the labeled, biotinylated nucleosomes to 10-100 pM in a buffer containing 0.1 mg/ml BSA, 10-100 nM unlabeled nucleosomes, and 1X oxygen scavenger (*see* **Note 7** and the previous paragraph). Inject the sample in the flow chamber and seal by covering the holes with a glass slide. Immobilization is virtually instantaneous. Record the fluorescence with a widefield microscope. Example data is shown in figure 2.4.a-c.

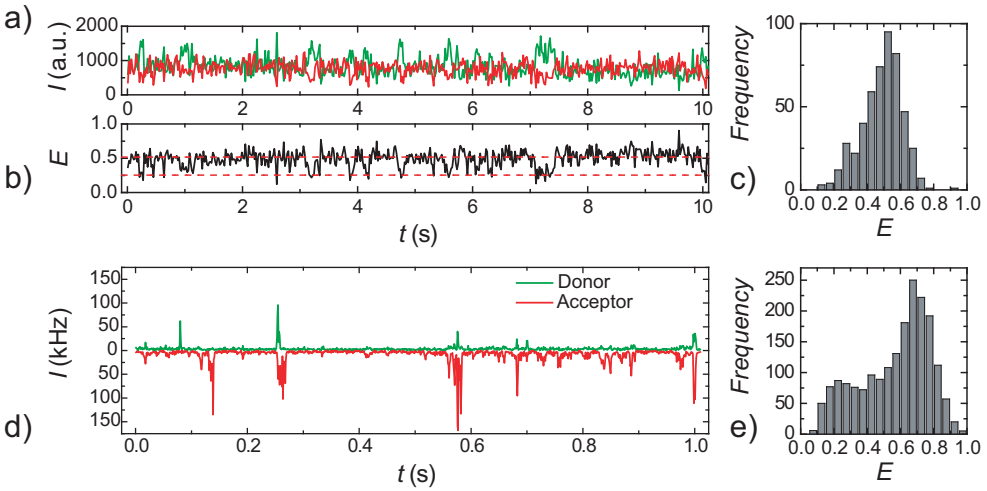

Figure 2.4: Single-pair FRET microscopy on nucleosomes. a) Fluorescence intensity time trace of donor and acceptor fluorescence of a single immobilized nucleosome. b) Resulting FRET efficiency E as a function of time. Fluctuations in E are caused by breathing dynamics of the nucleosome. c) FRET efficiency histogram of the time trace in b). d) Fluorescence intensity time trace of fluorescence originating from freely diffusing molecules. Bursts of fluorescence arise from the passage of a single molecule through the excitation volume. e) Histogram of FRET efficiencies calculated from bursts as in d). A high and a low FRET population can clearly be distinguished. These reflect different conformations of the nucleosome.

Single-pair FRET confocal microscopy

1. Alternatively, image freely diffusing molecules using confocal microscopy. Immobilization to a functionalized cover slide is not needed in this case, so the surface passivation and functionalization steps described in section 2.4.5 can be omitted. The observation time is limited to a few ms per molecule.

2. Mount a clean cover slide on the microscope, and place a droplet (~50 µl) of 10-100 pM labeled nucleosomes in a buffer containing 0.1 mg/ml BSA, and 10-100 nM unlabeled nucleosomes. Focus 25 µm above the glass surface, and record the fluorescence. Example data is shown in figure 2.4.d and e.

2.5 Notes

1. Unless stated otherwise, all solutions are prepared with 18.2 MΩ·cm MilliQ water. This standard is referred to as "water" in the text.

2. StarPEGs are not commercially available. With commercially available linear PEGs, we observed non-specific adsorption and dissociation of nucleosomes [9]. It has been reported that a repeated PEGylation step may increase the specificity and reduce non-specific adsorption of slides coated with linear PEGs however [17].

3. Care must be taken to avoid autofluorescent contamination of buffers, samples and microscope slides. Work at a clean lab bench, using clean glassware, and always wear gloves. Buffers for single molecule imaging are sterile filtrated with a 0.02 µm syringe filter (Whatman Anotop 25). This removes virtually all autofluorescent impurities.

4. We recommend to use Alternating Laser EXcitation (ALEX) [18] to virtually sort molecules based on their label stoichiometry, and to discriminate residual bleaching and blinking events from real conformational transitions.

5. Store the nucleosomes at the highest concentration possible (preferably >100 nM) to prevent dilution-driven dissociation. The use of low protein-binding tubes is recommended to minimize sticking to the tube.

6. If desired, 50 µl aliquots 50X glucose oxidase and catalase can be stored at -80 °C for several weeks. Although it is recommended not to freeze the catalase, we did not observe a major loss in oxygen scavenging activity from these aliquots.

7. Buffers for single molecule imaging are degassed prior to use, to remove the oxygen already in solution. When using oxygen scavenger the sample can be imaged for 30 min;

after that the pH will drop as a result of the production of gluconic acid as a byproduct of the oxygen scavenging reaction.

2.6 Conclusion

The methods presented here provide a simple and straightforward way to generate mononucleosomes with a FRET pair at various locations in the nucleosome. A careful design of the DNA template leads to exactly positioned nucleosomes, with fluorescent labels at the desired location. Salt dialysis reconstitution with stoichiometric amounts of histones directs the assembly of a homogeneous sample of nucleosomes, as deduced from PAGE and bulk fluorescence measurements. These well-characterized nucleosome constructs allow detailed single-molecule measurements of nucleosome structure and dynamics. Widefield TIRF microscopy on immobilized molecules allows the monitoring of individual nucleosomes for tens of seconds to minutes. Fluorescence microscopy on freely diffusing molecules in a femtoliter confocal detection volume allows a fast characterization of nucleosome conformational distributions free from possible interactions with the cover slide. The bottom-up approach for studying mononucleosome structure and dynamics presented here can pave the way for understanding the physical mechanisms underlying gene regulation.

The nucleosome is the fundamental building block of DNA organization *in vivo*. DNA programmability is of crucial importance for designing and constructing nucleosomes as a model system of this higher-order DNA structure: modified nucleotides allow the incorporation of fluorescent and biotin labels in the nucleosome, while the use of a nucleosome positioning sequence directs the formation of the nucleosome to a specific position on the DNA. The predictable structure of the resulting nucleosome could facilitate the architecture of new DNA-protein scaffolds and higher-order structures. Therefore, it could be exploited as a structural motif in DNA nanotechnology.

Acknowledgments

We thank Andrew Routh (MRC Cambridge) for samples of micrococcal nuclease digested nucleosome core particles and useful discussion, Alexander Brehm (University of Marburg) for histone octamer preparations, and Jürgen Groll (RWTH Aachen) for providing samples of the NCO-star PEG material and support with the coating procedure.

This work is part of the research programme of the 'Stichting voor Fundamenteel Onderzoek der materie (FOM)', which is financially supported by the 'Nederlandse Organisatie voor Wetenschappelijk Onderzoek (NWO)'.

Bibliography

[1] Seeman, N. and Lukeman, P. Nucleic acid nanostructures: bottom-up control of geometry on the nanoscale. *Rep. Prog. Phys.* **68**, 237–270 (2005).

[2] Seeman, N. DNA nanotechnology: Novel DNA constructions. *Annu. Rev. Biophys. Biomol. Struct.* **27**, 225–248 (1998).

[3] Chen, J. and Seeman, N. Synthesis from DNA of a molecule with the connectivity of a cube. *Nature* **350**, 631–633 (1991).

[4] Goodman, R., Schaap, I., Tardin, C., Erben, C., Berry, R., Schmidt, C., and Turberfield, A. Rapid chiral assembly of rigid DNA building blocks for molecular nanofabrication. *Science* **310**, 1661–1665 (2005).

[5] Rothemund, P. Folding DNA to create nanoscale shapes and patterns. *Nature* **440**, 297–302 (2006).

[6] Luger, K., Mader, A., Richmond, R., Sargent, D., and Richmond, T. Crystal structure of the nucleosome core particle at 2.8 Å resolution. *Nature* **389**, 251–260 (1997).

[7] Luger, K. Dynamic nucleosomes. *Chromosome Res.* **14**, 5–16 (2006).

[8] Koopmans, W. J. A., Brehm, A., Logie, C., Schmidt, T., and van Noort, J. Single-pair FRET microscopy reveals mononucleosome dynamics. *J. Fluoresc.* **17**, 785–795 (2007).

[9] Koopmans, W. J. A., Schmidt, T., and van Noort, J. Nucleosome Immobilization Strategies for Single-Pair FRET Microscopy. *ChemPhysChem* **9**, 2002–2009 (2008).

[10] Dyer, P., Edayathumangalam, R., White, C., Bao, Y., Chakravarthy, S., Muthurajan, U., and Luger, K. Reconstitution of nucleosome core particles from recombinant histones and DNA. *Chromatin and Chromatin Remodeling Enzymes, Pt A* **375**, 23–44 (2004).

[11] Lowary, P. and Widom, J. New DNA sequence rules for high affinity binding to histone octamer and sequence-directed nucleosome positioning. *J. Mol. Biol.* **276**, 19–42 (1998).

[12] Gansen, A., Hauger, F., Toth, K., and Langowski, J. Single-pair fluorescence resonance energy transfer of nucleosomes in free diffusion: Optimizing stability and resolution of subpopulations. *Anal. Biochem.* **368**, 193–204 (2007).

[13] Kelbauskas, L., Chan, N., Bash, R., Yodh, J., Woodbury, N., and Lohr, D. Sequence-dependent nucleosome structure and stability variations detected by Förster resonance energy transfer. *Biochemistry* **46**, 2239–2248 (2007).

[14] Davey, C., Sargent, D., Luger, K., Maeder, A., and Richmond, T. Solvent mediated interactions in the structure of the nucleosome core particle at 1.9 Å resolution. *J. Mol. Biol.* **319**, 1097–1113 (2002).

[15] Claudet, C., Angelov, D., Bouvet, P., Dimitrov, S., and Bednar, J. Histone octamer instability under single molecule experiment conditions. *J. Biol. Chem.* **280**, 19958–19965 (2005).

[16] Clegg, R. Fluorescence resonance energy-transfer and nucleic-acids. *Methods Enzymol.* **211**, 353–388 (1992).

[17] Roy, R., Hohng, S., and Ha, T. A practical guide to single-molecule FRET. *Nat. Methods* **5**, 507–516 (2008).

[18] Kapanidis, A., Lee, N., Laurence, T., Doose, S., Margeat, E., and Weiss, S. Fluorescence-aided molecule sorting: Analysis of structure and interactions by alternating-laser excitation of single molecules. *Proc. Natl. Acad. Sci. U.S.A.* **101**, 8936–8941 (2004).

Chapter 3

Single-pair FRET Microscopy reveals Mononucleosome Dynamics[1]

Abstract We applied spFRET microscopy for direct observation of intranucleosomal DNA dynamics. Mononucleosomes, reconstituted with DNA containing a FRET pair at the dyad axis and exit of the nucleosome core particle, were immobilized through a 30 bp DNA tether on a polyethyleneglycol functionalized slide and visualized using Total Internal Reflection Fluorescence microscopy. FRET efficiency time-traces revealed two types of dynamics: acceptor blinking and intramolecular rearrangements. Both Cy5 and ATTO647N acceptor dyes showed severe blinking in a deoxygenated buffer in the presence of 2% β-mercaptoethanol. Replacing the triplet quencher β-mercaptoethanol with 1 mM Trolox eliminated most blinking effects. After suppression of blinking three subpopulations were observed: 90% appeared as dissociated complexes; the remaining 10% featured an average FRET efficiency in agreement with intact nucleosomes. In 97% of these intact nucleosomes no significant changes in FRET efficiency were observed in the experimentally accessible time window ranging from 10 ms to 10s of seconds. However, 3% of the intact nucleosomes showed intervals with reduced FRET efficiency, clearly distinct from blinking, with a lifetime of 120 ms. These fluctuations can unambiguously be attributed to DNA breathing. Our findings illustrate not only the merits but also typical caveats encountered in single-molecule FRET studies on complex biological systems.

[1]This chapter is based on: W. J. A. Koopmans, A. Brehm, C. Logie, T. Schmidt, and J. van Noort, Single-pair FRET Microscopy reveals Mononucleosome Dynamics. *Journal of Fluorescence* **17**, 785-795 (2007)

3.1 Introduction

Fluorescence (or Förster) Resonance Energy Transfer (FRET) is a process in which the energy of an excited donor fluorophore is transferred non-radiatively to an acceptor molecule [1]. The efficiency of energy transfer E is given by:

$$E = \frac{1}{1 + \left(\frac{R}{R_0}\right)^6}, \tag{3.1}$$

where R is the distance between donor and acceptor and R_0 is the Förster radius, at which 50% energy transfer occurs (typically 5 nm for Cy3-Cy5, a commonly used FRET pair). FRET is a powerful tool to study the structure and function of biological molecules, such as DNA. When extended to the single-molecule level, single pair FRET (spFRET) can potentially be applied to determine the conformational distribution of an ensemble of molecules and the dynamics of individual molecules [2–4]. We exploited spFRET to study the structure and dynamics of single nucleosomes, the fundamental units of compaction and organization of eukaryotic DNA.

The nucleosome core particle consists of ~50 nm DNA wrapped nearly twice around a histone-octamer protein-core [5]. Nucleosomal DNA has to unwrap from the nucleosome core to sterically allow processes such as transcription, replication and repair. Accessibility to nucleosomal DNA is facilitated by ATP-dependent remodeling enzymes *in vivo* [6]. However, it is known that spontaneous conformational changes of the nucleosome expose occluded sites in the DNA as well [7]. DNA breathing, the transient unwrapping and rewrapping of a stretch of DNA from the nucleosome core, has recently been studied in detail with a variety of fluorescence techniques. The equilibrium constant of this process was determined with bulk FRET measurements [8]. Unwrapping lifetimes of 10-50 ms were obtained with stopped-flow FRET measurements and Fluorescence Cross Correlation Spectroscopy (FCCS) [9]. Interestingly, based on their single pair FRET work, Tomschik *et al.* concluded that unwrapping of nucleosomal DNA occurs to a much larger extent than was previously anticipated [10]: they suggested that 30-60% of the nucleosomal DNA was unwrapped with a lifetime on the order of ~150 ms before rewrapping.

Although the conceptual beauty of FRET studies is undisputed, there are a number of important caveats in single-molecule FRET studies of biomolecules, such as fluorophore blinking, photobleaching and sample immobilization. Here, we addressed these issues. spFRET microscopy on mononucleosomes revealed two dominant types of dynamics: acceptor blinking and intramolecular rearrangements that we attribute to DNA breathing, which only became apparent after suppression of blinking. Upon immobilization, we observed three different populations: 90% of the nucleosomes dissociated or represented donor-only species,

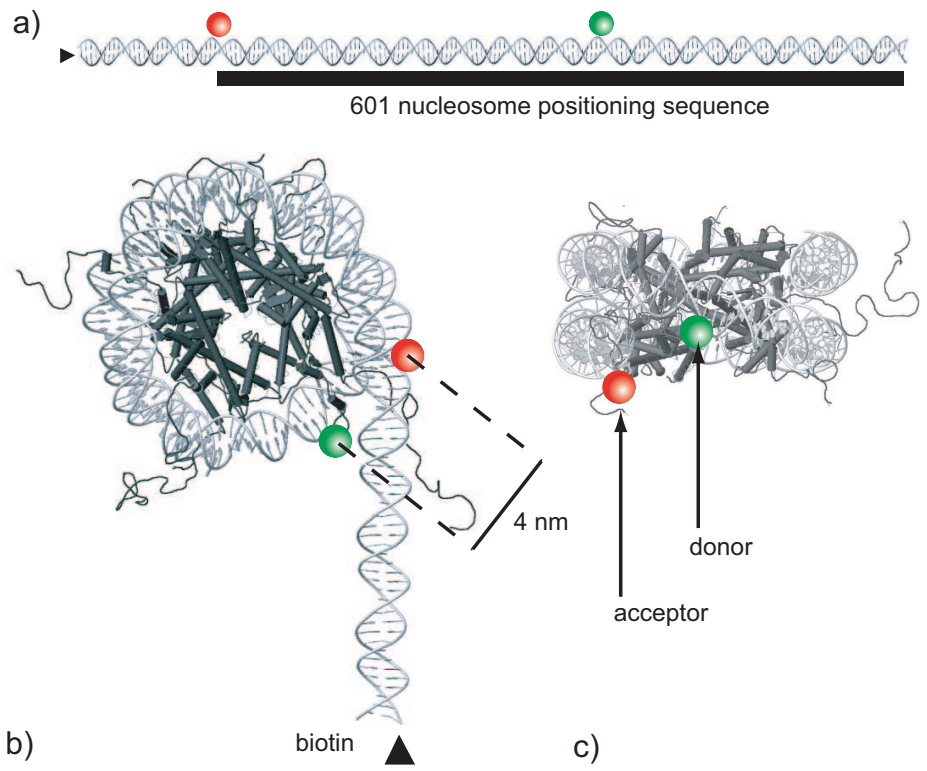

Figure 3.1: FRET system for the study of mononucleosome dynamics. a) The 177 bp DNA construct, indicating the position of the labels 80 bp apart in a fragment containing the 601 nucleosome positioning sequence. A biotin label allowed for immobilization of the construct. b) and c) Illustrations of the mononucleosome structure, indicating the position of donor and acceptor upon reconstitution. The distance between the labels was ~4 nm, at which efficient FRET takes place. Unwrapping of the DNA from the nucleosome core will be accompanied by a decrease in FRET due to increasing separation between donor and acceptor.

and 10% remained intact. Of these fully wrapped nucleosomes, 97% showed stable FRET on timescales between 0.01-10 s, while 3% showed dynamics with a dwell time of 120 ms that we attribute to conformational changes in the nucleosome.

3.2 Material and Methods

DNA preparation A 177 base pair (bp) DNA was constructed by PCR using the 601 nucleosome positioning element [11] as template. PCR primers were as follows. Forward primer: 5'-biotin-TTTGAATTCCCAGGGAATTGGGCGGCCGCCCTGGAGAATCCCGGTGCC-GAGGCCGC-3' (acceptor labeled nucleotide is underlined). Reverse primer: 5'-ACAGGA-

TGTATATATCTGACACGTGCCTGGAGACTAGGGAGTAATCCCCTTGGCGGTTAA-AACGCGGGGGGACAGCGCGTACG-3' (donor labeled nucleotide is underlined). We used either Cy3-Cy5 or ATTO550-ATTO647N as donor-acceptor FRET pair. PCR products were purified with a GFX PCR DNA & Gel Band Purification Kit (GE Healthcare). The position of the labels was chosen such that after reconstitution the acceptor was located at the nucleosome exit, and the donor near the dyad axis, as illustrated in figure 3.1. Donor and acceptor were predicted to be ~4 nm apart, as deduced from the nucleosome crystal structure [12], resulting in a FRET efficiency E of approximately 0.8 for the Cy3-Cy5 pair (R_0 ~5 nm), and of approximately 0.9 for the ATTO550-ATTO647N pair (R_0 ~6 nm).

Nucleosome reconstitution Recombinant histone octamers were mixed with the DNA construct at a 1:1 ratio, in TE (1 mM EDTA, 10 mM Tris.HCl pH 8.0) and 2 M NaCl. Mononucleosomes were reconstituted by salt dialysis against 0.85, 0.65, 0.5 and finally against 0.1 M NaCl, all buffered with TE.

Bulk fluorescence measurements Bulk fluorescence experiments were carried out on a Luminescence Spectrometer (LS55, Perkin Elmer). All experiments were performed at room temperature (22 ºC). The nucleosome concentration was 10-50 nM. The donor dye was excited at 515 nm and the emission was recorded from 535 to 700 nm. The acceptor dye was excited at 615 nm and the emission was recorded from 635 to 700 nm, to obtain acceptor-only emission spectra. The FRET efficiency was determined from the enhanced fluorescence of the acceptor using the $ratio_A$ method [13]:

$$E_{(ratio)A} = \frac{\varepsilon_A^{615} \frac{F_A^{515}}{F_A^{615}} - \varepsilon_A^{515}}{\varepsilon_D^{515} d^+}, \tag{3.2}$$

where ε_A^λ and ε_D^λ are the acceptor and donor extinction coefficient respectively at wavelength λ, F_A^λ is the fluorescence intensity of the acceptor when excited at wavelength λ, and d^+ is the fractional labeling coefficient of the donor. The fluorescence intensity of the acceptor was determined at its maximum value. d^+ was determined from DNA and fluorophore absorption peaks in an absorption spectrum of the labeled DNA, measured from 230 to 700 nm with a spectrophotometer (Pharmaspec UV-1700, Shimadzu).

Single-molecule FRET measurements Cleaned glass slides were amino functionalized with 10 µg/ml poly-D-lysine, and subsequently incubated for 4 hours with an amine reactive poly ethylene glycol (PEG) mixture: 20% mPEG-succinimidyl propionate 5,000 molecular weight (Nektar Therapeutics) and 0.2% biotin-PEG-n-hydroxysuccinimide 3,400 molecular weight (Nektar Therapeutics) in 0.1 M sodium carbonate buffer (pH 8.2). A flow cell was assem-

bled by sealing a poly-dimethylsiloxane channel with a PEG functionalized slide. A 0.1 mg/ml streptavidin (Roche) solution was incubated for 5 minutes, and subsequently washed away. A sample, which typically consists of 10-50 pM of labeled mononucleosomes in 50-200 mM NaCl, 10 mM Tris.HCl pH 8.0, 0.03% NP-40, and 10-50 nM unlabeled mononucleosomes, was injected in the channel and immobilized. An enzymatic oxygen scavenger system (1% glucose, 2% β-mercaptoethanol (βME) or 1 to 2 mM Trolox (Sigma), 0.2 mg/ml glucose oxidase, and 0.04 mg/ml catalase), was added to the buffer to extend the lifetime of the fluorophores before photobleaching. The buffer was degassed prior to use to further reduce the oxygen concentration. The flow cell was mounted on a microscope equipped with a 100X oil-immersion TIRF microscope objective (NA = 1.45, NIKON) and temperature-stabilized at 22 °C using a water circulating bath connected to all parts of the setup in contact with the sample. The 514 nm line of an Ar+ laser (Coherent) was used to illuminate an area of ~600 μm² with a power of 0.9 mW. In the case of alternating excitation, a 636 nm diode laser (Power Technology) was used to illuminate an area of ~900 μm² with a power of 0.3 mW. Both beams were circularly polarized and were displaced parallel to the optical axis of the objective, so that an evanescent excitation field was generated by total internal reflection of the light at the glass-water interface. The excitation intensity at the interface in the evanescent field is ~4 times higher than the incident beam intensity at the critical angle [14]. We therefore estimated that the resulting excitation intensities at the interface were ~0.6 kW/cm² for the 514 nm excitation and ~0.13 kW/cm² for the 636 nm excitation respectively. The fluorescence was collected by the objective and filtered through a custom-made dual color band pass filter (Chroma), that rejects scattered laser light, and a long pass filter (OG530, Schott). The fluorescence was further split into a donor and an acceptor channel by a custom-made dichroic wedge mirror (0.5° angle, center wavelength of 630 nm, Chroma) placed in the infinity path of the microscope [15]. A +150 mm achromatic lens (Thorlabs) projected the separate images on a multiplication gain CCD camera (Cascade 512B, Roper Scientific) operating at a frame rate of 20 to 100 Hz.

Data analysis The simultaneously acquired donor and acceptor images (typically 80 by 80 pixels) were aligned with respect to one another through their cross correlation. The first 50 donor and acceptor frames were overlaid, and their intensities averaged. Low frequency background signal was filtered out with a high-pass FFT filter. The location of the fluorophores was then determined by applying a threshold of two times the background noise level. A time-trace of donor and acceptor intensities was then calculated by integrating the pixel intensities 1.5 pixel around the fluorophore center for each frame and each image. In the case of alternating excitation, the acceptor intensity upon direct excitation was retrieved by deinterleaving the acceptor time-trace. The FRET efficiency E was calculated from [2]:

$$E = \frac{I_A}{I_A + \gamma I_D}, \tag{3.3}$$

where I_A and I_D are acceptor and donor intensity respectively, and $\gamma = \frac{\Phi_A \eta_A}{\Phi_D \eta_D}$ is a parameter to correct for photophysical properties of the dyes. Φ_A and Φ_D are acceptor and donor quantum yield, and η_A and η_D are acceptor and donor detector efficiency respectively. As a first approximation γ was set to unity. A more accurate estimate for γ was obtained from experimental intensity time traces where donor bleaching took place after acceptor bleaching. In these cases the FRET efficiency could also be calculated from donor quenching:

$$E = 1 - \frac{I_D}{I_{D0}}, \tag{3.4}$$

where I_{D0} is the donor intensity after bleaching of the acceptor. Combining eqs. (3.3) and (3.4) results in:

$$\gamma = \frac{I_A}{I_{D0} - I_D}. \tag{3.5}$$

3.3 Experimental Results

3.3.1 Bulk fluorescence spectra reveal proper reconstitution of mononucleosomes

The results of bulk fluorescence and absorption experiments on reconstituted mononucleosomes are shown in figure 3.2. The reconstituted sample showed efficient FRET, indicated by a distinct peak of fluorescence at the acceptor maximum emission wavelength (670 nm for ATTO647N, see figure 3.2.a). This peak was not present in the labeled DNA-only sample, confirming that the donor and the acceptor were in close proximity due to mononucleosome reconstitution. As a control, we diluted the mononucleosome sample in 2 M NaCl, as this high ionic strength disrupts nucleosome structure [16]. As predicted, over 90% of the energy transfer signal was lost. The observed average FRET efficiency in the reconstituted mononucleosomes was 0.75 ± 0.1, which is in good agreement with FRET values predicted by the position of the FRET pair in the nucleosome. From the bulk FRET experiments, and a predicted maximum FRET efficiency of ~0.9 for a mononucleosome with the ATTO550-ATTO647N FRET-pair, we estimated the reconstitution yield to be at least 85%. The residual donor emission can be accounted for by incomplete acceptor labeling. With absorption measurements on the DNA construct (figure 3.2.b) we determined that the molar ratio acceptor:donor:DNA was 0.7:0.9:1. Together, these bulk data show that the labeled DNA construct and the histone proteins properly formed mononucleosomes upon reconstitution (see figure 3.1).

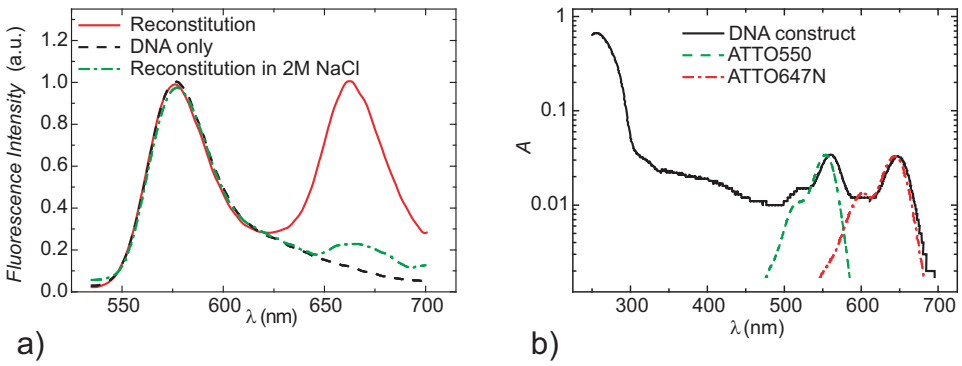

Figure 3.2: Bulk fluorescence emission and absorption spectra revealed proper reconstitution of mononucleosomes. a) Bulk fluorescence emission spectra. A distinct peak of fluorescence at the acceptor emission wavelength was seen after reconstitution, which was not present for the labeled DNA only. The peak disappeared upon dilution of the reconstituted material in 2 M NaCl, an ionic strength at which nucleosome structure is disrupted. b) Bulk absorption spectrum of the fluorescently labeled DNA construct. The stoichiometry of the labels was obtained by comparison with the absorption spectra of ATTO550 and ATTO647N (as provided by the manufacturer), which are plotted with dotted lines.

3.3.2 spFRET microscopy reveals individual nucleosomes together with a large population of dissociated nucleosomes

To investigate mononucleosome subpopulations and dynamics, spFRET measurements were performed in a wide field microscope. Figure 3.3 shows an example of typical single-molecule fluorescence images of immobilized mononucleosomes. In figure 3.3.a, an acceptor channel image was superimposed on a donor channel image. 10% of the immobilized fluorophores showed efficient FRET, as indicated by colocalized fluorescent spots in the acceptor channel upon donor excitation, and thus represent fully reconstituted mononucleosomes. In contrast, 90% of the fluorophores did not show FRET at all. This conflicts with the bulk experiments, where after correction for incomplete labeling an average FRET efficiency of 0.75 was found. As mentioned before, there was a fraction of donor only labeled species (~30%), but this alone could not explain the observed discrepancy between bulk and single-molecule measurement. When we directly excited the acceptor fluorophores (see figure 3.3.b), we found that most of the donors were colocalized with an acceptor. Therefore we conclude that FRET signal was lost during the single-molecule measurement, due to disassembly of a large fraction of the nucleosomes. It is known that nucleosomes become unstable and dissociate when they are diluted to low concentrations [17, 18]. For our wide field spFRET measurements we diluted to pM fluorophore concentrations to resolve individual fluorophores. We ensured that the nucleosome

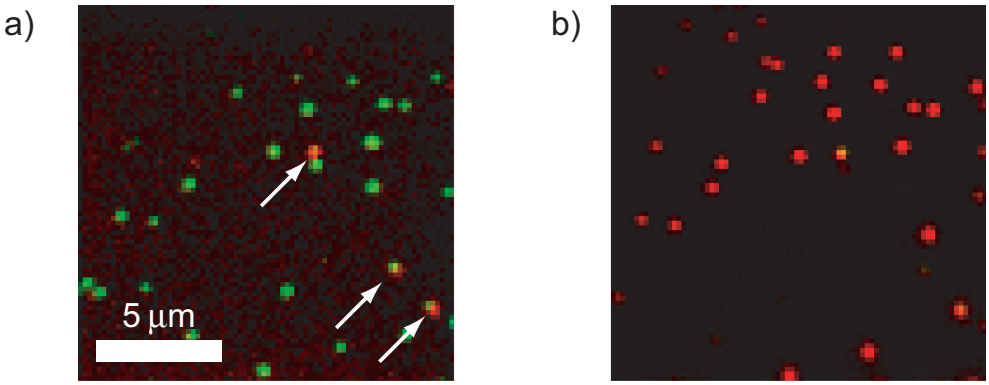

Figure 3.3: Single molecule fluorescence image of immobilized mononucleosomes. a) False color representation of averaged donor and acceptor channel images, excited at 514 nm. The arrows point at molecules that featured efficient FRET from donor to acceptor. The majority of the molecules however did not show FRET and appears in red. b) The same field of view excited at 636 nm, allowing for unambiguous identification of acceptor fluorophores.

concentration was always above 10-50 nM by adding an excess of unlabeled mononucleosomes and 0.03% non-ionic detergent (NP-40) to our buffer. Thåström *et al.* [19] reported that under these conditions nucleosomes do not dissociate in bulk solutions. We found that even 50 nM of unlabeled nucleosomes, far above the dilution-driven dissociation threshold, did not retain proper nucleosome folding, excluding dilution effects to be the cause. It is known that H2A-H2B histone dimers can spontaneously be exchanged from the protein core [20], which in our case would result in a transient loss of FRET. However, we found the same amount of disassembled nucleosomes upon immobilization when the octamer protein core was crosslinked by dialysis against 0.05% glutaraldehyde in 1 mM EDTA. We confirmed that the crosslinking itself did not dissociate nucleosomes with bulk fluorescence experiments. This suggests that not the histone protein core dissociates, but rather that the wrapped DNA loosens or significantly rearranges itself around the protein core. We confirmed that mononucleosomes in free solution (in the same buffer used for single-molecule experiments) remain stable for hours at room temperature using bulk fluorescence measurements. Therefore we consider the dissociation of the nucleosomes described here to be associated with their immobilization to the functionalized cover glass. As an alternative immobilization strategy we performed experiments with biotinylated BSA-functionalized cover glasses instead of PEGs. Biotinylated BSA is often used for single-molecule studies involving nucleic acids, whereas PEGs are often used for studies involving DNA-protein complexes [21]. Biotinylated BSA yielded even less intact nucleosomes. The exact nature of the interactions of the nucleosomes with the modified cover slides remains unclear, but the destabilizing effect of the surface forms a hurdle for obtaining

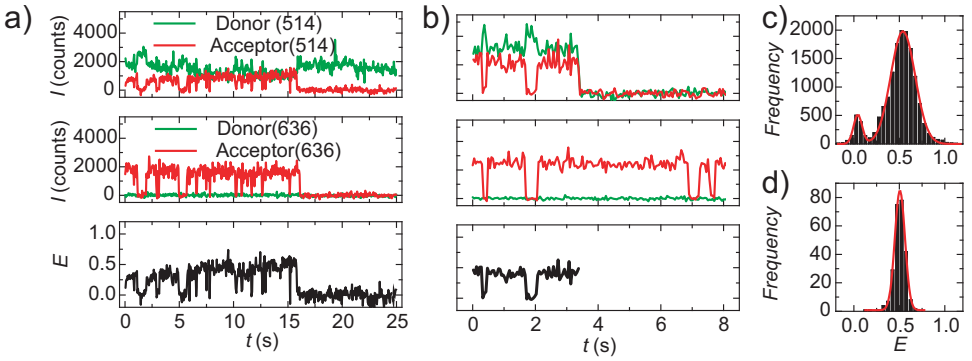

Figure 3.4: Single molecule FRET traces from individual mononucleosomes. The top panels in a) and b) show the intensity time traces of donor and acceptor for green excitation; the middle panel shows the intensity time traces of donor and acceptor for red excitation, which were acquired in alternation with the green excitations. The bottom panels show the calculated FRET efficiency. The fluctuations between high and low FRET states featured perfect correlation with the corresponding acceptor intensity traces excited at 636 nm. c) Histogram of the FRET efficiencies of multiple single molecule traces. d) Histogram of the FRET efficiencies of a single trace. The spread in FRET efficiency was larger between different traces than within a single trace.

large datasets of spFRET measurements. On the 10% immobilized mononucleosomes showing FRET, irreversible loss of FRET was only found after photobleaching, implying that their nucleosomal structure remained intact after immobilization.

3.3.3 Single-molecule fluorescence footprint of individual nucleosomes

Example intensity time-traces of intact single nucleosomes are shown in figure 3.4.a and b. Donor and acceptor intensity were clearly anti-correlated, indicative of their FRET interaction. The intensity of a single donor (Cy3) was $1.4 \pm 0.3 \cdot 10^3$ counts/10 ms at a signal to noise ratio (SNR) of 5. When the donor was quenched by FRET, both the intensity and SNR decreased. The intensity of an acceptor (Cy5) excited via FRET was $0.9 \pm 0.2 \cdot 10^3$ counts/10 ms at a SNR of 3. After ~4 s of continuous illumination at ~0.6 kW/cm² either donor or acceptor photobleached, limiting the observational window to a few seconds. The total number of emitted photons until bleaching from a FRET pair was ~10^5 (calculated with gain G = 33 counts/photon, detection efficiency η_A and η_D ~ 15%). The observed average FRET efficiency of the high FRET level was 0.5 ± 0.13, slightly lower than the values measured in the bulk. From the traces where donor bleaching takes place after acceptor bleaching, we estimated the correction factor γ for photophysical parameters of Cy3/Cy5 to be 0.7 ± 0.3 (*see* eq.(3.5)). The

corrected FRET efficiency was then 0.6 ± 0.3, in good agreement with values obtained from bulk measurements. We found that the standard deviation in FRET efficiency of the high FRET state of the entire population (0.13) was larger than the standard deviation within individual traces (0.06), as shown in the histograms in figures 3.4.c and d. This observation can be accounted for either by different nucleosome populations with slight variations in FRET efficiency, or by local differences in rotational freedom of the dyes due to immobilization.

3.3.4 Acceptor blinking is the dominant source of spFRET dynamics

The FRET traces shown in figure 3.4.a and b are highly dynamic and fluctuate between a high FRET state ($E \sim 0.6$, lifetime 2.5 s) and a low FRET state ($E \sim 0.1$, lifetime 0.13 s). Interestingly, the characteristics of these fluctuations, i.e. both on and off time, and the low FRET level, are remarkably similar to those observed by Tomschik *et al.* [10] who performed analogous experiments. This similarity however, is remarkable in view of the completely different FRET-label location. Tomschik *et al.* labeled the nucleosome opposite to the dyad axis and probed the DNA at the most internal position of the nucleosome, whereas our substrate has labels at the most exterior position. Polach and Widom have previously shown that the enzymatic accessibility of the DNA inside a nucleosome strongly reduces as the DNA is more internal in the nucleosome [7], suggesting a higher frequency of unwrapping events in our experiments. Because of the nearly complete absence of acceptor emission, we investigated the nature of these fluctuations in order to exclude reversible transitions of the acceptor to an inactive state (acceptor blinking, resulting in a Förster radius of effectively zero [22]) as the origin of these events. By alternating donor excitation with direct acceptor excitation we could directly monitor the acceptor condition as shown in figure 3.3.b. After deinterleaving the data into two time-traces, one for green excitation and one for red excitation, it became obvious that the fluorescence intensity of the acceptor upon direct excitation correlated perfectly with the enhanced emission of the acceptor due to FRET. Thus, the low FRET state must be attributed to blinking, due to a dark-state level of the acceptor. Further evidence that these fluctuations were caused by acceptor blinking was provided by experiments with alternative acceptor dye (ATTO647N, emission spectrum similar to Cy5). Alternating excitation of the acceptor dye revealed a strong positive correlation between sensitized emission of the acceptor and direct excitation of the acceptor. In this case the low FRET state was also present, but with a much shorter lifetime of 0.046 s. In conclusion, our data confirm that the fluctuations between a high and a low FRET state reflect photophysical processes in the acceptor dye rather than nucleosome conformational changes.

We further analyzed the single-molecule FRET traces for dynamics other than blinking. Therefore we filtered out blinking events by the application of a threshold on low FRET efficiencies ($\leq \sim$0.1-0.2, dependent on the noise in the measurement). Although careful inspection

did occasionally reveal anticorrelated features of donor and acceptor channel, these features had a lifetime below the time resolution of our measurements. To confirm that we did not overlook any dynamics, we analyzed the fluorophore intensity noise in the high FRET state, which in the absence of dynamics should be limited by shot noise. The theoretical noise σ_{tot} in the measurement was estimated by [23]:

$$\sigma_{tot} = \sqrt{G^2F^2S\Phi + G^2F^2D + \sigma_R}, \tag{3.6}$$

where G is the multiplication gain factor, F is the excess noise factor due to the multiplication gain register, S is the number of photons that reach the camera, Φ is the camera quantum yield, D is the dark count, and $\sigma_R$is the readout noise. The first contribution represents photon shot noise after multiplication, the second contribution represents the camera dark noise after multiplication, and the third the ADC converter electronic noise. Readout noise and dark noise were calculated from the standard deviation of an area of the chip that was not illuminated by fluorescence to be 130 counts/10 ms. The actual noise σ in the single-molecule fluorescence traces was estimated by the standard deviation of the measured fluorophore intensity. The measured and calculated noise were tested for equality with an F-test:

$$F_{\alpha,\nu1,\nu2} \geq \frac{\sigma^2}{\sigma_{tot}^2} \tag{3.7}$$

where α is the significance level at which the test was performed (0.05), and ν_1 , $\nu_2$are the degrees of freedom used to calculate σ and σ_{tot} respectively. We found that the total measured noise was significantly (typically 1.5 times) higher than that predicted by photon statistics and camera noise only. This implied that the traces contained dynamic events that cannot be fully resolved, originating from either photophysical processes (short blinking events, or intersystem crossing), or fast nucleosome dynamics. Hence, to accurately capture these events, blinking had to be further suppressed, and the sampling frequency had to be increased.

3.3.5 Suppression of blinking

In order to suppress blinking, we first tested a different acceptor dye (ATTO647N), which was reported to have superior photochemical stability compared to Cy5 [24]. As mentioned before, this acceptor dye showed blinking as well, as seen in the example traces and histograms of figure 3.5.a and b. Although a small fraction of molecules did not show any dynamics in FRET, the majority significantly blinked. In the case of Cy5 93% of all acceptors excited via FRET showed significant blinking, with a lifetime of 0.13 ± 0.05 s, and lifetime of the high state of 0.8 ± 0.1 s. In the case of ATTO647N, 94% of all acceptors excited via FRET showed blinking, with a lifetime of 0.046 ± 0.02 s, and lifetime of the high state of 1.2 ± 0.2 s. In conclusion, the

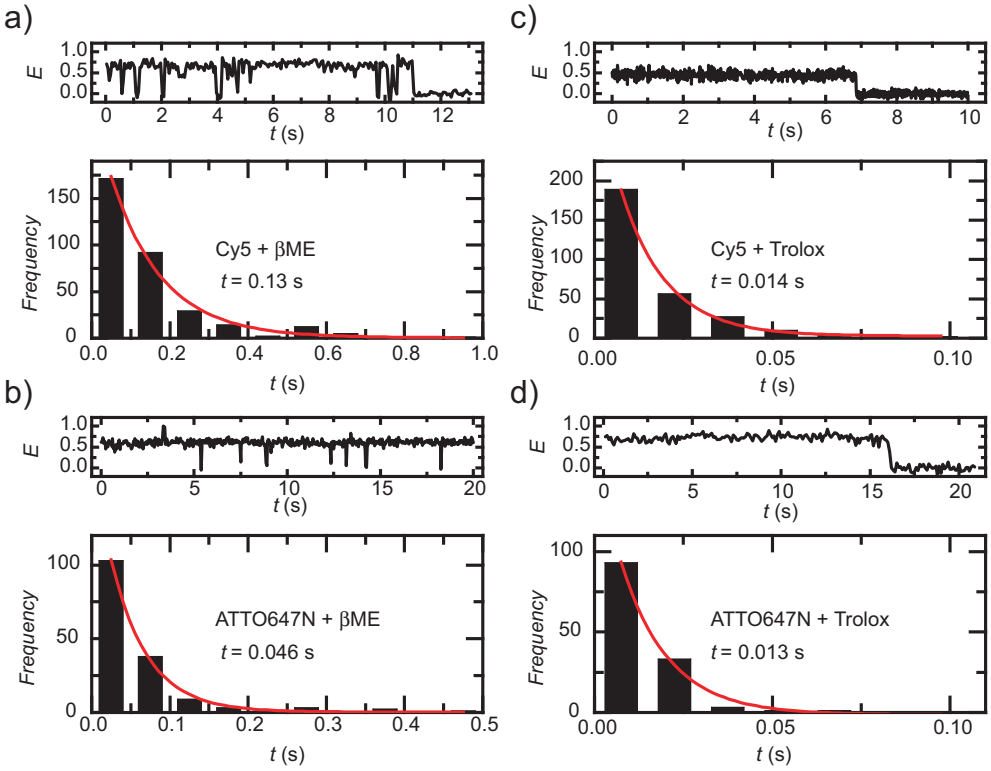

Figure 3.5: Fluorophore blinking in spFRET traces obtained from mononucleosomes. In the presence of βME, nucleosomes labeled with Cy5 (a) or ATTO647N (b) both show severe blinking in 95% of the traces. Example traces (top) and blinking lifetime histograms (bottom) are shown. In the presence of an alternative triplet quencher, Trolox, blinking of both dyes is significantly suppressed, (c, d). The example traces (top) show the absence of blinking in 90% of the traces, while the blinking lifetime histograms (bottom) show a small but finite amount of fast blinking still present in ~ 10% of the traces.

use of a different dye did not suppress blinking to the required level, but just yielded different blinking statistics. Recently a different approach to reduce blinking was described by Rasnik *et al.* [25]. They replaced the triplet quencher βME in the oxygen scavenger system by a water-soluble analog of vitamin E, Trolox. Using this approach, Cy5 blinking in single-molecule FRET measurements on DNA constructs was eliminated. We tested the effect of Trolox in the imaging buffer on blinking of FRET pair labeled mononucleosomes. Results are shown in example traces and histograms in figure 3.5.c and d. For both Cy5 and ATTO647N blinking was dramatically suppressed in the presence of 1 to 2 mM Trolox: over 90% of the traces showed no observable blinking. Noise analyses of the intensity fluctuations in most of these traces were fully accounted for by camera noise and photon statistics (shot noise) only. Thus, within our time resolution (10 ms), no effect of short time scale blinking, or inter system crossing, was detected. Surprisingly, less than 10% of the observed FRET pairs still showed some extent of blinking indicated by fast excursions into a FRET state below 0.2, with a typical off time of 14 ± 1 and 13 ± 1 ms respectively, as shown in the histograms in figure 3.5.c and d. Because the lifetime of these blinking events was on the order of the smallest sampling time used, blinking events were not identified by alternating excitation of the acceptor dye, but only by FRET efficiencies below the noise threshold. Direct excitation of the acceptor did only reveal some occasional blinking in the acceptor traces, with the same lifetime of 13-14 ms. To confirm that a small but finite amount of fast blinking still occurred in the presence of Trolox, we performed spFRET measurements on a FRET pair that was separated by 11 basepair duplex DNA. This construct does not exhibit structural changes that affect the FRET intensity. In this case we also observed a small, but finite amount of blinking in a number of traces (data not shown), with a lifetime similar to that measured on mononucleosomes.

3.3.6 A fraction of the immobilized nucleosomes shows dynamics clearly distinct from blinking

The suppression of blinking finally allowed us to unambiguously identify non-blinking dynamic events in the FRET traces. From a sample of 236 mononucleosomes that showed FRET, we found that over 95% of the traces essentially show stable FRET efficiency, as illustrated in figure 3.6.a and b; all anti-correlated features in the FRET efficiency were short-lived and fall within the noise of the measurement. Thus, the upper limit for dynamic events that could have been missed in this population was 10 ms (the sampling time used). Interestingly, 3% of the traces showed dynamic events clearly distinct from blinking (examples shown in figure 3.6.c and d), as judged by the following criteria: 1) the acceptor signal of a low FRET event was significantly higher than zero. 2) No correlated change in acceptor intensity was detected using alternating excitation. 3) Events persisted for at least two data-points. We found 14 events

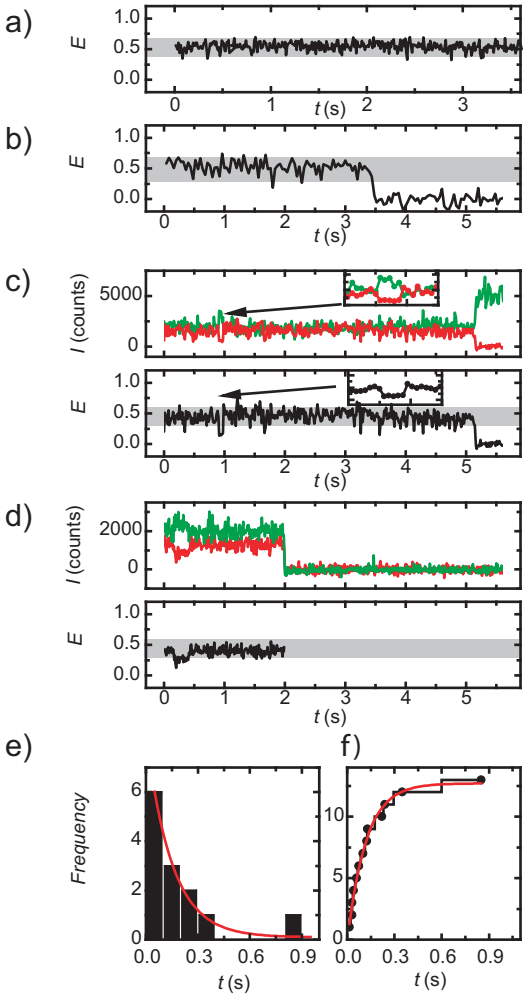

Figure 3.6: A fraction of the immobilized nucleosomes showed dynamics clearly distinct from blinking. a) and b) After suppression of blinking with Trolox, over 95% of the FRET traces do not show FRET dynamics. The theoretical photon and instrument noise is approximately indicated by the grey bars. c) and d) ~ 3% of the intensity traces (top panels) showed FRET fluctuations (bottom panels) clearly distinct from blinking: the acceptor intensity was significantly higher than zero, and events persisted multiple data points (see insets). These fluctuations clearly exceeded the noise. e) Histogram and cumulative distribution plot (f) of the lifetime of the dynamic events. An exponential fit to the data gave an average lifetime of 120 ms.

with an average FRET change $\triangle E$ of -0.23 and an average dwell time of 120 ± 5 ms, as summarized in the histogram and cumulative distribution function in figure 3.6.e and f respectively. The lifetime was determined by fitting a cumulative exponential distribution to the data, independent of binning and therefore a more accurate way of determining the lifetime when using small datasets (figure 3.6.f) than fitting a distribution to binned data. The lifetime of the high FRET state could not be determined accurately, due to the short time window that was available due to photobleaching. Since we explicitly checked the vitality of both fluorophores, we ruled out photodynamics and we could unambiguously attribute the observed features to DNA breathing dynamics.

3.4 Discussion and conclusion

Time-traces of spFRET microscopy on single reconstituted mononucleosomes revealed two types of dynamics: acceptor blinking and intramolecular rearrangements. Intramolecular rearrangements became only apparent after suppression of blinking. Both Cy5 and ATTO647N showed severe blinking in a deoxygenated buffer in the presence of 2% βME. Replacing the triplet quencher βME with Trolox effectively eliminated most blinking effects. The lifetime of DNA unwrapping that we obtained after rigorous elimination of blinking events (~120 ms) was comparable to the 150-180 ms obtained by Tomschik *et al.* [10], despite the very different location of the labels in the nucleosome, and probably less important, the different DNA sequence and origin of the histones. However, we observed a very similar lifetime (~130 ms) for Cy5 blinking under comparable buffer conditions (2% βME). The FRET efficiency of the open states in our experiments was significantly above the detection threshold, so we can explicitly exclude photophysics as the origin of the observed changes in FRET efficiency. Our single-molecule measurements revealed at least three subpopulations in the reconstituted and immobilized nucleosome sample: 90% of the fluorophores represented dissociated nucleosomes or donor only species, 10% represented intact nucleosomes. Of these, 97% remained stable on time-scales ranging from 10 ms to 10s of seconds, while 3% showed intervals with reduced FRET efficiency and a lifetime of 120 ms clearly distinct from blinking. Why most nucleosomes dissociate upon immobilization to the cover slip remains unknown. Immobilization of the molecules is necessary for extension of the available observation time. The time limit is given by photobleaching, one of the key advantages of this method with respect to, for example, Fluorescence Correlation Spectroscopy. However, the close proximity to the surface provides ample opportunity for interactions with it. Surface induced nucleosome dissociation has been reported before in Atomic Force Microscopy (AFM) studies. Using AFM in liquid, Nikova *et al.* observed an unwrapping of ~25 nm of DNA from nucleosomes absorbed to a mica surface [26]. This unwrapping was attributed to a depletion of H2A-H2B histone dimers

induced by the high surface charge of the mica, resulting in unwrapping of DNA. Although PEGs are neutral polymers that are commonly used to reduce non-specific surface binding of proteins, they may affect nucleosomes in different ways: PEG molecules have been reported to interact strongly with unfolded proteins [21], and could therefore possibly interact with histone tails. Furthermore, histone proteins are known to be adhesive to glass or plastic [27]. The large fraction of dissociated nucleosomes we report here was not observed by Tomschik *et al.* [10]. Because of the internal position of the labels they used, at least 50 bp of DNA had to be detached from the histone core before FRET was completely lost. We labeled the DNA at the very end of the histone bound part, and accordingly a detachment of 10-20 bp of DNA would already result in complete loss of FRET. Furthermore, the exterior part of the DNA is largely constrained by the mobile H2A-H2B dimer, whereas the labeled part of the DNA in the nucleosomes used by Tomschik *et al.* is mostly constrained by the more stable H3-H4 tetramer. A labeling strategy by Li *et al.* [8, 9], who end-labeled a 601 nucleosome positioning element together with either histone H3 or H2A, provides a more comparable construct. Based on stopped-flow FRET and FCCS experiments they deduced an unwrapping rate of 4 s^{-1} and an unwrapping lifetime of 10-50 ms. The 3% of our traces that showed dynamics typically featured multiple unwrapping events before photobleaching. Though photobleaching obstructs quantification of the unwrapping rate, it is of the same order of magnitude as observed by Li *et al.* The lifetime of the unwrapped state we observed is 5 to 10 times larger. This discrepancy may in part be explained by differences in experimental conditions and nucleosome constructs; we can however not exclude the possibility that we overlook short-lived unwrapped states, biasing our data to a longer lifetime. The absence of observations of DNA unwrapping in the majority of the intact nucleosomes reported in this study is in strong contrast with the extent of DNA breathing dynamics found by Li *et al.* [8, 9]. Two possible explanations could account for this difference: 1) The most frequently occurring DNA unwrapping occurs at a rate that exceeds the time resolution of our experiment. The rare dynamics (3%) that we observe would reflect the release of multiple histone-DNA contacts, a process that would occur less often and on longer time scales than unwrapping of only the first DNA-octamer. However, unwrapping of 10-20 bp of DNA would induce a more dramatic reduction in FRET efficiency than the reduction we observed, which is consistent with unwrapping of 10 bp or less. 2) The immobilized nucleosomes did not undergo breathing dynamics. It should be kept in mind that because of the disruption of 90% of the nucleosome upon immobilization, we only probed a subset of nucleosomes that do not dissociate upon immobilization. These nucleosomes could either be resistant to unwrapping of the DNA, or immobilized in such a way that DNA dynamics are inhibited due to interactions with the surface, while still retaining proper folding. In either case, immobilization is expected to have major impact on nucleosome dynamics, emphasizing the need for a more inert immobilization than point attachment to a PEG coated surface. Our

findings demonstrate that experimental conditions can have a profound impact on the data obtained when probing nucleosome structure and conformational dynamics. Immobilization effects and blinking dynamics have to be accounted for, and where possible suppressed in order to extract biologically relevant data from spFRET experiments. We have shown that DNA breathing kinetics obtained from carefully optimized spFRET experiments approaches values obtained from bulk experiments, opening the way to more complex single-molecule studies of chromatin dynamics.

Acknowledgements

We would like to thank Jon Widom for providing a plasmid containing the 601 sequence; Jesper Donsmark, John van Egmond and Ineke de Boer for technical assistance, and Paige Shaklee for help with the manuscript. AB, CL, and JvN acknowledge support from the EuroDYNA eurocores program. This work is part of the research programme of the 'Stichting voor Fundamenteel Onderzoek der Materie (FOM)', which is financially supported by the 'Nederlandse Organisatie voor Wetenschappelijk Onderzoek (NWO)'.

Bibliography

[1] Förster, T. Delocalized excitation and excitation transfer. In Modern Quantum Chemistry, Sinanoglu, O., editor, 93–137. Academic Press, New York (1965).

[2] Ha, T. Single-molecule fluorescence resonance energy transfer. *Methods* **25**, 78–86 (2001).

[3] Ha, T., Rasnik, I., Cheng, W., Babcock, H., Gauss, G., Lohman, T., and Chu, S. Initiation and re-initiation of DNA unwinding by the Escherichia coli Rep helicase. *Nature* **419**, 638–641 (2002).

[4] Rasnik, I., Myong, S., Cheng, W., Lohman, T., and Ha, T. DNA-binding orientation and domain conformation of the E-coli Rep helicase monomer bound to a partial duplex junction: Single-molecule studies of fluorescently labeled enzymes. *J. Mol. Biol.* **336**, 395–408 (2004).

[5] Luger, K., Mader, A., Richmond, R., Sargent, D., and Richmond, T. Crystal structure of the nucleosome core particle at 2.8 Å resolution. *Nature* **389**, 251–260 (1997).

[6] Saha, A., Wittmeyer, J., and Cairns, B. Chromatin remodelling: the industrial revolution of DNA around histones. *Nat. Rev. Mol. Cell Biol.* **7**, 437–447 (2006).

[7] Polach, K. and Widom, J. Mechanism of Protein Access to Specific DNA-Sequences in Chromatin - A Dynamic Equilibrium-Model for Gene-Regulation. *J. Mol. Biol.* **254**, 130–149 (1995).

[8] Li, G. and Widom, J. Nucleosomes facilitate their own invasion. *Nat. Struct. Mol. Biol.* **11**, 763–769 (2004).

[9] Li, G., Levitus, M., Bustamante, C., and Widom, J. Rapid spontaneous accesibility of nucleosomal DNA. *Nat. Struct. Mol. Biol.* **12**, 46–53 (2005).

[10] Tomschik, M., Zheng, H., van Holde, K., Zlatanova, J., and Leuba, S. Fast, long-range, reversible conformational fluctuations in nucleosomes revealed by single-pair fluorescence resonance energy transfer. *Proc. Natl. Acad. Sci. U.S.A.* **102**, 3278–3283 (2005).

[11] Lowary, P. and Widom, J. New DNA sequence rules for high affinity binding to histone octamer and sequence-directed nucleosome positioning. *J. Mol. Biol.* **276**, 19–42 (1998).

[12] Davey, C., Sargent, D., Luger, K., Maeder, A., and Richmond, T. Solvent mediated interactions in the structure of the nucleosome core particle at 1.9 Å resolution. *J. Mol. Biol.* **319**, 1097–1113 (2002).

[13] Clegg, R. Fluorescence resonance energy-transfer and nucleic-acids. *Methods Enzymol.* **211**, 353–388 (1992).

[14] Thompson, N., Pearce, K., and Hsieh, H. Total Internal-Reflection Fluorescence Microscopy - Application to Substrate-Supported Planar Membranes. *Eur. Biophys. J.* **22**, 367–378 (1993).

[15] Cognet, L., Harms, G., Blab, G., Lommerse, P., and Schmidt, T. Simultaneous dual-color and dual-polarization imaging of single molecules. *Appl. Phys. Lett.* **77**, 4052–4054 (2000).

[16] Yager, T., Mcmurray, C., and Vanholde, K. Salt-Induced Release of DNA from Nucleosome Core Particles. *Biochemistry* **28**, 2271–2281 (1989).

[17] Claudet, C., Angelov, D., Bouvet, P., Dimitrov, S., and Bednar, J. Histone octamer instability under single molecule experiment conditions. *J. Biol. Chem.* **280**, 19958–19965 (2005).

[18] Godde, J. and Wolffe, A. Disruption of Reconstituted Nucleosomes - the Effect of Particle Concentration, $MgCl_2$ and KCl Concentration, the Histone Tails, and Temperature. *J. Biol. Chem.* **270**, 27399–27402 (1995).

[19] Thåström, A., Gottesfeld, J., Luger, K., and Widom, J. Histone - DNA binding free energy cannot be measured in dilution-driven dissociation experiments. *Biochemistry* **43**, 736–741 (2004).

[20] Eickbush, T. and Moudrianakis, E. Histone core complex - octamer assembled by 2 sets of protein-protein interactions. *Biochemistry* **17**, 4955–4964 (1978).

[21] Rasnik, I., Mckinney, S., and Ha, T. Surfaces and orientations: Much to FRET about? *Acc. Chem. Res.* **38**, 542–548 (2005).

[22] Sabanayagam, C., Eid, J., and Meller, A. Long time scale blinking kinetics of cyanine fluorophores conjugated to DNA and its effect on Förster resonance energy transfer. *J. Chem. Phys.* **123**, – (2005).

[23] Roper Scientific. On-chip multiplication gain. Technical report, Tucson, AZ, (2003).

[24] Eggeling, C., Widengren, J., Brand, L., Schaffer, J., Felekyan, S., and Seidel, C. Analysis of photobleaching in single-molecule multicolor excitation and forster resonance energy transfer measurement. *J. Phys. Chem. A* **110**, 2979–2995 (2006).

[25] Rasnik, I., Mckinney, S., and Ha, T. Nonblinking and longlasting single-molecule fluorescence imaging. *Nat. Methods* **3**, 891–893 (2006).

[26] Nikova, D., Pope, L., Bennink, M., van Leijenhorst-Groener, K., van der Werf, K., and Greve, J. Unexpected binding motifs for subnucleosomal particles revealed by atomic force microscopy. *Biophys. J.* **87**, 4135–4145 (2004).

[27] Lusser, A. and Kadonaga, J. Strategies for the reconstitution of chromatin. *Nat. Methods* **1**, 19–26 (2004).

Chapter 4

Nucleosome Immobilization Strategies for Single-Pair FRET Microscopy[1]

Abstract All genomic transactions in eukaryotes take place in the context of the nucleosome, the basic unit of chromatin, which is responsible for DNA compaction. Overcoming the steric hindrance that nucleosomes present for DNA-processing enzymes requires significant conformational changes. The dynamics of these have been hard to resolve. Single-pair Fluorescence Resonance Energy Transfer (spFRET) microscopy is a powerful technique for observing conformational dynamics of the nucleosome. Nucleosome immobilization allows the extension of observation times to a limit set only by photobleaching, and thus opens the possibility of studying processes occurring on timescales ranging from milliseconds to minutes. It is crucial however, that immobilization itself does not introduce artifacts in the dynamics. Here we report on various nucleosome immobilization strategies, such as single point attachment to polyethylene glycol (PEG) or bovine serum albumin (BSA) coated surfaces, and confinement in porous agarose or polyacrylamide gels. We compared the immobilization specificity and structural integrity of immobilized nucleosomes. A crosslinked star polyethylene glycol coating performed best with respect to tethering specificity and nucleosome integrity, and enabled us for the first time to reproduce bulk nucleosome unwrapping kinetics in single nucleosomes without immobilization artifacts.

[1]This chapter is based on: W. J. A. Koopmans, T. Schmidt, and J. van Noort, Nucleosome Immobilization Strategies for Single-Pair FRET Microscopy. *ChemPhysChem* **9**, 2002-2008 (2008)

4.1 Introduction

Nucleosomes form the basic unit of DNA organization in eukaryotic nuclei. A nucleosome core particle comprises 147 base pairs (bp) of DNA wrapped 1.7 turns around a histone octamer protein core [1]. This tight compaction makes most of the nucleosomal DNA inaccessible to proteins involved in processes such as transcription, replication, and repair. However, several pathways that provide accessibility to nucleosomal DNA [2] have been identified, including transient DNA unwrapping [3], thermal and ATP-driven enzymatic nucleosome repositioning [4], and histone exchange [5]. These processes occur on various time scales, ranging from milliseconds for DNA unwrapping to minutes or hours for thermal nucleosome repositioning. Single-pair Fluorescence (or Förster) Resonance Energy Transfer [6] (spFRET) microscopy has the potential to reveal these mechanisms in individual nucleosomes with unprecedented detail, since it is sensitive to conformational changes of 2-10 nm. In recent spFRET experiments on nucleosomes, energy transfer was detected from short bursts of fluorescence as single nucleosomes diffused through a small confocal detection volume [7–9]. Since the average diffusion time was on the order of 1 ms, it was not possible to resolve slow (>10 ms) conformational dynamics with this approach, limiting the applications to only a small subset of the anticipated conformational changes. Sample immobilization can provide the extended observation time needed for directly observing slow dynamics as demonstrated by two spFRET studies on nucleosomes tethered to a surface. Tomschik *et al.* placed a FRET pair far inside the nucleosome, thereby targeting major disruptions of nucleosomal structure [10]. However, reevaluation of their data led to the conclusion that the observed FRET dynamics was dominated by photoblinking of the dyes [11]. In a slightly different approach, we performed spFRET microscopy, under conditions that suppressed blinking, on immobilized mononucleosomes that were labeled at the dyad axis and the nucleosome exit [12]. We observed DNA unwrapping dynamics in only 3% of the nucleosomes. We found however that the vast majority of nucleosomes was disrupted, resulting in an absence of FRET. Furthermore, the observed kinetics were much slower than anticipated based on bulk experiments by Li *et al.* [13] From these effects we concluded that both nucleosome structure and DNA breathing dynamics were influenced by immobilization of nucleosomes to the surface. In this study we explore a number of immobilization strategies that were successful in other single-molecule assays for their ability to reduce surface artifacts. The physical properties of nucleosomes require a tailored solution to provide an inert local environment. The high level of bending of the nucleosomal DNA effectively renders the nucleosome to be a loaded spring [14]. Nucleosomes rapidly dissociate to form sub-stoichiometric DNA-histone complexes [15, 16] at the 10-100 pM concentrations needed for single-molecule detection. Furthermore, the pronounced charge distribution on the nucleosome surface, with negatively charged DNA bound to positively charged

histones, makes the nucleosome a highly salt-sensitive structure [17]. Finally, histone proteins are known to stick to many types of glass and plastic surfaces [18]. Thus, nucleosomes provide a magnificent challenge to be immobilized such, that they don't interact non-specifically with the surface, and that they retain their canonical structure. In single-molecule fluorescence microscopy several immobilization schemes have been employed successfully (reviewed by Rasnik [19]), such as specific tethering to BSA-biotin [20] or polyethylene glycol (PEG) [21] coated surfaces, encapsulation in lipid vesicles [22], and immobilization in the aqueous pores of polyacrylamide (PA) [23] or agarose gels [24]. Although each immobilization scheme has its own merits, a universal strategy does not exist: for example, BSA surface coatings were too adhesive for studies involving Rep helicase protein [21] but PEG coated surfaces provided a good alternative. In a different study however, it was shown that RNaseH denatured when immobilized to PEG coated surfaces [25]. Thus, each DNA-protein complex requires a tailored immobilization strategy for single-molecule fluorescence microscopy studies. In order to find an optimal strategy for immobilizing complex multi-subunit DNA-protein assemblies like the nucleosome, we systematically tested several immobilization procedures on fluorescently labeled nucleosomes: immobilization in PA and agarose gels, and specific tethering to BSA-biotin or PEG coated surfaces. We used total internal reflection fluorescence (TIRF) microscopy and alternating excitation [26] (ALEX) to identify donor- and acceptor-only species, and to resolve bleaching and blinking events. Both gel immobilization procedures resulted in unacceptable signal-to-noise ratios (SNR). We subsequently characterized surfaces for their resistance to non-specific binding of nucleosomes, and the effect of the surface on nucleosome structural integrity, as judged by the FRET efficiency of individual nucleosomes. A crosslinked star PEG coating [27] performed best with respect to tethering specificity and nucleosome integrity, and enabled us to reproduce the nucleosome unwrapping kinetics determined by Li *et al.* [13] using bulk fluorescence methods, in single nucleosomes.

4.2 Results and Discussion

Mononucleosomes were prepared on a fluorescently labeled, biotinylated DNA construct as schematically shown in figure 4.1. As determined by absorption measurements, the labeling efficiency of the primer DNA was 70% for the acceptor and 90% for the donor, despite HPLC purification after primer synthesis. Upon reconstitution with stoichiometric amounts of histone proteins, the 601 nucleosome positioning sequence [28] places the donor and acceptor at the nucleosome dyad axis and exit respectively. The average FRET efficiency of the nucleosome sample in solution was 0.3, as determined by bulk fluorescence measurements (figure 4.1.b). In previous single molecule experiments we measured the FRET efficiency of single nucleosomes with dyes at the same locations to be 0.6. Accordingly, taking incomplete labeling

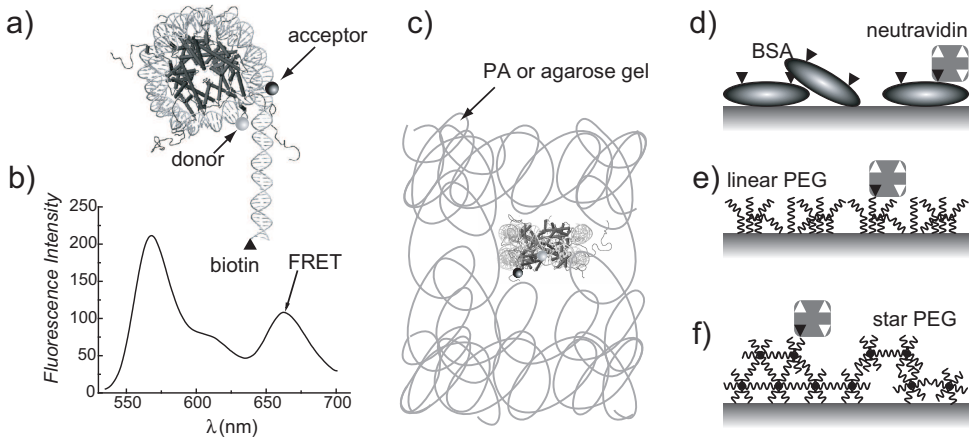

Figure 4.1: Overview of the tested nucleosome immobilization strategies. a) Schematic of the nucleosome construct. The label positions of donor and acceptor are indicated with circles, a biotin modification at the DNA end is indicated with a triangle. b) Bulk fluorescence spectrum of reconstituted nucleosomes. The distinct acceptor emission peak is indicative of reconstituted nucleosomes. c) Gel immobilization, by trapping nucleosomes in the aqueous pores of a polyacrylamide or agarose gel matrix. d)-f) Surface immobilization, by tethering nucleosomes to a glass slide with (d) a BSA-biotin coating, (e) a linear PEG coating, or (f) a crosslinked star PEG coating, through biotin-neutravidin-biotin linkage.

of the primers into account, 33% of the DNA molecules were properly reconstituted into nucleosomes and showed efficient FRET, while another 33% was doubly-labeled free DNA. Thus, when nucleosome integrity is not affected by immobilization we expect a maximum yield of nucleosomes with efficient spFRET of 33%. We tested five nucleosome immobilization strategies, as illustrated in figure 4.1. First, we studied confinement in the aqueous pores of (i) PA gel or (ii) agarose gel matrices (figure 4.1.c). Both agarose and polyacrylamide gel electrophoresis are routinely employed to separate and isolate nucleosomes from free DNA. Since nucleosomes migrate in sharp bands and retain their proper folding in native gel electrophoresis assays, we reasoned that agarose and PA gels are relatively inert to nucleosomes. Alternatively, we studied nucleosome tethered to (iii) BSA-biotin coatings (figure 4.1.d), (iv) linear PEG coatings (figure 4.1.e), and (v) crosslinked star PEG coatings (figure 4.1.f), which all have been successfully employed in single-molecule fluorescence experiments[19].

4.2.1 Immobilization through confinement in gels

Polyacrylamide gels In PA, gel formation occurs due to polymerization and crosslinking reactions between monomers. At the conditions chosen, i.e. 8% PA, the average pore diameter was ~8 nm [29], sufficiently small to immobilize the 11x6 nm sized nucleosomes. Indeed, we

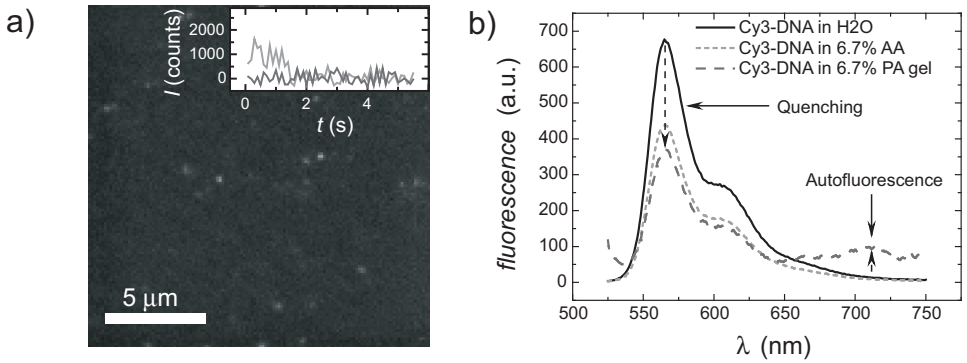

Figure 4.2: Immobilization in PA gels. a) Fluorescence image of 100 pM Cy3-ATTO647N labeled nucleosomes in an 8% PA gel. The fluorescence intensity was reproducibly low, and often either donor or acceptor was already bleached (inset). b) Bulk fluorescence emission spectrum of Cy3-labeled DNA in water, in a 6.7% acrylamide solution, and in a 6.7% PA gel. Fluorescence emission was quenched in acrylamide gels, and autofluorescence was observed at ~700 nm.

observed many immobilized fluorophores, as depicted in figure 4.2.a. We found however that only a small fraction of the molecules was doubly labeled when immobilized in PA. Most of the fluorescence originated from donor-only (45%) or acceptor-only (25%) species, as deduced by alternating excitation (ALEX). Therefore 40% of the donor and 40% of the acceptor were absent in the gel, probably due to bleaching by free radicals that catalyze the polymerization process. Next to the degradation of the dyes, the observed signal intensity from a single fluorophore was low ($0.9 \pm 0.4 \cdot 10^3$ counts), as compared to the background noise of $0.2 \cdot 10^3$ counts, leading to signal-to-noise ratio (SNR) of 2 and signal-to-background ratio (SNB) of 5. In comparison, at similar excitation intensity (0.75 kW/cm^2) and illumination time (40 ms), the intensity of either donor or acceptor from individual nucleosomes immobilized to a coated surface was $2.2 \pm 0.3 \cdot 10^3$ counts, resulting in a SNR and SNB of 8 and 11, respectively. The reason for the low SNR and SNB in single-molecule experiments was inferred from bulk fluorescence experiments on Cy3-labeled DNA oligomers immobilized in 6.7% PA (figure 4.2.b). We found a 30% decrease of fluorescence intensity for Cy3 in 6.7% acrylamide (AA), which is a known fluorescence quencher [30]. Upon polymerization into PA, the fluorescence intensity dropped an additional 20%. Furthermore a broad band of autofluorescence around 700 nm emerged. This autofluorescence was also observed in gels without immobilized fluorophores, and should therefore be attributed to the PA gel itself. In conclusion, we observed an increase in donor-only and acceptor-only species, a decrease in fluorescence intensity and a low SNR and SNB due to a combination of bleaching by free radicals, quenching by unpolymerized AA

and background autofluorescence from the PA gel. How does this compare to previous studies using the same methodology? We did not obtain a high SNR as obtained by Dickson *et al.* for Nile red in a 18% PA gel [23] or GFP in a 15% PA gel [31]. However, nile red probably showed an acceptable SNR because of its high quantum yield (0.7), in combination with the high excitation intensity (5 kW/cm^2) and long exposure time (100 ms) used by Dickson *et al.* Due to rapid photobleaching under these illumination conditions, the observation time was limited to ~10 data points however. In the case of GFP, bleaching by free radicals or quenching by unpolymerized AA is unlikely to occur, because the fluorophore is protected by a protein barrel. In summary, nucleosome immobilization in PA gels is not productive because of the low SNR and the loss of doubly labeled molecules.

Agarose Gels Alternatively, we immobilized nucleosomes in 3% agarose gels [24]. Unlike polymer gels like PA, where gel formation occurs by chemical polymerization and crosslinking reactions between monomers, agarose forms a physical gel upon cooling below the gelling temperature (~35 °C for low melting agarose). Furthermore, agarose is not known to quench fluorescence. Using epifluorescence we imaged number of immobilized nucleosomes in the agarose gel. The SNR (~3) and SNB (~4) were poor however compared to TIRF imaging, and did not improve with longer exposure times. We attribute this to out-of-focus fluorescence emission from nucleosomes in the agarose gel, and from the buffer layer, where freely diffusing nucleosomes accumulated. Using TIRF, we observed that the agarose gel did not adhere to the cover slide, resulting in a 1-2 µm layer of buffer between the glass and the agarose gel. Nucleosomes could freely diffuse in this layer. This gap was always present, even when we prepared the agarose film using spincoating, or with thin intermediate coatings such as methylcellulose, poly-D-lysine, or sigmacote (Sigma). TIRF imaging of immobilized nucleosomes in the gel was therefore not possible, since the evanescent excitation field only extended a few 100 nm into the buffer. On top of the accumulation of free nucleosomes between the gel and the surface we did not achieve sufficient protein immobilization in agarose gels to allow for extended imaging times using epifluorescence, unlike Lu *et al.* [24]. Immobilization by confinement alone however is unlikely in a 1% gel with an average pore diameter of ~140 nm, as noticed by Gai et al, who also reported a buffer layer between the gel and the cover slide [32]. Kelbauskas *et al.* confirmed, using FCS, that nucleosomes embedded in a 3% agarose gel show reduced diffusion only by a factor of 10-100 slower [9]. In conclusion, for various reasons gel immobilization did not work for studying long term dynamics of nucleosomes, and alternative immobilization strategies, such as immobilization to a surface, are needed.

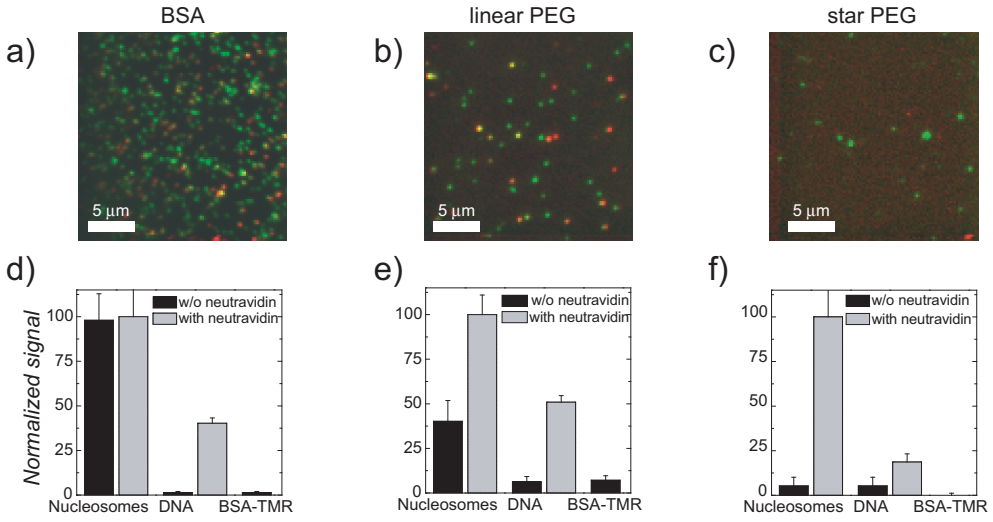

Figure 4.3: Nucleosome binding specificity. Fluorescence image of 100 pM Cy3-ATTO647N labeled nucleosomes bound non-specifically to BSA (a), linear PEG (b), or star PEG (c) coated cover slides, when neutravidin incubation was omitted. Non-specific binding was quantified through a comparison with the amount of fluorescent spots when the same concentration of nucleosomes was bound to BSA (d), linear PEG (e), or star PEG (f) coated slides after incubation with neutravidin. Non-specific binding of 100 pM Cy3-ATTO647N labeled DNA or 100 pM BSA-TMR was negligible on all surface coatings.

4.2.2 Surface immobilization: binding specificity

We immobilized biotinylated nucleosomes to BSA, linear PEG, or star PEG treated glass cover slides through biotin-neutravidin-biotin attachment. We exposed these surfaces to 100 pM fluorescently labeled nucleosomes, and imaged the fluorescence. The specificity of immobilization was tested by quantification of non-specific adhesion of nucleosomes to surfaces prepared without neutravidin. The resulting single- molecule fluorescence images are shown in figure 4.3.a-c. The large number of fluorescent spots shows that nucleosomes readily adhere to BSA-coated glass (figure 4.3.a). The linear PEG coating prevented non-specific adsorption to some extent (figure 4.3.b). Star PEG coatings however were superior, and showed negligible nucleosome binding when the neutravidin incubation was omitted (figure 4.3.c). We quantified the amount of non-specific adhesion by counting the number of fluorescent spots in each image (figure 4.3.d-f), and normalized this to the amount of binding observed on surfaces which were incubated with neutravidin. For BSA we found no significant difference between neutravidin treated and untreated surfaces. For linear PEG coatings we found that ~40% of the molecules were immobilized non-specifically, while for star PEG coatings this was less than 10%. We repeated these experiments for neutravidin treated surfaces with non-biotinylated nucleosomes, to test whether nucleosomes interacted non-specifically with the neutravidin. The same trend was observed: nucleosomes showed significant binding to the BSA (~1 /μm²), limited binding to the linear PEG (~0.2 /μm²), and negligible binding to the star PEG (~0.03 /μm²) coated glass. Therefore, non-specific binding should be attributed to the surface rather than to the neutravidin. To resolve nucleosome-specific properties of these surface coatings and to relate these previous reports [19] we tested them for preventing DNA and BSA adsorption (figure 4.3.d-f). Non-specific binding of the DNA construct alone was negligible on all surfaces. None of the surface coatings showed any fluorescence when exposed to fluorescently labeled BSA. Thus, though all tested surfaces prevented non-specific interactions with DNA and BSA-protein, only star PEG coatings provided sufficient resistance to nucleosome adsorption. Since no DNA binding was observed, nucleosome adhesion to bare glass, BSA coatings, and PEG coatings must be mediated through the histone proteins in the octamer core. BSA coatings did not prevent nucleosome adsorption at all: the number of fluorescent spots was comparable to that of nucleosomes on bare glass. It is known that physisorbed BSA coatings are inhomogeneous [25]. It is therefore possible that parts of the glass surface were still exposed, resulting in nucleosome adsorption. BSA itself is negatively charged and could interact with the positively charged histone proteins as well. Interactions with DNA are effectively screened though, presumably through electrostatic repulsion. An excess of BSA was always present in the buffer, which explains why all non-specific interactions with labeled BSA-TMR were blocked. The linear PEG coating showed a strong reduction in non-specific interactions with nucleosomes. The covalently attached PEGs form a ~1 nm thick polymer brush that prevents protein adsorption

to the glass surface. Indeed, fluorescently labeled DNA, BSA and streptavidin (data not shown) did not bind non-specifically to the PEG surface. However, 40% of the nucleosomes were attached non-specifically, pointing at interactions between the histones and the PEG polymers. Although PEG surfaces are inert for many protein interactions, they have been reported to interact strongly with unfolded proteins [19]. The unstructured histone tails that protrude from the nucleosome core are likely to mediate similar interactions. Furthermore, nucleosomes can undergo large conformational fluctuations under the chosen conditions (H2A-H2B dimer exchange, DNA unwrapping), which may transiently expose the histone proteins. This could facilitate hydrophobic interactions between the PEG chain ends and the histone proteins, resulting in persistent non-specific adsorption [25]. Star PEG coatings however showed almost no non-specific binding of nucleosomes. This exceptional blocking of protein adsorption has been demonstrated before with a number of small proteins [27, 33]. Crosslinking of the PEG extremes results in a higher grafting density of the PEG chains, which blocks the underlying glass surface to a greater extent than linear PEG coatings. Furthermore, crosslinking results in an increased layer thickness and a lower density of PEG chain ends, which may result in a more inert surface coating. In summary, the nucleosome binding specificity was poor on BSA, fair on the linear PEG, but excellent on the star PEG coated surfaces.

4.2.3 Surface immobilization: nucleosome integrity

In order to study intrinsic nucleosome conformational fluctuations, it is necessary that nucleosomes maintain their structural integrity when bound to the surface. With the nucleosome labeling strategy described, we could perform spFRET experiments to test whether nucleosomes remained properly folded upon surface immobilization. With the acceptor positioned at the exit point in the nucleosome any conformational change of the nucleosome, be it DNA unwrapping, dimer dissociation or more rigorous mechanisms, will result in a loss of FRET. We used ALEX [26] to distinguish donor- and acceptor-only species from doubly labeled species. For each molecule on the surface we calculated the FRET efficiency E

$$E = \frac{I_A^{514}}{I_A^{514} + I_D^{514}}, \tag{4.1}$$

and the label stoichiometry S

$$S = \frac{I_A^{514} + I_D^{514}}{I_A^{514} + I_D^{514} + I_A^{636}}, \tag{4.2}$$

where I_D^{514} is the donor intensity when excited at 514 nm, and where I_A^{514} and $I_A^{636}$are the acceptor intensities when excited at 514 nm and 636 nm respectively. Properly folded nucleosomes labeled with both donor and acceptor can be identified by having both high E is high

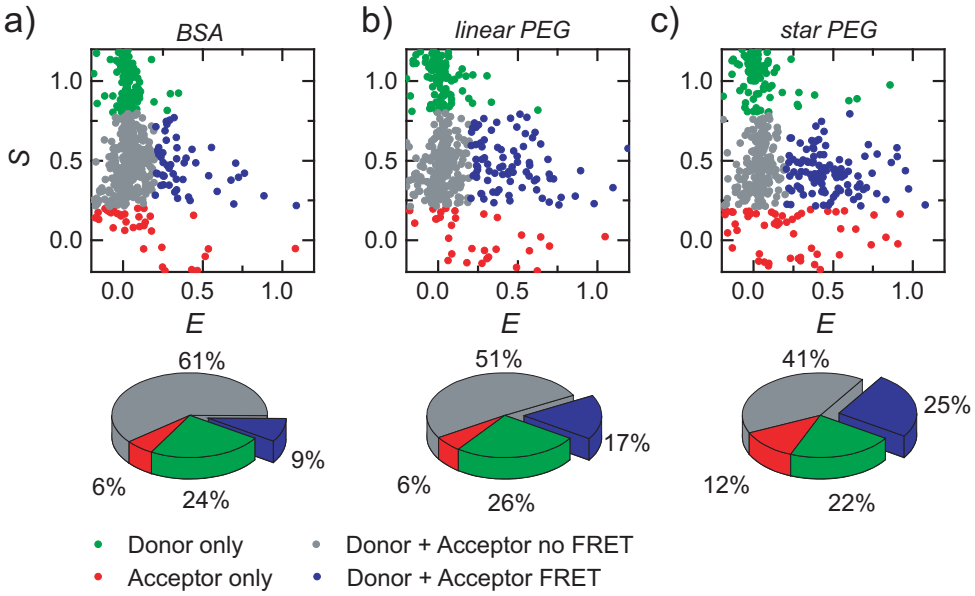

Figure 4.4: Nucleosome structural integrity. 2D scatter plots of the label stoichiometry S versus the FRET efficiency E for nucleosomes bound to BSA (a), linear PEG (b) and star PEG (c) coated cover slides. Each data point represents the average E and S value for a trace until either donor or acceptor bleached. We identified donor-only (S = 1), acceptor-only (S=0) and doubly labeled species (S ~ 0.5). A fraction of the doubly labeled species showed FRET (E > 0.2). This fraction was used as an indicator of nucleosome structural integrity on each surface coating. The relative size of all fractions are summarized in pie-charts (bottom panels)

and S approaching 0.5, assuming comparable quantum yields, absorption cross sections and detector efficiencies for donor and acceptor. The resulting scatter plots of S vs. E for the entire population of nucleosomes are shown in figure 4.4. Each point represents the time averaged E and S value of a fluorescent spot up to either donor or acceptor bleached. We classified fluorescent spots into four categories: canonical nucleosomes with both labels present and showing FRET ($0.2<E<1.2$ and $0.2<S<0.8$); unfolded nucleosomes and bare DNA with both labels present but not showing FRET ($E<0.2$ and $0.2<S<0.8$); donor-only species ($0.8<S$); and acceptor only species ($S<0.2$). The thresholds between the different categories were based on separate measurements (data not shown) of single molecule fluorescence intensity time traces from doubly labeled bare DNA that did not show FRET: from traces where the acceptor bleached first we deduced that $S>0.8$ for donor-only species; from traces where the donor bleached first we deduced that $S<0.2$ for acceptor-only species; from traces before bleaching of either fluorophore, we deduced that $E<0.2$ for bare DNA, since background fluorescence, direct excitation of the acceptor, and crosstalk of donor emission into the acceptor channel never resulted in apparent FRET efficiencies above 0.2 for doubly labeled, bare DNA. On all surfaces the donor-only and acceptor-only populations amounted to ~25% and ~10% respectively, which agreed well with the stoichiometry deduced from bulk absorption measurements on the DNA construct. The population of properly folded nucleosomes, with both labels showing FRET, was 9% for the BSA surface (a), 17% for the linear PEG surface (b) and 25% for the star PEG surface (c), while the population showing no FRET was 61%, 51% and 41% respectively. From the bulk measurements, we estimated that 32% of the molecules were doubly labeled and properly folded. Thus all surfaces featured a destabilization of nucleosomes by the surface. The star PEG surface prevented disassembly of the nucleosomes better than BSA or linear PEG, with 78% of the initial nucleosomes intact. It is known that nucleosomes can be destabilized at low concentrations, presumably due to disassembly of the histone octamer core [15, 16, 34]. This might explain the observed loss in FRET, since the experiments were carried out a low (100 pM) nucleosome concentration in order to get a low enough density of fluorescent spots to resolve individual nucleosomes. However, when the labeled nucleosomes were mixed in a buffer containing 10 nM unlabeled nucleosomes, we found a similar loss in FRET. Consistent with this, we found pronounced differences in nucleosome integrity on the different surface coatings. Thus, surface immobilization, rather than dilution, caused the observed nucleosome disassembly. The linear PEG surface performed better than the BSA coating, but still induced nucleosome destabilization. Conformational changes upon binding to a linear PEG coated surface have been observed before: Heyes *et al.* observed a denaturing of RNaseH when immobilized to a PEG 5000 surface [25]. They attributed this to the flexible PEG chains interacting with the hydrophobic interior of the protein, and/or interactions with the underlying amino functionalized surface. In the case of nucleosomes, these mechanisms

could play a role as well, as demonstrated by the correlation between non-specific adhesion, and a loss of nucleosome integrity. Compared to our previous work [12] using linear PEGs, using star PEGs increased the yield of intact nucleosomes by a factor of 5. The results of our comparison of various nucleosome immobilization strategies are summarized in Table 4.1 on page 62. Since star PEG coatings showed little non-specific binding of nucleosomes and allowed the majority of the nucleosomes to retain their structural integrity, this should put us in a good position to measure nucleosome dynamics without interference of the surface.

Table 4.1: Comparison of various nucleosome immobilization strategies.

Strategy	Immobilization (observation time (s))	SNR	Specificity	Integrity
PA Gel	~1	2	-	-
Agarose Gel	~0.1	3	-	-
BSA-biotin	>10[a]	8	2%	28%
Linear PEG	>10[a]	8	60%	53%
Star PEG	>10[a]	8	90%	78%

[a] limited by photobleaching

4.2.4 Nucleosome breathing dynamics

Spontaneous unwrapping of nucleosomal DNA was previously reported by Li *et al.* [13], who performed FRET based stopped-flow, protein association, and fluorescence correlation spectroscopy experiments on nucleosomes labeled at the histone octamer surface and the DNA exit, probing similar DNA mechanics as in our constructs. From these combined experiments with nucleosomes in solution, on and off times of 250 ms and 10-50 ms respectively could be deduced. Our spFRET experiments allow for direct observation of such DNA breathing in individual nucleosomes, but up to now we could not reproduce the kinetics [12]. To capture all breathing dynamics we performed fast spFRET microscopy (10 ms time resolution) and analyzed the fluorescence intensity traces of nucleosomes immobilized to star PEG coated surfaces. From the traces that showed FRET (25% of the total number of spots), we rejected the traces which had a low SNR (20%), showed photoblinking (5%), uncorrelated intensity changes (10%), or traces with crosstalk from a neighboring FRET pair (8%). In this filtered dataset, we can exclude photoblinking and attributed all FRET dynamics to nucleosome breathing (figure 4.5.a). The FRET efficiency fluctuated reversibly between a high FRET state (E=0.55), originating from a fully wrapped nucleosome, and a distinct low FRET state (E=0.2) originating from an unwrapped state of the nucleosome. A photon and instrument noise analysis [12] enabled us to discriminate between noise and opening events. The lifetime of the closed state was 280 ms, and the lifetime of the open state was 25 ms (figure 4.5.b). These lifetimes are ap-

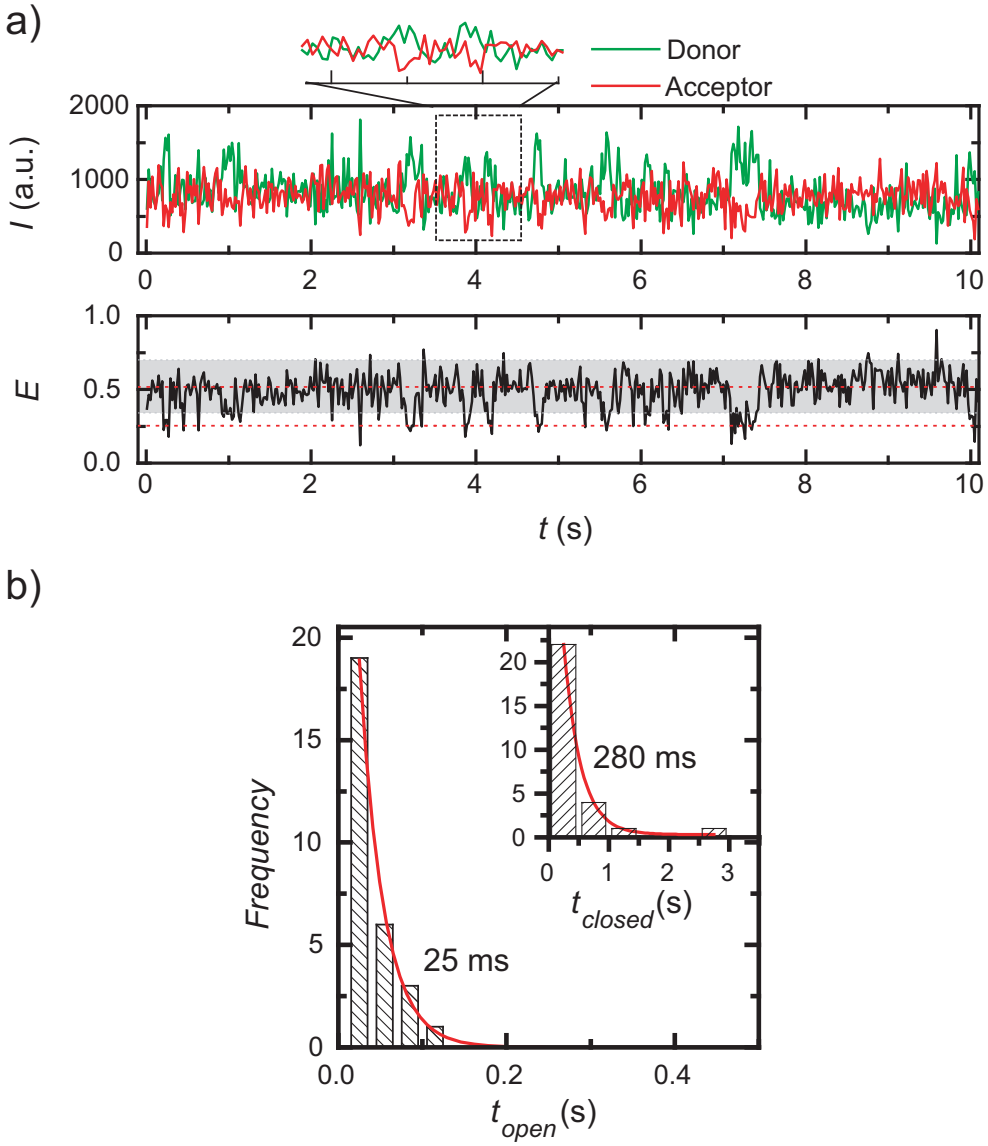

Figure 4.5: Dynamics of nucleosomes immobilized to a star PEG coated surface. a) Fluorescence intensity time trace (top) and corresponding FRET efficiency time trace (bottom). The FRET efficiency fluctuated between a high and a low FRET state, corresponding to a closed and an open nucleosome conformation, respectively. The grey bar indicates a 96% confidence interval for the theoretical photon and instrument noise. b) Histograms of the lifetime of the open and closed (inset) state. The solid lines are exponential fits to the data, yielding lifetimes of 25 ms for the open state and of 280 ms for the closed state.

proximately 5 times faster than the dynamics we observed on linear PEG coated surface (1.5 s closed state, 120 ms open state) but agree perfectly with the nucleosome breathing kinetics of nucleosomes in solution [13]. Thus, nucleosomes can be specifically immobilized on star PEG coatings, while maintaining their structural integrity and their dynamic nature.

4.3 Conclusion

We tested various immobilization strategies for time resolved spFRET microscopy on nucleosomes. Imaging nucleosomes immobilized in polyacrylamide gels was not possible, because of fluorescence quenching, fluorophore bleaching, and autofluorescence. Agarose gels showed limited reduction of diffusion and accumulation of free nucleosomes between the gel and the glass slide, demonstrating the limited applicability of gel immobilization. Surface immobilization allows unlimited observation times but requires a surface tailored to the physical properties of nucleosomes. BSA surfaces were too adhesive, and most nucleosomes disassembled upon immobilization. Linear PEG coatings showed less non-specific adsorption than BSA coatings, but still a large fraction of the nucleosomes disassembled upon immobilization. Crosslinked star PEG coatings however prevented non-specific adsorption and reduced nucleosome disassembly significantly. Using this strategy we were able for the first time to follow DNA breathing dynamics in single nucleosomes yielding the same kinetics as observed for nucleosomes in solution. This opens opportunities to reveal the mechanisms of more complex nucleosomal conformational changes in real time and at the single-molecule level using spFRET. For example assessment of the effect of nucleosome-nucleosome interactions, ATP-dependent remodelers and/or posttranslational modifications on nucleosome stability will provide insight in the physical aspects of gene regulation.

4.4 Experimental Section

Preparation of DNA and nucleosomes Mononucleosomes were reconstituted on a fluorescently labeled 177 basepair (bp) DNA template containing a 601 nucleosome positioning sequence as described [12]. Briefly, the template DNA was prepared by PCR and was labeled with biotin, Cy3 (donor) and ATTO647N (acceptor) by incorporation of fluorescently labeled, HPLC purified primers (IBA GmbH). PCR primers were as follows: forward primer 5'-biotin-TTTGAATTCCCAGGGAATTGGGCGGCCGCCCTGGAGAATCCCGGTGCCGAGGCCGC-3' (acceptor labeled nucleotide is underlined). Reverse primer: 5'-ACAGGATGTATATATCTGACACGTGCCTGGAGACTAGGGAGTAATCCCCTTGGCGGTTAAAACGCGGGGGACAGCGCGTACG-3' (donor labeled nucleotide is underlined. In the DNA template donor and acceptor were located 81 bp (24 nm) apart. Nucleosomes were reconstituted by salt

gradient dialysis with recombinant histones. After reconstitution, donor and acceptor were folded at the dyad axis and nucleosome exit respectively, approximately 4 nm apart, resulting in efficient FRET.

Cover slide preparation Glass cover slides (Assistant, Germany) were sonicated in 1% RBS-50 anionic detergent at 90 °C for 15 minutes, rinsed with milliQ water, sonicated for 1 hour in ethanol (96%), rinsed with milliQ water, dried over a flame, and finally cleaned with a UVO UV ozone cleaning device (Jelight, USA). Slides cleaned in this way showed no detectable residual fluorescence.

Confinement in polymer gels Beaded low melting temperature agarose (BMA, Rockland, ME, USA) was suspended in 1X TE at a 3% w/v ratio. The agarose suspension was melted at 90 °C, and cooled down to 50 °C. Nucleosomes (~100 pM final concentration) were added to the melted gel. The mixture was poured on a cover slide and formed a gel upon cooling to room temperature. In an 8% polyacrylamide gel nucleosomes were immobilized following Dickson *et al.* [23]. Nucleosomes were added to a 8% 29:1 acrylamide:bisacrylamide solution in 1X TE (10 mM Tris.HCl pH 8, 1 mM EDTA), to a final concentration of 100 pM. Polymerization was initiated by adding tetramethylenediamine (0.2% final concentration) and ammonium persulfate (0.05% final concentration). The solution was pipetted on a cover slide, and spread evenly on the slide by covering it with a second slide. Polymerization was complete after 5 minutes.

Surface passivation and functionalization:

BSA coatings Cleaned slides were exposed to biotinylated BSA (0.1 mg/ml, Sigma) for 5 minutes, and rinsed with milliQ water.

Linear PEG Cleaned glass slides were amino functionalized with poly-D-lysine (0.01 mg/ml, Sigma), and subsequently incubated for 4 hours with an amine reactive poly ethylene glycol (PEG) mixture: 20% mPEG-succinimidyl propionate (MW 5 kDa, NOF) and 0.2% biotin-PEG-n-hydroxysuccinimide (MW 3.4 kDa, Nektar Therapeutics) in sodium carbonate buffer (0.1 M, pH 8.2).

Star PEG Six arm NCO PEG stars (MW 12 kDa) were dissolved in tetrahydrofuran (THF) at a concentration of 20 mg/ml, and diluted in milliQ water to a concentration of 2 mg/ ml. Biocytin (Sigma) was added to a final concentration of 1 μg/ml. Five minutes after mixing, the solution was filtered through a 0.22 μm syringe filter (MilliQ), onto the amino functionalized cover slide. When the substrate was fully covered, the slide was spincoated for 45 seconds at

2500 rpm. The slides were incubated at room temperature overnight to complete the crosslinking reaction and were stored in the dark for up to 1 week.

Neutravidin incubation Biotinylated slides were incubated with neutravidin (2 µg/ml, Pierce) for 5 minutes, and were rinsed with milliQ water.

Buffers Experiments were performed in a buffer containing Tris (10 mM, pH 8.0), NaCl (50 mM), and NP-40 (0.03%). For non-specific binding and nucleosome integrity experiments, $MgCl_2$ (2 mM), and BSA (0.1 mg/ml) were added. In some experiments we included unlabeled nucleosomes (10 nM) in the buffer. For nucleosome dynamics measurements, an oxygen scavenger system (glucose oxidase (0.2 mg/ml, Sigma), catalase (0.04 mg/ml, Roche), glucose (4% w/v), and Trolox [35](2 mM)) was added to the buffer, to minimize photobleaching and –blinking.

Single-molecule fluorescence microscopy Single-molecule fluorescence experiments were performed on a setup as described before [12]. Briefly, molecules were imaged on a CCD camera (Cascade 512B, Roper Scientific) through a home-built inverted total internal reflection microscope with an oil immersion objective (100X, 1.45 NA, NIKON). Alternating excitation was achieved by switching between 514 nm and 636 nm laser lines through an AOTF (A.A. Opto-Electronic). Donor and acceptor fluorescence were imaged simultaneously on separate areas of the CCD chip using a dichroic mirror wedge [36].

Acknowledgements

We thank Dr. Jürgen Groll (RWTH Aachen) for providing samples of the NCO-star PEG material and support with the coating procedure, Ineke de Boer and John van Egmond for technical assistance, and Prof. Dr. Alexander Brehm (Philipps-Universtät Marburg) for histone octamer preparations. This work is part of the research programme of the 'Stichting voor Fundamenteel Onderzoek der materie (FOM)', which is financially supported by the 'Nederlandse Organisatie voor Wetenschappelijk Onderzoek (NWO)'.

Bibliography

[1] Luger, K., Mader, A., Richmond, R., Sargent, D., and Richmond, T. Crystal structure of the nucleosome core particle at 2.8 Å resolution. *Nature* **389**, 251–260 (1997).

[2] Luger, K. Dynamic nucleosomes. *Chromosome Res.* **14**, 5–16 (2006).

[3] Li, G. and Widom, J. Nucleosomes facilitate their own invasion. *Nat. Struct. Mol. Biol.* **11**, 763–769 (2004).

[4] Flaus, A. and Owen-Hughes, T. Dynamic properties of nucleosomes during thermal and ATP-driven mobilization. *Mol. Cell. Biol.* **23**, 7767–7779 (2003).

[5] Kimura, H. and Cook, P. Kinetics of core histones in living human cells: Little exchange of H3 and H4 and some rapid exchange of H2B. *J. Cell Biol.* **153**, 1341–1353 (2001).

[6] Ha, T. Single-molecule fluorescence resonance energy transfer. *Methods* **25**, 78–86 (2001).

[7] Gansen, A., Hauger, F., Toth, K., and Langowski, J. Single-pair fluorescence resonance energy transfer of nucleosomes in free diffusion: Optimizing stability and resolution of subpopulations. *Anal. Biochem.* **368**, 193–204 (2007).

[8] Kelbauskas, L., Chan, N., Bash, R., Yodh, J., Woodbury, N., and Lohr, D. Sequence-dependent nucleosome structure and stability variations detected by Förster resonance energy transfer. *Biochemistry* **46**, 2239–2248 (2007).

[9] Kelbauskas, L., Chan, N., Bash, R., DeBartolo, P., Sun, J., Woodbury, N., and Lohr, D. Sequence-dependent variations associated with H2A/H2B depletion of nucleosomes. *Biophys. J.* **94**, 147–158 (2008).

[10] Tomschik, M., Zheng, H., van Holde, K., Zlatanova, J., and Leuba, S. Fast, long-range, reversible conformational fluctuations in nucleosomes revealed by single-pair fluorescence resonance energy transfer. *Proc. Natl. Acad. Sci. U.S.A.* **102**, 3278–3283 (2005).

[11] Correction for Tomschik et al. , Fast, long-range, reversible conformational fluctuations in nucleosomes revealed by single-pair fluorescence resonance energy transfer. *Proc. Natl. Acad. Sci. U.S.A.* **105**, 10632–10632 (2008).

[12] Koopmans, W. J. A., Brehm, A., Logie, C., Schmidt, T., and van Noort, J. Single-pair FRET microscopy reveals mononucleosome dynamics. *J. Fluoresc.* **17**, 785–795 (2007).

[13] Li, G., Levitus, M., Bustamante, C., and Widom, J. Rapid spontaneous accesibility of nucleosomal DNA. *Nat. Struct. Mol. Biol.* **12**, 46–53 (2005).

[14] Schiessel, H. The physics of chromatin. *J. Phys.: Condens Matter* **15**, R699–R774 (2003).

[15] Claudet, C., Angelov, D., Bouvet, P., Dimitrov, S., and Bednar, J. Histone octamer instability under single molecule experiment conditions. *J. Biol. Chem.* **280**, 19958–19965 (2005).

[16] Thåström, A., Gottesfeld, J., Luger, K., and Widom, J. Histone - DNA binding free energy cannot be measured in dilution-driven dissociation experiments. *Biochemistry* **43**, 736–741 (2004).

[17] Yager, T., Mcmurray, C., and Vanholde, K. Salt-Induced Release of DNA from Nucleosome Core Particles. *Biochemistry* **28**, 2271–2281 (1989).

[18] Lusser, A. and Kadonaga, J. Strategies for the reconstitution of chromatin. *Nat. Methods* **1**, 19–26 (2004).

[19] Rasnik, I., Mckinney, S., and Ha, T. Surfaces and orientations: Much to FRET about? *Acc. Chem. Res.* **38**, 542–548 (2005).

[20] Zhuang, X., Bartley, L., Babcock, H., Russell, R., Ha, T., Herschlag, D., and Chu, S. A single-molecule study of RNA catalysis and folding. *Science* **288**, 2048–2051 (2000).

[21] Rasnik, I., Myong, S., Cheng, W., Lohman, T., and Ha, T. DNA-binding orientation and domain conformation of the E-coli Rep helicase monomer bound to a partial duplex junction: Single-molecule studies of fluorescently labeled enzymes. *J. Mol. Biol.* **336**, 395–408 (2004).

[22] Boukobza, E., Sonnenfeld, A., and Haran, G. Immobilization in surface-tethered lipid vesicles as a new tool for single biomolecule spectroscopy. *J. Phys. Chem. B* **105**, 12165–12170 (2001).

[23] Dickson, R., Norris, D., Tzeng, Y., and Moerner, W. Three-dimensional imaging of single molecules solvated in pores of poly(acrylamide) gels. *Science* **274**, 966–969 (1996).

[24] Lu, H., Xun, L., and Xie, X. Single-molecule enzymatic dynamics. *Science* **282**, 1877–1882 (1998).

[25] Heyes, C., Kobitski, A., Amirgoulova, E., and Nienhaus, G. Biocompatible surfaces for specific tethering of individual protein molecules. *J. Phys. Chem. B* **108**, 13387–13394 (2004).

[26] Kapanidis, A., Laurence, T., Lee, N., Margeat, E., Kong, X., and Weiss, S. Alternating-laser excitation of single molecules. *Acc. Chem. Res.* **38**, 523–533 (2005).

[27] Amirgoulova, E., Groll, J., Heyes, C., Ameringer, T., Rocker, C., Moller, M., and Nienhaus, G. Biofunctionalized polymer surfaces exhibiting minimal interaction towards immobilized proteins. *ChemPhysChem* **5**, 552–555 (2004).

[28] Lowary, P. and Widom, J. New DNA sequence rules for high affinity binding to histone octamer and sequence-directed nucleosome positioning. *J. Mol. Biol.* **276**, 19–42 (1998).

[29] Chrambach, A. and Rodbard, D. Polyacrylamide gel electrophoresis. *Science* **172**, 440–451 (1971).

[30] Lackowicz, J. *Principles of Fluorescence Spectroscopy*, volume 2nd. Kluwer Academic / Plenum Publishers, New York, (1999).

[31] Dickson, R., Cubitt, A., Tsien, R., and Moerner, W. On/off blinking and switching behaviour of single molecules of green fluorescent protein. *Nature* **388**, 355–358 (1997).

[32] Gai, H., Griess, G., Demeler, B., Weintraub, S., and Serwer, P. Routine fluorescence microscopy of single untethered protein molecules confined to a planar zone. *J. Microsc.* **226**, 256–262 (2007).

[33] Groll, J., Ameringer, T., Spatz, J., and Moeller, M. Ultrathin coatings from isocyanate-terminated star PEG prepolymers: Layer formation and characterization. *Langmuir* **21**, 1991–1999 (2005).

[34] Godde, J. and Wolffe, A. Disruption of Reconstituted Nucleosomes - the Effect of Particle Concentration, $MgCl_2$ and KCl Concentration, the Histone Tails, and Temperature. *J. Biol. Chem.* **270**, 27399–27402 (1995).

[35] Rasnik, I., Mckinney, S., and Ha, T. Nonblinking and longlasting single-molecule fluorescence imaging. *Nat. Methods* **3**, 891–893 (2006).

[36] Cognet, L., Harms, G., Blab, G., Lommerse, P., and Schmidt, T. Simultaneous dual-color and dual-polarization imaging of single molecules. *Appl. Phys. Lett.* **77**, 4052–4054 (2000).

Chapter 5

spFRET using ALEX and FCS reveals Progressive DNA Unwrapping in Nucleosomes[1]

Abstract Accessibility to DNA wrapped in nucleosomes is essential for nuclear processes such as DNA transcription. Large conformational changes in nucleosome structure are required to facilitate protein binding to target sites within nucleosomal DNA. Transient unwrapping of DNA from nucleosome ends can provide an intrinsic exposure of wrapped DNA, allowing proteins to bind DNA that would otherwise be occluded in the nucleosome. The molecular details underlying these mechanisms remain to be resolved. Here we show how DNA unwrapping occurs progressively from both nucleosome ends. We performed single-pair Fluorescence Resonance Energy Transfer (spFRET) spectroscopy with Alternating Laser Excitation (ALEX) on nucleosomes either in free solution or confined in a gel after PAGE separation. We combined ALEX-spFRET with a correlation analysis on selected bursts of fluorescence, to resolve a variety of unwrapped nucleosome conformations. The experiments reveal that nucleosomes are unwrapped with an equilibrium constant of $\sim 0.2 - 0.6$ at nucleosome ends and ~ 0.1 at a location 27 basepairs inside the nucleosome, but yet remain stably associated. Our findings, obtained using a powerful combination of single-molecule fluorescence techniques and gel electrophoresis, emphasize the delicate interplay between DNA accessibility and condensation in chromatin.

[1] This chapter is based on a manuscript accepted for publication in Biophysical Journal: W.J.A. Koopmans, R. Buning, T. Schmidt, and J. van Noort, spFRET using Alternating Excitation and FCS reveals Progressive DNA Unwrapping in Nucleosomes. *Biophysical Journal* (2009)

5.1 Introduction

DNA-protein complexes are transient by nature. To understand the reaction mechanisms that control DNA metabolism it is important to relate the association and dissociation kinetics of these complexes to the conformational changes that are associated with DNA binding. All transactions involving eukaryotic DNA occur in the context of the nucleosome, the ubiquitous DNA-protein complex that forms the fundamental unit of chromatin organization. A nucleosome core particle consists of 50 nm of DNA wrapped in nearly two turns around a histone-octamer core [1]. Since nucleosomes sterically hinder enzymes that bind the nucleosomal DNA, they play an important role in gene regulation [2]. Large conformational changes in nucleosome structure are required to accommodate enzymatic processes such as transcription, replication, and repair. A variety of mechanisms that promote accessibility to nucleosomal DNA has been identified [3, 4], such as nucleosome repositioning, transient DNA unwrapping or breathing, and exchange of histone dimers between nucleosomes. However, the molecular mechanisms underlying these processes remain to be resolved.

Fluorescence Resonance Energy Transfer (FRET) is ideally suited to studying nucleosome structure and dynamics, since it is sensitive to conformational changes of 2-10 nm [5]. Li and Widom used ensemble FRET experiments to demonstrate that under physiological conditions the end of nucleosomal DNA transiently unwraps and rewraps from the histone core with an equilibrium constant K_{eq} of 0.02–0.1 [6]. The dynamic opening and closing of the nucleosome ends is termed DNA breathing. With additional fluorescence correlation spectroscopy (FCS) and stopped-flow FRET experiments, Li *et al.* measured the unwrapping and rewrapping rates of the DNA breathing process [7]. Due to the ensemble nature of their experiments, Li *et al.* could not resolve whether DNA unwraps in a single step as assumed in their model, or through multiple intermediate states, as speculated by Anderson *et al.* [8].

On the single-molecule level, single-pair FRET (spFRET) has the power to probe the conformational distribution and dynamics of an ensemble of molecules, and other heterogeneities with unprecedented detail [9]. In recent years, spFRET experiments provided valuable information on nucleosome destabilization and disassembly, and partially resolved structural heterogeneity in the nucleosome sample [10–14]. However, these studies used single-wavelength excitation, and therefore FRET populations attributed to dissociated nucleosomes could not be discriminated from incompletely labeled donor-only or free DNA molecules, which display identical FRET. Also, it remained unclear whether the DNA unwraps symmetrically from both nucleosome ends, and whether intermediate states exist in this process. Finally, it is not straightforward how to relate the irreversible nucleosome disassembly studied in the latter experiments to the reversible nucleosome breathing kinetics observed by Li *et al.* [6]. Therefore, a comprehensive study of DNA dynamics in nucleosomes should both discriminate sub-

stoichiometric labeling and nucleosome disassembly.

Many of the uncertainties in the analysis described in the previous paragraph are resolved by applying Alternating Laser Excitation (ALEX) [15]. ALEX complements the applicability of spFRET by simultaneously reporting on fluorophore stoichiometry (S) and FRET efficiency (E) of the molecule of interest. This additional information is obtained by rapidly alternating donor and acceptor excitation. ALEX also allows the determination of correction factors for the detection efficiencies and quantum yields of donor and acceptor, needed for accurate FRET measurements [16]. Thus, using ALEX it is possible to further disentangle the heterogeneity that is inherent in nucleosome studies.

In previous studies, we observed and quantified DNA breathing dynamics on individual immobilized nucleosomes imaged with widefield TIRF microscopy [17, 18]. We employed ALEX to separate photoblinking and photobleaching artifacts from true conformational dynamics, and obtained unwrapping and rewrapping rates similar to Li *et al.* [7]. Despite careful optimization of sample immobilization and surface passivation, we found that nucleosome immobilization affected the conformational distribution and disrupted a large fraction of the nucleosomes [18].

Here, we prevent immobilization artifacts by measuring ALEX-spFRET on free, diffusing nucleosomes using confocal microscopy. Because the observation time is limited to the diffusion time of a nucleosome in the confocal volume, it is necessary to acquire statistics over a large number of different molecules. This inevitably results in mixing differently wrapped DNA molecules, despite ALEX selection. To both separate properly folded nucleosomes from substoichiometric histone-DNA assemblies, and increase the diffusion time, allowing for longer observation time and better statistics of each molecule, we observed nucleosomes in a polyacrylamide gel after electrophoresis. Using this strategy, we compared equilibrium constants of DNA breathing at different locations within the nucleosome, and studied a variety of nucleosome conformations with a correlation analysis on selected bursts.

5.2 Materials and methods

Preparation of DNA and nucleosomes Mononucleosomes were reconstituted on a fluorescently labeled 155 (bp) DNA template containing a 601 nucleosome positioning sequence as described [17]. Briefly, the template DNA was prepared by PCR and was labeled with Cy3B (donor) and ATTO647N (acceptor) by incorporation of fluorescently labeled, HPLC purified primers (IBA GmbH, Göttingen, Germany). PCR primers were as follows (modified dT or dC underlined): Cy3B labeled forward primer: 5'-TTGGC<u>X</u>GGAGAATCCCGGTGCCGAGGC-CGC<u>Y</u>CAATTGGTCGTAGACAGCTCTAGCACCGCTTAAACGCACG<u>Z</u>ACGCGCTG-3'; ATTO647N labeled reverse primer 5'-biotin-TTGGA<u>Z</u>AGGATGTATATATCTGACACG-

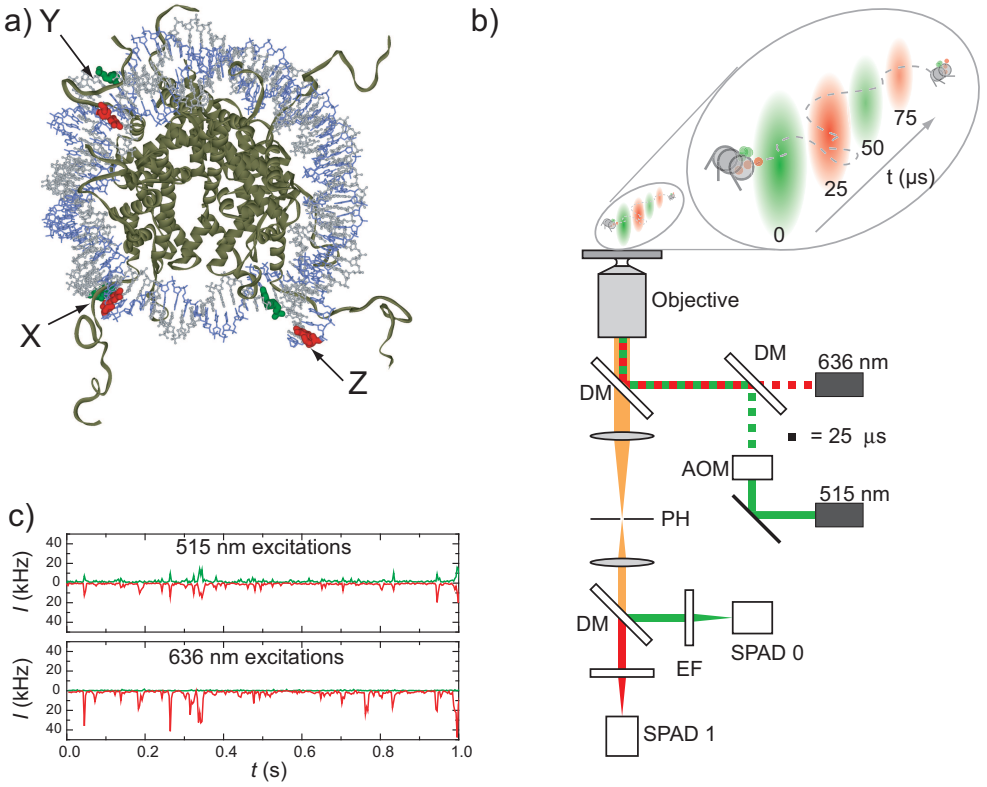

Figure 5.1: Experimental system and setup. a) A FRET labeled nucleosome. X,Y,Z indicate the locations of various FRET labeling positions used in this work. b) ALEX-FRET fluorescence microscope. DM: dichroic mirror; AOM: acousto-optical modulator; PH: pinhole; EF: emission filter; SPAD: single-photon avalanche diode c)Typical fluorescence intensity time traces of the four different photon streams acquired with the setup in b).

TGCCTGGAGACTAGGGAGTAAYCCCCTTGGCGGTTAAAACGXGGGGGACAGC-3'. We generated three DNA templates with a FRET pair (Cy3B-ATTO647N, R_0~ 5.5 nm) at either of the nucleosome extremes (labels at position X, or at position Z), and a position 27 base pair (bp) from one nucleosome end that we refer to as internally labeled in this work (labels at position Y), as shown in figure 5.1.a. In all DNA templates donor and acceptor were located ~80 bp (24 nm) apart. Nucleosomes were reconstituted by salt gradient dialysis with chicken erythrocyte histones as described [17]. After reconstitution donor and acceptor were approximately 4 nm apart, resulting in efficient FRET, as confirmed by bulk fluorescence spectroscopy. Native gel electrophoresis, as described below, was used to determine the reconstitution yield, which were 70%, 90%, and 85% for reconstitutions X, Y, and Z respectively.

Sample preparation Nucleosomes in free solution were diluted to a concentration of 100-200 pM in a buffer containing 10 mM Tris.HCl (pH 8), 0.1 mg/ml BSA, and 0.03 % NP-40. Reliable experiments could only be performed in the presence of 0.03% NP-40 anionic detergent, similar to the conditions established by Thåström *et al.* [19]. If the NP-40 was omitted, no reproducible data could be taken and we observed a decrease in the number of bursts over time that we attributed to precipitation. For most experiments 2 mM Trolox (Sigma, Zwijndrecht, The Netherlands) was added to the buffer [20]. A drop of 50 µl was placed on a glass cover slide (#1.5, Menzel, Braunschweig, Germany), and imaged as described below. Unless stated otherwise, experiments in this work were performed with nucleosomes labeled at position Y (see figure 5.1.a).

Nucleosomes in gel were imaged at single molecule concentration by excising the desired band from the gel. The gel slice was placed on a glass cover slide. A drop of 20 µl buffer was used to match the refractive of the gel and to prevent drying of the gel during the experiment.

Poly-acrylamide gel electrophoresis Nucleosome reconstitutions were analyzed with 5% native poly-acrylamide gel electrophoresis (PAGE). A sample of 0.1-1 pmol was loaded on the gel (29:1 bis:acrylamide, 0.2X TB). The gel was run at 19 V/cm at 4 °C for 80 min to separate nucleosomes from free DNA. The fluorescence was imaged with a gel imager (Typhoon 9400, GE, Waukesha, WI, USA).

Single molecule fluorescence microscopy Single nucleosomes were imaged with a home-built confocal microscope equipped with a 60X water-immersion microscope objective (NA = 1.2, Olympus, Zoeterwoude, The Netherlands), as schematically depicted in figure 5.1.b. A 515 nm diode pumped solid state laser (Cobolt, Solna, Sweden) and a 636 nm diode laser (Power Technology, Little Rock, AR, USA) were used as excitation sources. The lasers were alternated at 20 kHz by analog modulation, either directly (636 nm) or with an AOM (515 nm;

Isomet, Springfield, VA, USA). The beams were spatially filtered with a single-mode fiber, and focused 25 µm above the glass-buffer interface by the objective. The confocal volumes were 1.5 fl and 2.0 fl for 515 nm and 636 nm excitation respectively, as determined from fluorescence correlation spectroscopy (FCS) calibration experiments on 100 nm tetraspeck fluorescent beads (Invitrogen, Breda, The Netherlands). The excitation power was 80 µW for 515 nm excitation, and 50 µW for 636 nm excitation. The collected fluorescence was spatially filtered with a 50 µm pinhole in the image plane, and was split into a donor and an acceptor channel by a dichroic mirror (640dcxr, Chroma, Rockingham, VT, USA). The fluorescence was filtered with emission filters (hq570/100m for the donor channel, hq700/75m for the acceptor channel, Chroma, USA) to minimize crosstalk, and was imaged on the active area of single photon avalanche photodiodes (SPCM AQR-14, Perkin-Elmer (EG&G), Waltham, MA, USA). The photodiodes were read out with a TimeHarp 200 photon counting board (Picoquant GmbH, Berlin, Germany). In a typical experiment, data was collected for 10 min and 1000-5000 bursts of fluorescence were detected.

Data-analysis Photon arrival times in the donor and acceptor channel were sorted according to excitation period, resulting in four photon streams: I^D_{515}, donor emission during green excitation; I^A_{515}, acceptor emission during green excitation; I^D_{636} , donor emission during red excitation; I^A_{636}, acceptor emission during red excitation. Example data is shown in figure 5.1.c. The total fluorescence emission was analyzed with a burst detection scheme [21]. A burst was detected if a minimum of 100 photons arrived subsequently, with a maximum interphoton time of 100 µs. For each burst we calculated the apparent FRET efficiency E (also known as proximity ratio):

$$E = \frac{N^A_{515}}{N^A_{515} + \gamma N^D_{515}}, \tag{5.1}$$

and the apparent label stoichiometry S:

$$S = \frac{N^A_{515} + \gamma N^D_{515}}{N^A_{515} + \gamma N^D_{515} + N^A_{636}}, \tag{5.2}$$

where N^D_{515}, N^A_{515}, and N^A_{636} are number of photons in the burst from the different photon streams, and $\gamma = \frac{\Phi_A \eta_A}{\Phi_D \eta_D}$ is a parameter to correct for photophysical properties of the dyes. Φ_A and Φ_D are acceptor and donor quantum yield, and η_A and η_D are acceptor and donor detector efficiency respectively. Since we only compared relative changes, γ was set to unity. The excitation powers were chosen such that $N^A_{515} + \gamma N^D_{515} \approx N^A_{636}$ for doubly labeled molecules, resulting in $S \sim 0.5$. E and S were not corrected for donor crosstalk to the acceptor channel

(11%) and direct excitation of the acceptor fluorophore (<2%). The relative size of a certain population was determined from the number of bursts matching defined E, S-thresholds. The equilibrium constant K_{eq} for DNA unwrapping was calculated as

$$K_{eq} = \frac{unwrapped\ fraction}{wrapped\ fraction}. \tag{5.3}$$

Correlation curves $G(\tau)$

$$G_{1,2}(\tau) = \frac{\langle I_1(t)\, I_2(t+\tau)\rangle}{\langle I_1(t)\, I_2(t)\rangle} - 1, \tag{5.4}$$

where $I_1(t)$, $I_2(t)$ are the photon streams of interest, and τ is the lag time, were computed with the multi-tau algorithm described by Wahl *et al.* [22]. The correlation curves were smoothed by averaging out the periodic contribution that comes from alternating excitation, and were corrected for afterpulsing as described [23]. Correlation curves were constructed from photons during 515 nm excitation, selected from bursts matching defined E, S criteria. Although in principle any auto- or cross correlation (e.g. $\left(I_1 = I_2 = I^A_{615}\right)$ or $\left(I_1 = I^A_{515},\ I_2 = I^D_{515}\right)$) curve can be computed from the selected photons, we used a particular autocorrelation function $\left(I_1 = I_2 = I^D_{515} + I^A_{515}\right)$. This ensures that bursts are weighted based on their intensity and not on their FRET efficiency, facilitating a comparison of the correlation of different E-species.

5.3 Results

5.3.1 ALEX-spFRET resolves nucleosome sample heterogeneity

To characterize label stoichiometries and determine appropriate thresholds between different species, we used fluorescently labeled DNA samples that served as donor-only (D-only), acceptor-only (A-only), and doubly labeled species (D+A, no FRET). The corresponding 2D E, S-histograms revealed a single dominant population for each sample with the predicted E, S signature (figures 5.2.a-c and table 5.1). Considerable D-only and A-only species were present in the doubly labeled sample, effects of photobleaching. We used these results to determine the following thresholds for the experiments on nucleosomes: D-only: $S > 0.8$, and A-only: $S < 0.2$; free DNA and unwrapped nucleosomes without FRET: $E < 0.25$; wrapped nucleosomes with significant FRET: $E > 0.25$. Since the number of molecules with E, S-values close to the thresholds was small, the number of bursts in each fraction was only marginally dependent on the position of the threshold.

The 2D E, S-histogram obtained from reconstituted nucleosomes labeled at position Y are shown in figure 5.2.d and summarized in table 5.1. We observed a distinct, dominant pop-

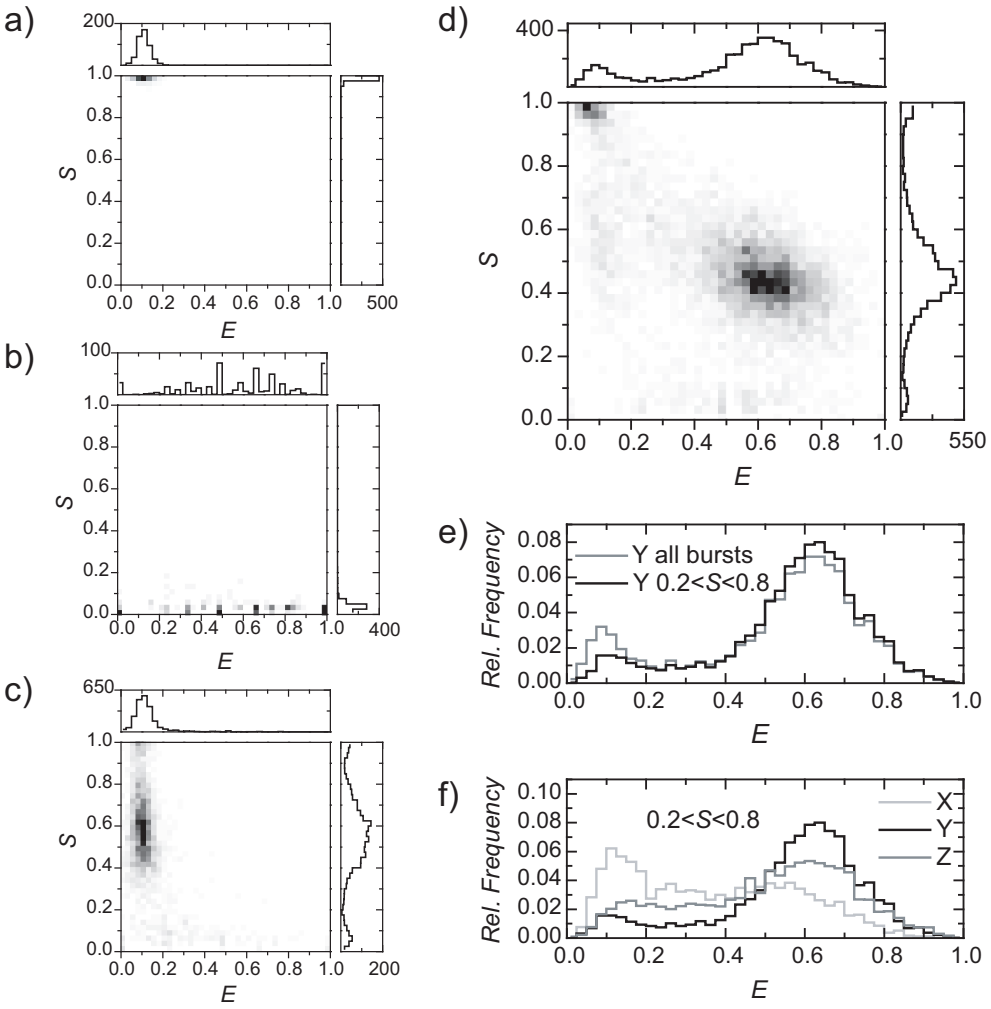

Figure 5.2: E, S footprint of nucleosomes and reference samples. a) Donor-only ssDNA b) Acceptor-only ssDNA c) Donor and acceptor labeled dsDNA used in reconstitutions. d) Reconstituted nucleosomes, label position Y. e) FRET histogram of all bursts (grey) and of doubly labeled bursts (black). The low FRET population is reduced considerably by filtering out D-only species. f) D-only filtered E-histograms for label positions X,Y, and Z in the nucleosome. Note the considerable population at intermediate FRET efficiency.

Table 5.1: E, S signature of the dominant populations in figure 5.2.a-d.

Sample	E (mean±σ)	S (mean±σ)	fraction size
Donor-only	0.11 ± 0.06	1.00 ± 0.03	100%
Acceptor-only	0.6 ± 0.6	0.02 ± 0.02	100%
Doubly labeled DNA	0.11 ± 0.07	0.56 ± 0.28	80%
Reconstituted nucleosomes	0.63 ± 0.22	0.45 ± 0.17	78%

ulation of doubly labeled and fully wrapped nucleosomes (78%), with $E = 0.63 \pm 0.22$, and $S = 0.45 \pm 0.17$. Three other populations could be clearly resolved: doubly labeled unreconstituted DNA or unwrapped nucleosomes (8%), and photobleached or partially labeled D-only (8%) and A-only (6%) populations,. These single-molecule characteristics agree well with results obtained from separate bulk experiments (data not shown): using UV-VIS absorption spectroscopy, bulk fluorescence spectra, and PAGE we deduced that the sample consisted of ~80% doubly labeled reconstituted nucleosomes with $E = 0.75$, ~8% doubly labeled unreconstituted DNA, and incompletely labeled species (~5% for D-only or A-only). These results demonstrate a powerful advantage of combining spFRET with ALEX: a single experiment is sufficient to resolve the heterogeneity in the sample.

5.3.2 ALEX selection resolves DNA breathing in nucleosomes

In the FRET histogram constructed from all detected bursts (similar to the case of single-wavelength excitation), 16% of the bursts falls in the $E < 0.25$ (low FRET) population, as shown in figure 5.2.e. When only bursts are selected that contain both donor and acceptor labels, 9% fall in this population that we can attribute to free DNA or unwrapped nucleosomes present in the sample.

This D-only correction enabled us to characterize and compare nucleosome reconstitutions at different label positions X,Y, and Z within their 1D E-histograms, unaffected by bleaching and labeling artifacts which amounts to 40% of the low FRET population. We compared the resulting selected FRET histograms shown in figure 5.2.f. The results are summarized in table 5.2. For each reconstituted nucleosome (X,Y and Z) the size of the low FRET population agreed well with the observed fraction of unreconstituted free DNA in PAGE experiments. Each wrapped nucleosome population showed a clear peak, with slightly different FRET efficiencies that reflect the different label attachment positions for the FRET pairs on the different DNA templates. Importantly, each distribution showed a pronounced tail extending from the peak towards intermediate FRET values. The histogram could not be fitted with a sum of two Gaussian distributions, indicating the presence of a third population of considerable size. These intermediate FRET values cannot be explained by the simultaneous transit of multiple

Table 5.2: Comparison of FRET characteristics and high ($E > 0.4$), intermediate ($0.25 < E < 0.4$), and low ($E < 0.25$) FRET populations of end-labeled (X,Z) and internally labeled (Y) nucleosome reconstitutions, based on the FRET histograms in figure 5.2.f.

Nucleosome	$E < 0.25$	$0.25 < E < 0.4$	$E > 0.4$	K_{eq}	E of main population
X	36%	19%	45%	0.37	0.53 ± 0.3
Y	8%	6%	86%	0.07	0.63 ± 0.22
Z	17%	13%	70%	0.19	0.61 ± 0.27

species through the detection volume, since the concentration is low enough (100-200 pM) that the presence of more than a single molecule in the spot is highly improbable. Control measurements at 20 pM concentration showed the same intermediate FRET population. Here we assign the tails in the FRET distribution to molecules in which spontaneous unwrapping or rewrapping of DNA [6] occurred during their transit through the excitation volume. The observed intermediate FRET value corresponds to ~10 bp unwrapped DNA from nucleosomes X and Z, and ~35 bp from nucleosome Y. The smaller fraction in Y this suggests that the first ~10-35 bp of the nucleosomal DNA progressively unwrap, starting from either end. It must be noted that the amount of unwrapped DNA mentioned here is a rough estimate, given the many assumptions needed to convert a FRET efficiency to a distance (e.g. freely rotating dyes, $\gamma = 1$, the conformation of the unwrapped DNA). We used different label positions to monitor the unwrapping of nucleosomal DNA in order to avoid this complexity for the most part.

The size of the distribution allowed us to determine the equilibrium constant for DNA unwrapping. The equilibrium constants we observed were $K_{eq} = 0.19 - 0.37$ for end-labeled nucleosomes Z and X, and $K_{eq} = 0.07$ for internally labeled nucleosomes Y. The value of the equilibrium constant was only marginally dependent on the thresholds between the different populations, or on the thresholds used for burst detection: the number of bursts close to the thresholds E, S-values was small, and the relative size of the populations only changed a few percent when using different burst detection criteria (50 instead of 100 photons per burst, or 150 instead of 100 µs interphoton time).

5.3.3 Monovalent salt promotes DNA unwrapping and nucleosome disassembly

Although the low FRET population agrees well with the fraction of unreconstituted DNA, it may also indicate dissociation of the nucleosomes in the sample, as reported before [10]. Kelbauskas *et al.* [13] reported that nucleosomes are less stable at physiological conditions that contain >100 mM NaCl than at the low salt concentrations used in many studies of nucleosome dynamics [7, 13]. To follow the structural integrity of the nucleosomes, we analyzed E, S-populations for different salt concentrations in time. We quantified the number of bursts

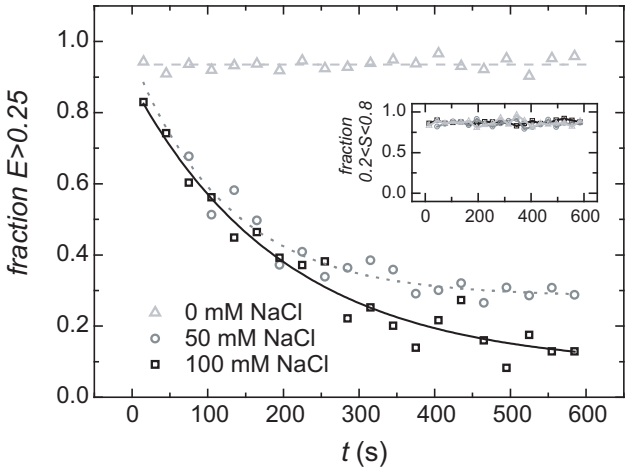

Figure 5.3: Nucleosome disassembly kinetics for several salt concentrations in time. The fraction of intact nucleosomes ($E > 0.25$) in time for different monovalent salt concentrations, buffered with 10 mM Tris.HCl (pH 8). The lines are linear (0 mM NaCl) or exponential (50 and 100 mM NaCl) fits to the data. *Inset* The fraction of doubly labeled ($0.2 < S < 0.8$) molecules in time. For each salt concentration tested, this fraction is constant over time.

in each population for 30 s bins and compared the relative size of each fraction as a function of time. The fraction of intact nucleosomes was monitored by evaluating the ratio of the number of $E > 0.25$ to all doubly labeled molecules, as shown in figure 5.3.

In 10 mM Tris.HCl the fraction of intact nucleosomes was constant over time, and was equal to the reconstitution yield as determined with PAGE (90%). In contrast, at 50 and 100 mM NaCl (both + 10 mM Tris.HCl) we observed pronounced nucleosome disassembly: the fraction of intact nucleosomes decreased exponentially with a decay time of 200 ± 30 s after the addition of NaCl. At 100 mM NaCl only 10% of the nucleosomes remained folded, whereas 30% was retained in 50 mM NaCl. The disassembly process was irreversible upon subsequent lowering of the salt concentration. A comparison of the FRET distributions for 0 mM and 50-100 mM NaCl was not straightforward, because of this instability. The fraction of bursts with intermediate E compared to those with high E was on average higher (15%) at 50-100 mM than at 0 mM NaCl (7%), indicating that breathing dynamics was promoted at higher salt conditions. The fraction of doubly labeled species did not change over time for all salt concentrations, as shown in figure 5.3 (*inset*). This indicates that photobleached species did not accumulate near the detection volume, but were continuously redistributed by diffusion.

In summary, 50-100 mM monovalent salt promotes both reversible nucleosome breathing kinetics and irreversible nucleosome disassembly processes at low nucleosome concentration.

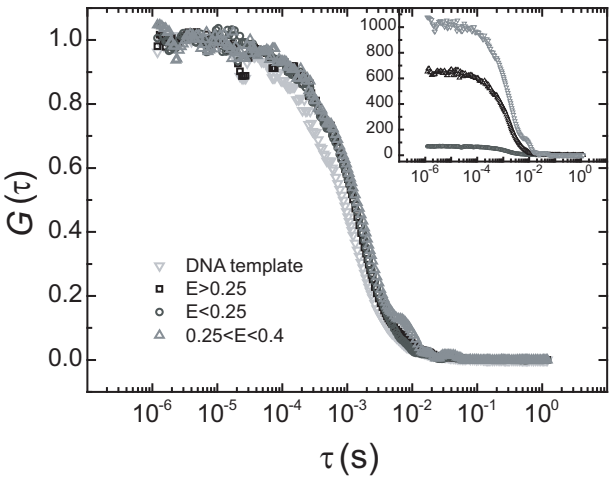

Figure 5.4: Correlation curves *(inset:* Unscaled correlation curves) of selected bursts in a nucleosome sample, and of a free DNA sample. The nucleosomes show an increased diffusion time compared the DNA. Nucleosome fraction can only be separated based on FRET; the diffusion time in free solution is unaffected by conformational changes within the nucleosome.

5.3.4 Fluorescence correlation analysis of selected nucleosome populations shows unwrapping at low FRET

By performing fluorescence correlation spectroscopy (FCS), ALEX-spFRET allowed us to monitor the conformation of nucleosomes. FCS was applied to selected bursts to determine the diffusion time, which is directly related to the hydrodynamic radius of the nucleosomes in the selected population. We first mapped out the composition of the sample with ALEX, and only included particular bursts of fluorescence selected on both E and S value in FCS-analysis. To characterize the hydrodynamic radius of a population matching defined criteria in E and S, we performed FCS on doubly labeled bursts in a defined E-range to characterize their diffusion behavior. We calculated the auto-correlation curve $G(\tau)$ from all photons from both detection channels during green excitation, and separated three populations: $E > 0.25$ (all nucleosomes), $E < 0.25$ (free DNA or unwrapped nucleosomes) and $0.25 < E < 0.4$ (partially unwrapped nucleosomes), shown in figure 5.4.

The individual correlation curves showed a qualitatively similar decay as FCS diffusion curves reported in literature [24] that were not composed of selected E,S-bursts. In the limit of small correlation times τ, G was constant with an amplitude that was inversely related to the number of bursts (see *inset* in figure 5.4). For larger lag times, G decreased at $\tau = 1$ ms towards its final value $G = 0$. We determined the time lag at half amplitude ($\tau_{\frac{1}{2}}$) as the characteristic

diffusion time from an FCS curve from selected bursts. Uncertainties were estimated from the change in $\tau_{\frac{1}{2}}$ corresponding to a change of one standard deviation in the initial amplitude of the correlation curve. The standard deviation in the amplitude was calculated using a bootstrap method, i.e. by dividing one measurement in smaller data packages analogous to Wohland *et al.* [25]. The characteristic times were $\tau_{\frac{1}{2}} = 1.2 \pm 0.1$ ms, $\tau_{\frac{1}{2}} = 1.3 \pm 0.2$ ms, and $\tau_{\frac{1}{2}} = 1.4 \pm 0.3$ ms for $E > 0.25$, $E < 0.25$ and $0.25 < E < 0.4$ respectively. The obtained values were the same within the statistical uncertainty, and hence the three populations were indistinguishable based on diffusion. Control measurements on a DNA template sample yielded $\tau_{\frac{1}{2}} = 0.84 \pm 0.04$ ms, significantly shorter than any of the populations in the nucleosome sample. This shows that the $E < 0.25$ fraction in the nucleosome sample does not only contain unreconstituted DNA, but also a significant amount of unwrapped nucleosomes with larger hydrodynamic radius.

The correlation curves of the nucleosome species did not follow a simple diffusion model typically fitted to FCS curves. We further noted that the selection process results in reduced data-sets that produce a smaller signal-to-noise ratio (SNR). The benefits of selecting specific species in a heterogeneous sample may in certain applications outweigh the reduced SNR associated with the combination of ALEX-spFRET-FCS. In summary, using FCS on selected populations, we deduced that the low FRET population contains a significant amount of unwrapped nucleosomes, apart from the unreconstituted DNA.

5.3.5 Gel separated nucleosomes are transiently unwrapped in a progressive way from both nucleosome ends

To better resolve difference in nucleosome conformation, we used native PAGE to separate nucleosomes from DNA. Nucleosomes confined in a gel are expected to diffuse slower, resulting in a longer observation time, better photon statistics, and enhanced sensitivity to molecular conformation. An additional advantage of this approach is that virtual E, S-sorting is supplemented by sorting based on gel separation [26]. This results in a well-defined nucleosome band, not contaminated with free, unreconstituted DNA and nucleosome aggregates, two species that cannot be separated based on S alone.

Low resolution fluorescence images of the gel are shown in figure 5.5.a-d (*left panels*). All lanes with the nucleosome reconstitutions showed a sharp band of nucleosomes which migrated slower through the gel than the free DNA band. The ratio of nucleosomes to free DNA was 8:1 for the reconstitution at label position X, and 9:1 for the reconstitutions at label positions Y and Z. The nucleosomes migrated in a sharp band, indicating that dilution driven dissociation was not occurring during gel electrophoresis (~3h), despite the elevated ionic strength of 40 mM in the gel. Trace amounts of fluorescence were detected outside these two bands, indicating that aggregation or formation of non-nucleosomal particles was small, and that these

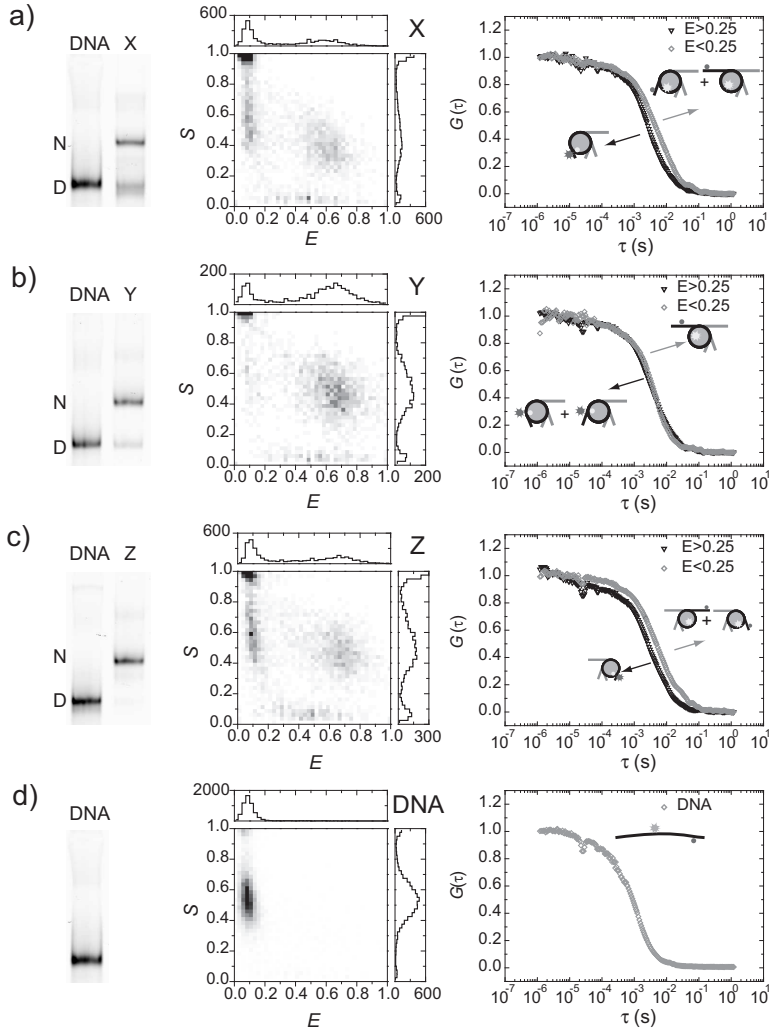

Figure 5.5: ALEX-spFRET spectroscopy on gel separated nucleosomes a) X, b) Y, c) Z and d) DNA from template Z. *Left panels* Fluorescence image (acceptor excitation) of PAGE analysis of reconstituted nucleosomes and the corresponding DNA templates. N: nucleosome band, D: DNA band. *Middle panels E*, *S*-histograms of ALEX-spFRET experiments in gel in the nucleosome bands, and DNA band Z depicted. A low FRET peak can be observed in all nucleosome bands, which points at progressive DNA unwrapping from the nucleosome ends. *Right panels* Burst-wise FCS analysis on nucleosome populations in gel. For nucleosomes X and Z, a clear difference in correlation time can be seen for different FRET efficiencies, reflecting different conformations. For nucleosome Y, the difference is smaller. All nucleosome populations diffuse significantly slower than the DNA.

were successfully separated.

The fluorescence images allow for a quantitative measurement of the FRET efficiency of purified nucleosomes. However, transient nucleosome conformations cannot be resolved in these images. To detect these, we applied ALEX-spFRET experiments in excised gel bands of interest. The corresponding 2D E, S histograms are shown in the *middle panels* in figure 5.5.a-d. We observed a clear high FRET population in all nucleosome bands, with the same characteristic E and S values as those observed in free solution. Surprisingly, in all nucleosome bands we observed a rather large fraction of bursts with $S = 0.5$, $E < 0.25$, amounting to 38% for the end labeled nucleosomes X and Z, and 10% for internally labeled nucleosome Y after correction for D-only species (see figure 5.6 and table 5.3). This fraction could not originate from free DNA and sub-stoichiometric histone-DNA complexes, since these result in different bands in the gel. Even though the ionic strength of the buffer was 40 mM we did not observe irreversible nucleosome disassembly during the experiment (10 min per gel band, ~1h in total) in the time evolution of the E, S-histograms, in contrast to similar experiments in free solution. Therefore, this fraction probably reflects the nucleosomes that temporarily lose FRET by transient unwrapping. The unwrapped fractions had the same size for nucleosomes X and Z, indicating that DNA unwrapping is symmetric from both ends. Since also a considerably smaller unwrapped fraction was observed in internally labeled nucleosomes Y, we conclude that DNA unwrapping occurs progressively with a lower probability as the DNA is located further in the nucleosome. We again observed a significant fraction with intermediate FRET values (20% for X and Z, 10% for Y), that we assigned to either partially unwrapped nucleosomes, or transient unwrapping and rewrapping events during the diffusion through the confocal excitation volume.

In all gel experiments, A-only and D-only populations (12% and 20% respectively) were more pronounced than in free solution (8% and 10% respectively). Since nucleosomes diffuse slower in the gel, the attached FRET pair is longer exposed to the excitation light, increasing the probability that either fluorophore bleaches. ALEX allows a label stoichiometry based sorting, and hence the presence of such bleached species did not interfere with the detection of correctly labeled low FRET species.

In order to gain more insight into the underlying molecular conformations, we analyzed the diffusion characteristics of the various fractions ($E > 0.25$ and $E < 0.25$) with an FCS analysis on selected bursts. The results are shown in figure 5.5 (*right panels*), and summarized in table 5.3. The correlation times for nucleosomes were approximately three times longer in gel than in free solution, reflecting a slower diffusion process. Furthermore, the bursts in the nucleosomes bands showed considerably longer correlation times, showing that gel-based FCS has a larger resolving power than solution-based FCS. For all nucleosomes (i.e. X, Y, and Z), the unwrapped nucleosomes diffused slower than nucleosomes with $E > 0.25$. This is consis-

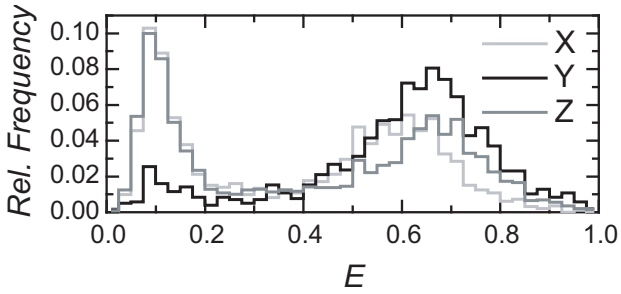

Figure 5.6: D-only corrected E-histograms for nucleosomes X,Y, and Z in in gel. A low FRET population can clearly be observed at all three labeling positions. The low FRET population is 38% for X and Z, and 10% for Y, indicating progressive and pronounced nucleosome unwrapping from both ends.

tent with the predicted larger hydrodynamic radius of unwrapped nucleosomes as compared to the more compact fully wrapped nucleosomes, schematically depicted in the cartoons in figures 5.5.a-c (*right panels*). We note that nucleosomes that show FRET can still represent a heterogeneous population: although the FRET pair only reports on unwrapping at the side where it is located, X and Z feature symmetric unwrapping behavior. Therefore, in terms of hydrodynamic radius it can be expected that a fraction of nucleosomes is unwrapped on either side. How unwrapping of one end of the nucleosome affects the DNA at the other end remains an open question, however. Nucleosomes Y with $E > 0.25$ were anticipated to be partially unwrapped from the nucleosome end in 28% of the bursts, resulting in a more open structure and larger hydrodynamic radius, and therefore in slower diffusion than for completely wrapped end-labeled nucleosomes. The observed difference in diffusion time is comparable to the uncertainty however, and better statistics are needed to confirm whether this difference is significant. Nucleosomes Y with $E < 0.25$ are unwrapped for at least 30-40 bp in 10% of the bursts ($K_{eq} \sim 0.1$). Nucleosomes X and Z without FRET are unwrapped in 38% of the bursts ($K_{eq} \sim 0.6$), and must therefore be either unwrapped for 10-20 bp (28%, $K_{eq} \sim 0.4$) or for 30-40 bp (10%, $K_{eq} \sim 0.1$). Surprisingly, this fraction showed the slowest diffusion of all fractions tested, even though the suggested conformation from the FRET signature does not correspond to the most unwrapped and extended state of the nucleosome. The differences in correlation times between nucleosome fractions can probably be more completely understood in the light of gel-retardation studies [27].

In conclusion, the combined PAGE-ALEX-spFRET-FCS data resolve an even more accessible set of conformations than obtained in solution.

Table 5.3: Correlation analysis of nucleosome populations in gel

	Wrapped fraction		Unwrapped fraction		
Sample	$\tau_{\frac{1}{2}}$ (ms)	Fraction size	$\tau_{\frac{1}{2}}$ (ms)	Fraction size	K_{eq}
X	2.7 ± 0.3	61%	4.5 ± 0.8	39%	0.6
Y	3.1 ± 0.3	90%	3.5 ± 1.2	10%	0.1
Z	2.7 ± 0.3	62%	4.7 ± 0.8	38%	0.6
DNA	-	-	0.90 ± 0.05	98%	-

5.4 Discussion and Conclusion

Combining PAGE, ALEX-spFRET and FCS To resolve the intrinsic dynamic heterogeneity of nucleosomes, it was necessary to combine PAGE-ALEX-spFRET and FCS in a single experiment. Each technique complements the others and here we show that the techniques can be performed simultaneously on the same sample. The combination ALEX-spFRET has proven itself capable of accurately mapping stoichiometric heterogeneity, allowing for exclusion of the unwanted D-only fraction from data-analysis (see e.g. Kapanidis *et al.* [28]). Here, we used ALEX to exclude a photobleached D-only fraction from data-analysis to allow for correct observation of low FRET populations. This D-only correction is even more essential for the experiments in gel because of increased photobleaching due to slower diffusion. ALEX-spFRET allowed us to strengthen the evidence for earlier conclusions obtained by others. We confirmed that breathing is enhanced at higher salt concentrations [6], that disassembly is promoted at higher salt and picomolar nucleosome concentration [12], that nucleosome ends are less stable than internal regions [14], and that broadening of the FRET histogram is indicative of nucleosome dynamics [11]. Our new findings reveal that nucleosomes are unwrapped with a higher equilibrium constant than demonstrated earlier [6], but yet remain stably associated. Pronounced breathing does not directly result in disassembly of the nucleosome into sub-stoichiometric DNA-histone complexes.

PAGE-ALEX-spFRET is a new and powerful combination of techniques whose potential has only recently been pointed out by Santoso *et al.* [26]. We successfully used it to remove unreconstituted DNA, which interferes with a correct observation of unwrapped nucleosomes with low and intermediate FRET characteristics, from our data-analysis. Optimized reconstitution protocols and titration reactions can minimize but never fully remove all free DNA; in the work presented by Gansen *et al.* [10] and in our work, a fraction of ~10% free DNA is mentioned. Reconstitution reactions can be further purified with for example sucrose gradient ultracentrifugation [6], or PAGE with gel elution [29]. This complicates sample preparation and does not necessarily result in a 100% pure nucleosome sample as the conditions for purification may result in disassembly itself [29].

FCS analysis can be included with ALEX-spFRET spectroscopy and PAGE separation without any modifications of the experimental setup, since it only requires a correlation analysis of the detected photon streams to report on the diffusion behavior. Although photon selection criteria are common practice in FCS (e.g. based on lifetime for time-gated FCS [30], or based on detection channel for a standard cross-correlation), the correlation analysis on selected bursts presented here has not been reported before. By using bursts from a selected nucleosome population for FCS analysis, a diffusion time can be recovered that is directly related to the hydrodynamic radius of the population, which in turn depends on its conformation. Here we quantitatively compared correlation curves based on the $\tau_{\frac{1}{2}}$, avoiding fitting of the curves with an analytical expression. A model that describes the correlation curve would need to encompass i) how the burst-selection algorithm affects the photon streams and how this influences the shape of the curve, ii) anomalous diffusion of nucleosomes in gel [24], as well as iii) an accurate description of DNA breathing conformational changes including its kinetics. A comprehensive analysis of these contributions is beyond the scope of this study, but could potentially uncover more details.

The application of this combined PAGE-ALEX-spFRET-FCS approach is not limited to the study of nucleosomes, but can in principle be exploited to study a variety of heterogeneous systems. Any process involving transient DNA-protein conformations, such as the action of ATP-dependent remodeling enzymes on nucleosomes, is dynamic and heterogeneous in nature. Only a single set of experiments is needed to extract a wealth of information about the conformational distribution and dynamics underlying such DNA-protein interactions.

Progressive nucleosome unwrapping The combined data for end-labeled and internally labeled nucleosomes, both in free solution and in gel, indicate that transient DNA unwrapping occurs progressively from both nucleosome ends. This is consistent with the DNA breathing model, where transient DNA release initiates at the nucleosome end and proceeds inward [31]. Progressive unwrapping from both ends implies that even in a homogeneous nucleosome population a variety of nucleosome conformations exists simultaneously. This was confirmed here based on diffusion times determined with FCS. Though the 601 DNA sequence used for nucleosome reconstitutions in this work is not palindromic, we did not observe sequence dependent DNA unwrapping from the nucleosome ends.

Our single-molecule observations of DNA breathing show much more pronounced unwrapping ($K_{eq} \sim 0.1 - 0.6$) than studies where DNA site exposure for different positions in the nucleosome was monitored using classical enzyme binding assays ($K_{eq} = 0.02 - 0.1$ at the nucleosome ends [6, 8]). This difference may in part result from differences in experimental conditions and nucleosome constructs. In particular, at the subnanomolar nucleosome concentrations used in this work, nucleosomes are known to be less stable due to weakened

interactions with the H2A-H2B histone dimer that binds the region close to DNA ends [32], which is preceded by DNA breathing.

Unwrapping and rewrapping rates obtained by Li *et al.* [7] and by our previous work on immobilized nucleosomes [17, 18] suggest that the lifetime of the unwrapped state is 10-50 ms. Fluctuations on this timescale cannot be resolved with our current approach, since the diffusion time is an order of magnitude smaller (~1 ms) than the predicted fluctuations. Fluctuations caused by nucleosome dynamics will affect the FRET value and the width of the distribution for different populations in an E-histogram. The latter information can be used to extract information about how the breathing rates compare to the diffusion time [33]. For example, since the experiments in gel reveal a clear low FRET population of unwrapped nucleosomes in the histogram, we deduce that no conformational fluctuations that broaden this peak occurred during diffusion through the confocal volume. This yields a lower limit (~4.5 ms in gel) for the lifetime of the unwrapped state.

Disassembly of nucleosomes into sub-stoichiometric histone-DNA complexes is increasingly recognized as a relevant process in chromatin structural maintenance [34]. It vastly complicates the analysis of the nucleosome sample, because of the large number of possible conformations. Despite the pronounced DNA unwrapping far into the nucleosome, we did not observe irreversible nucleosome disassembly at low salt conditions or in the gel: the fraction of nucleosomes at low salt concentration in free solution experiments was the same as the fraction obtained from bulk experiments (within experimental error), and a sharp, stable band of nucleosomes in gel indicated that irreversible disassembly was absent. Nucleosome disassembly can be prevented by using high concentrations of unlabeled nucleosomes, as was demonstrated by Gansen *et al.* [10]. This allowed us to perform experiments at physiological salt conditions in free solution (data not shown). In the experiments reported here, a gel matrix prevents dilution-driven nucleosome disassembly, possibly due to crowding. Crowded conditions may very well be physiologically relevant, since they closely resemble the situation in the cell nucleus.

In conclusion, our results show that the nucleosome is transiently unwrapped, but yet the histone proteins and the DNA remain stably associated. The nucleosome is more accessible to binding of regulatory proteins on the nucleosomal DNA than was shown previously [6]. Our findings, obtained using a powerful combination of single-molecule fluorescence techniques and gel electrophoresis, emphasize the delicate interplay between DNA accessibility and condensation in chromatin. The method presented here is not restricted to the study of nucleosomes, but can be exploited to resolve the dynamics of other heterogeneous DNA-protein complexes as well.

Acknowledgement

We thank Eyal Nir and Shimon Weiss for help with the realization of the ALEX-FRET setup, Andrew Routh and Daniela Rhodes for help with mononucleosome reconstitutions, and Alexander Gaiduk and Michel Orrit for helpful discussion on the correlation analysis. This work is part of the research programme of the 'Stichting voor Fundamenteel Onderzoek der Materie (FOM)', which is financially supported by the 'Nederlandse Organisatie voor Wetenschappelijk Onderzoek (NWO)'.

Bibliography

[1] Luger, K., Mader, A., Richmond, R., Sargent, D., and Richmond, T. Crystal structure of the nucleosome core particle at 2.8 Å resolution. *Nature* **389**, 251–260 (1997).

[2] Kornberg, R. and Lorch, Y. Twenty-five years of the nucleosome, fundamental particle of the eukaryote chromosome. *Cell* **98**, 285–294 (1999).

[3] Flaus, A. and Owen-Hughes, T. Mechanisms for ATP-dependent chromatin remodelling: farewell to the tuna-can octamer? *Curr. Opin. Genet. Dev.* **14**, 165–173 (2004).

[4] Luger, K. Dynamic nucleosomes. *Chromosome Res.* **14**, 5–16 (2006).

[5] Clegg, R. Fluorescence resonance energy-transfer and nucleic-acids. *Methods Enzymol.* **211**, 353–388 (1992).

[6] Li, G. and Widom, J. Nucleosomes facilitate their own invasion. *Nat. Struct. Mol. Biol.* **11**, 763–769 (2004).

[7] Li, G., Levitus, M., Bustamante, C., and Widom, J. Rapid spontaneous accesibility of nucleosomal DNA. *Nat. Struct. Mol. Biol.* **12**, 46–53 (2005).

[8] Anderson, J. and Widom, J. Sequence and position-dependence of the equilibrium accessibility of nucleosomal DNA target sites. *J. Mol. Biol.* **296**, 979–987 (2000).

[9] Ha, T. Single-molecule fluorescence resonance energy transfer. *Methods* **25**, 78–86 (2001).

[10] Gansen, A., Hauger, F., Toth, K., and Langowski, J. Single-pair fluorescence resonance energy transfer of nucleosomes in free diffusion: Optimizing stability and resolution of subpopulations. *Anal. Biochem.* **368**, 193–204 (2007).

[11] Gansen, A., Tóth, K., Schwarz, N., and Langowski, J. Structural Variability of Nucleosomes Detected by Single-Pair Förster Resonance Energy Transfer: Histone Acetylation, Sequence Variation, and Salt Effects. *J. Phys. Chem. B* **113**, 2604–2613 (2009).

[12] Kelbauskas, L., Chan, N., Bash, R., Yodh, J., Woodbury, N., and Lohr, D. Sequence-dependent nucleosome structure and stability variations detected by Förster resonance energy transfer. *Biochemistry* **46**, 2239–2248 (2007).

[13] Kelbauskas, L., Chan, N., Bash, R., DeBartolo, P., Sun, J., Woodbury, N., and Lohr, D. Sequence-dependent variations associated with H2A/H2B depletion of nucleosomes. *Biophys. J.* **94**, 147–158 (2008).

[14] Kelbauskas, L., Sun, J., Woodbury, N., and Lohr, D. Nucleosomal Stability and Dynamics Vary Significantly When Viewed by Internal Versus Terminal Labels. *Biochemistry* **47**, 9627–9635 (2008).

[15] Kapanidis, A., Laurence, T., Lee, N., Margeat, E., Kong, X., and Weiss, S. Alternating-laser excitation of single molecules. *Acc. Chem. Res.* **38**, 523–533 (2005).

[16] Lee, N., Kapanidis, A., Wang, Y., Michalet, X., Mukhopadhyay, J., Ebright, R., and Weiss, S. Accurate FRET measurements within single diffusing biomolecules using alternating-laser excitation. *Biophys. J.* **88**, 2939–2953 (2005).

[17] Koopmans, W. J. A., Brehm, A., Logie, C., Schmidt, T., and van Noort, J. Single-pair FRET microscopy reveals mononucleosome dynamics. *J. Fluoresc.* **17**, 785–795 (2007).

[18] Koopmans, W. J. A., Schmidt, T., and van Noort, J. Nucleosome Immobilization Strategies for Single-Pair FRET Microscopy. *ChemPhysChem* **9**, 2002–2009 (2008).

[19] Thåström, A., Gottesfeld, J., Luger, K., and Widom, J. Histone - DNA binding free energy cannot be measured in dilution-driven dissociation experiments. *Biochemistry* **43**, 736–741 (2004).

[20] Rasnik, I., Mckinney, S., and Ha, T. Nonblinking and longlasting single-molecule fluorescence imaging. *Nat. Methods* **3**, 891–893 (2006).

[21] Eggeling, C., Berger, S., Brand, L., Fries, J., Schaffer, J., Volkmer, A., and Seidel, C. Data registration and selective single-molecule analysis using multi-parameter fluorescence detection. *J. Biotechnol.* **86**, 163–180 (2001).

[22] Wahl, M., Gregor, I., Patting, M., and Enderlein, J. Fast calculation of fluorescence correlation data with asynchronous time-correlated single-photon counting. *Opt. Express* **11**, 3583–3591 (2003).

[23] Zhao, M., Jin, L., Chen, B., Ding, Y., Ma, H., and Chen, D. Afterpulsing and its correction in fluorescence correlation spectroscopy experiments. *Appl. Opt.* **42**, 4031–4036 (2003).

[24] Hess, S., Huang, S., Heikal, A., and Webb, W. Biological and chemical applications of fluorescence correlation spectroscopy: A review. *Biochemistry* **41**, 697–705 (2002).

[25] Wohland, T., Rigler, R., and Vogel, H. The standard deviation in fluorescence correlation spectroscopy. *Biophys. J.* **80**, 2987–2999 (2001).

[26] Santoso, Y., Hwang, L. C., Le Reste, L., and Kapanidis, A. N. Red light, green light: probing single molecules using alternating-laser excitation. *Biochem. Soc. Trans.* **36**, 738–744 (2008).

[27] Meersseman, G., Pennings, S., and Bradbury, E. Mobile nucleosomes -a general behavior. *EMBO J.* **11**, 2951 – 2959 (1992).

[28] Kapanidis, A., Margeat, E., Laurence, T., Doose, S., Ho, S., Mukhopadhyay, J., Kortkhonjia, E., Mekler, V., Ebright, R., and Weiss, S. Retention of transcription initiation factor sigma(70) in transcription elongation: Single-molecule analysis. *Mol. Cell* **20**, 347–356 (2005).

[29] Dyer, P., Edayathumangalam, R., White, C., Bao, Y., Chakravarthy, S., Muthurajan, U., and Luger, K. Reconstitution of nucleosome core particles from recombinant histones and DNA. *Chromatin and Chromatin Remodeling Enzymes, Pt A* **375**, 23–44 (2004).

[30] Lamb, D., Schenk, A., Rocker, C., Scalfi-Happ, C., and Nienhaus, G. Sensitivity enhancement in fluorescence correlation spectroscopy of multiple species using time-gated detection. *Biophys. J.* **79**, 1129–1138 (2000).

[31] Anderson, J., Thåström, A., and Widom, J. Spontaneous access of proteins to buried nucleosomal DNA target sites occurs via a mechanism that is distinct from nucleosome translocation. *Mol. Cell. Biol.* **22**, 7147–7157 (2002).

[32] Claudet, C., Angelov, D., Bouvet, P., Dimitrov, S., and Bednar, J. Histone octamer instability under single molecule experiment conditions. *J. Biol. Chem.* **280**, 19958–19965 (2005).

[33] Nir, E., Michalet, X., Hamadani, K. M., Laurence, T. A., Neuhauser, D., Kovchegov, Y., and Weiss, S. Shot-noise limited single-molecule FRET histograms: Comparison between theory and experiments. *J. Phys. Chem. B* **110**, 22103–22124 (2006).

[34] Zlatanova, J., Bishop, T., Victor, J., Jackson, V., and van Holde, K. The nucleosome family: dynamic and growing. *Structure* **17**, 160–171 (2009).

Summary

Nucleosomes form the first level of DNA compaction in eukaryotic nuclei. Nucleosomes sterically hinder enzymes that bind the nucleosomal DNA, and hence play an important role in gene regulation. In order to understand how accessibility to nucleosomal DNA is regulated, it is necessary to resolve the molecular mechanisms underlying conformational changes in the nucleosome. This thesis presents the results of an experimental study of nucleosome dynamics, using single-pair Fluorescence Resonance Energy Transfer (spFRET) as a reporter of nucleosome conformation at the single-molecule level. Each chapter was written as a separate research article focusing on specific aspects of nucleosome conformational changes and the experimental methodology used to study these.

Chapter 2 gives a detailed overview of the procedures that were established to reconstitute nucleosomes with a FRET pair exactly at the desired location, and to analyze them with ensemble and single-molecule techniques: we generated a DNA template containing a 601 nucleosome positioning sequence. Donor and acceptor were incorporated at specific locations in the DNA using a polymerase chain reaction (PCR) with fluorescently labeled primers. We reconstituted mononucleosomes from the template DNA and histone octamer proteins with salt dialysis. The reconstitution yield was approximately 90%, as observed with polyacrylamide gel electrophoresis (PAGE). Using widefield Total Internal Reflection Fluorescence (TIRF) microscopy on immobilized molecules, we observed and quantified DNA breathing dynamics on individual nucleosomes. Alternatively, fluorescence microscopy on freely diffusing molecules in a confocal detection volume allowed a fast characterization of nucleosome conformational distributions.

In **Chapter 3** we applied spFRET microscopy for direct observation of intranucleosomal DNA dynamics. Mononucleosomes, containing a FRET pair at the dyad axis and at the exit of the nucleosome core particle, were immobilized through a 30 bp DNA tether on a polyethylene glycol (PEG) functionalized slide and visualized using TIRF microscopy. FRET efficiency time-traces revealed two types of dynamics: acceptor blinking and intramolecular rearrangements. Both Cy5 and ATTO647N acceptor dyes showed severe blinking in a deoxygenated buffer in the presence of 2% β-mercaptoethanol (βME). Replacing the triplet quencher βME

with 1 mM Trolox eliminated most blinking effects. After suppression of blinking three subpopulations were observed: 90% appeared as dissociated complexes; the remaining 10% featured an average FRET efficiency in agreement with that found in intact nucleosomes. In 97% of these intact nucleosomes no significant changes in FRET efficiency were observed in the experimentally accessible time window ranging from 10 ms to 10s of seconds. However, 3% of the intact nucleosomes showed intervals with reduced FRET efficiency, clearly distinct from blinking. These fluctuations with a lifetime of 120 ms, could unambiguously be attributed to DNA breathing. The findings in this chapter illustrate the merits but also typical caveats encountered in single-molecule FRET studies on complex biological systems.

Because we observed that many immobilized molecules appeared as dissociated nucleosomes, we further explored the issue of nucleosome immobilization in **Chapter 4**. Immobilization has several advantages: it allows the extension of observation times to a limit set only by photobleaching, and thus opens the possibility of studying processes occurring on timescales ranging from milliseconds to minutes. It is crucial however, that immobilization itself does not introduce artifacts in the dynamics or affects nucleosome structure. We tested various nucleosome immobilization strategies, such as single point attachment to PEG or bovine serum albumin (BSA) coated surfaces, and confinement in porous agarose or polyacrylamide gels. We compared the immobilization specificity and structural integrity of immobilized nucleosomes for these strategies. A crosslinked star-PEG coating performed best with respect to tethering specificity and nucleosome integrity, and enabled us for the first time to reproduce bulk nucleosome unwrapping kinetics in single nucleosomes without immobilization artifacts.

In **Chapter 5** we chose a complementary approach to prevent immobilization artifacts and show how DNA unwrapping occurs progressively from both nucleosome ends. We performed spFRET spectroscopy with Alternating Laser Excitation (ALEX) on nucleosomes either in free solution or confined in a gel after PAGE separation. We combined ALEX-spFRET with a Fluorescence Correlation Spectroscopy (FCS) analysis on selected bursts of fluorescence to resolve a variety of unwrapped nucleosome conformations. The experiments revealed that nucleosomes are transiently unwrapped with an equilibrium constant of $\sim$ 0.2 – 0.6 at nucleosome ends, and $\sim$ 0.1 at a location 27 basepairs inside the nucleosome. The DNA and histones yet remain stably associated. Our findings, obtained using a powerful combination of single-molecule fluorescence techniques and gel electrophoresis, emphasize the delicate interplay between DNA accessibility and condensation in chromatin.

In conclusion, we resolved nucleosome dynamics by carefully applying single-pair fluorescence resonance energy transfer spectroscopy in two different microscope setups. We showed that nucleosomal DNA is frequently unwrapped, allowing for interactions with other DNA binding proteins. The versatile techniques presented in this thesis can further be exploited to study the dynamics of other heterogeneous DNA-protein complexes than the nucleosome.

Samenvatting

Nucleosoom Dynamica Ontrafeld met Enkel-Paar Fluorescentie Resonantie Energie Overdracht Spectroscopie

Het nucleosoom is de eerste stap van DNA condensatie in de celkern. Nucleosomen vormen obstakels voor enzymen die het opgevouwen DNA binden, en spelen om die reden een belangrijke rol in genregulatie. Om te begrijpen hoe de toegankelijkheid tot nucleosomaal DNA wordt gecontroleerd, is het noodzakelijk om de moleculaire mechanismen te ontrafelen die ten grondslag liggen aan vormveranderingen van het nucleosoom. Dit proefschrift doet verslag van een experimentele studie over de dynamica van nucleosomen, uitgevoerd met behulp van enkel-paar Fluorescentie Resonantie Energie Overdracht Spectroscopie (single-pair Fluorescence Resonance Energy Transfer, ofwel spFRET). Met spFRET is het mogelijk de structuur van het DNA in een enkel nucleosoom te volgen in de tijd. Elk hoofdstuk van dit proefschrift werd als losstaand onderzoekartikel geschreven en geeft een andere inkijk in nucleosoom dynamica of in de experimentele methodes die we hebben toegepast.

Hoofdstuk 2 beschrijft in detail de procedures die we hebben gebruikt om nucleosomen te maken met een FRET paar op de gewenste locatie, en hoe we deze nucleosomen met ensemble technieken en enkel-molecuul technieken hebben bestudeerd. We genereerden een kunstmatig stuk DNA op basis van de 601 sequentie, die een zeer hoge affiniteit voor de histon octameer heeft en daardoor een nucleosoom op één goed gedefinieerde plek vormt. De donor en de acceptor fluorofoor werden op een specifieke plek in het DNA ingebouwd met behulp van PCR met fluorescente primers. Nucleosomen werden geassembleerd uit dit DNA en losse histon eiwitten met behulp van zout dialyse. De opbrengst van deze reconstitutie reacties was ongeveer 90%, volgens metingen met polyacrylamide gel elektroforese (PAGE). Door middel van Totale Interne Reflectie Fluorescentie (TIRF) microscopie op geïmmobiliseerde moleculen, hebben wij de dynamica van het ontwinden van DNA in nucleosomen waargenomen en gekwantificeerd. Ook hebben we met een confocale fluorescentiemicroscoop de statistische verdeling van de verschillende conformaties van deze nucleosomen in kaart gebracht, terwijl ze vrij diffunderen in het confocaal detectievolume.

In **Hoofdstuk 3** hebben we spFRET microscopie toegepast om de dynamica van DNA in nucleosomen rechtstreeks te observeren. Mononucleosomen, met een FRET paar bij de dyade en de uitgang van het nucleosoom, werden geïmmobiliseerd door ze met een 30 bp lange streng DNA vast te binden aan een microscoopglaasje dat was gefunctionaliseerd met een coating van polyethyleen glycol (PEG). De moleculen werden vervolgens geobserveerd met TIRF microscopie. Het FRET signaal van enkele moleculen als functie van de tijd liet twee soorten dynamica zien: tijdelijke onderbrekingen in de fluorescentie van de acceptor en vormverandering in het nucleosoom. Zowel een Cy5 als ATTO647N acceptor fluorofoor vertoonde "fotoknipperen" in een zuurstofarme buffer met 2% β-mercaptoethanol (βME). Het vervangen van de triplet-afvanger βME door 1 mM Trolox verhielp dit effect. Na het onderdrukken van fotoknipperen werden drie sub-populaties waargenomen: 90% van de moleculen was gedissocieerd DNA-eiwit complex; de resterende 10% had een gemiddelde FRET efficiency die past bij intacte nucleosomen. In 97% van deze intacte nucleosomen vonden we geen significante veranderingen in de FRET efficiency, en dus geen DNA dynamica op een tijdschaal tussen 10 ms en tientallen seconden. Echter, in 3% van de intacte nucleosomen namen we kortstondige intervallen met een verminderde energie overdracht waar. Deze fluctuaties, met een gemiddelde levensduur van 120 ms, waren duidelijk anders dan "fotoknipperen" en konden ondubbelzinnig toegeschreven worden aan het "ademen" van nucleosomaal DNA - het tijdelijk loskomen en terugvouwen van DNA van de uiteinden van het nucleosoom. De bevindingen in dit hoofdstuk illustreren de verdiensten van spFRET microscopie, maar ook de valkuilen waar men op beducht moet zijn bij onderzoek aan complexe biologische systemen.

Omdat wij waarnamen dat veel geïmmobiliseerde nucleosomen waren gedissocieerd, hebben we het onderwerp van nucleosoom immobilisatie verder uitgediept in **Hoofdstuk 4**. Immobilisatie heeft een aantal voordelen: het staat het verlengen van observatietijden toe tot aan een limiet die slechts door photobleken wordt bepaald. Dit opent de mogelijkheid om processen te bestuderen die plaatsvinden met een tijdschaal tussen milliseconden en minuten. Het is wel essentieel dat immobilisatie zelf de dynamica of structuur van het nucleosoom niet beïnvloedt. Daarom hebben wij diverse strategieën voor het immobiliseren van nucleosomen getest, zoals specifieke verankering aan een oppervlak met een coating van polymeren (PEG) of eiwitten (BSA), en het opsluiten van nucleosomen in de waterige poriën van agarose of polyacrylamidegels. Voor elk van deze strategieën vergeleken we hoe specifiek de immobilisatie was, en hoeveel geïmmobiliseerde nucleosomen intact bleven. Een coating van stervormige PEG ketens die een netwerk vormen presteerde het best op deze twee aspecten. Deze coating stelde ons in het staat om kinetiek, zoals die was geobserveerd in een ensemble van nucleosomen, te reproduceren op het niveau van een enkel molecuul, terwijl we immobilisatieartefacten uit konden sluiten.

In **Hoofdstuk 5** hebben we gekozen voor een andere wijze om immobilisatieartefacten te

verhinderen. Wij pasten spFRET spectroscopie toe met Alternerende Laser Excitatie (ALEX) op nucleosomen in vrije oplossing, of opgesloten in een gel na zuivering met poly acrylamide gel elektroforese (PAGE). Daarnaast hebben we ALEX-spFRET gecombineerd met een Fluorescentie Correlatie Spectroscopie (FCS) analyse op geselecteerde reeksen van fluorescentie, waardoor we een verscheidenheid aan ontvouwde nucleosomen wisten te ontrafelen. Op die manier hebben we laten zien hoe het openvouwen van DNA voortschrijdt vanaf beide uiteinden van het nucleosoom. De experimenten laten zien dat het DNA kortstondig losvouwt van de eiwitkern, met een evenwichtsconstante van $\sim 0.2 - 0.6$ bij de uiteinden en ~ 0.1 op een plek 27 bp van het uiteinde in het nucleosoom, terwijl DNA en histonen toch op de lange termijn stabiel aan elkaar verbonden blijven. Onze bevindingen, die we hebben verkregen met een krachtige synthese tussen enkel-molecuul fluorescentie technieken en gelelektroforese, benadrukken de subtiele wisselwerking tussen toegankelijkheid en condensatie van DNA in chromatine.

Samenvattend, wij hebben nucleosoom dynamica bestudeerd door spFRET spectroscopie zorgvuldig toe te passen. We hebben laten zien dat DNA frequent loskomt van de histon kern, waardoor nucleosomen intrinsiek toegankelijk zijn voor enzymen op biologische relevante tijdschalen. De veelzijdige technieken die in dit proefschrift worden beschreven kunnen verder worden benut om de dynamica te bestuderen van andere heterogene DNA-eiwitcomplexen dan het nucleosoom alleen.

List of Publications

1. D. Stein, F. H. J. van der Heyden, W. J. A. Koopmans, and C. Dekker, Pressure-driven transport of confined DNA polymers in fluidic channels. *Proceedings of the National Academy of Sciences of the USA* **103**, 15853-15858 (2006)

2. W. J. A. Koopmans, A. Brehm, C. Logie, T. Schmidt, and J. van Noort, Single-pair FRET microscopy reveals mononucleosome dynamics. *Journal of Fluorescence* **17**, 785-795 (2007)

3. W. J. A. Koopmans, T. Schmidt, and J. van Noort, Nucleosome immobilization strategies for single-pair FRET microscopy. *ChemPhysChem* **9**, 2002-2008 (2008)

4. W. J. A. Koopmans, R. Buning, T. Schmidt, and J. van Noort, spFRET using alternating excitation and FCS reveals progressive DNA unwrapping in nucleosomes. *Biophysical Journal* **97**, (2009)

5. W. J. A. Koopmans, R. Buning, J. van Noort, Engineering mononucleosomes for single-pair FRET experiments. to appear as a chapter in *Methods in Molecular Biology: Protocols in DNA Nanotechnology* (ed. G. Zuccheri & B. Samori), Humana Press (2009)

6. M. J. M. Schaaf, W. J. A. Koopmans, T. Meckel, J. van Noort, E. Snaar-Jagalska, T. Schmidt and H. P. Spaink, Single-molecule microscopy in living zebrafish embryos. *Biophysical Journal* (2009), accepted for publication

7. D. Stein, Z. Deurvorst, F. H. J. van der Heyden, W. J. A. Koopmans, and C. Dekker, Electrokinetic DNA concentration in nanofluidic channels. under revision

Curriculum Vitae

Wiepke Koopmans werd geboren op 11 oktober 1980 te Papendrecht. In 1998 deed hij eindexamen in tien vakken en behaalde zijn gymnasium diploma aan het Raayland College te Venray. In datzelfde jaar begon hij aan een studie Technische Natuurkunde aan de TU Delft. In 2004 studeerde hij met lof af als natuurkundig ingenieur. Zijn afstudeeronderzoek naar de transporteigenschappen van individuele DNA moleculen in zeer kleine fluïde kanalen werd uitgevoerd in de Molecular Biophysics groep onder leiding van prof. dr. Cees Dekker. Dit onderzoek resulteerde in een publicatie in een gerenommeerd internationaal vaktijdschrift.

In 2005 kwam Wiepke als onderzoeker in opleiding in dienst bij stichting Fundamenteel Onderzoek der Materie (FOM), voor een promotieonderzoek bij de Physics of Life Processes groep aan de Universiteit Leiden. Onder begeleiding van dr. ir. John van Noort en prof. dr. Thomas Schmidt heeft hij hier tot begin 2009 onderzoek gedaan aan de dynamica van het nucleosoom, de fundamentele eenheid van DNA organisatie in de celkern. De resultaten van dit werk heeft hij onder andere gepresenteerd voor de onderzoeksgroep op UCLA (Los Angeles) van prof. Shimon Weiss -pionier op het gebied van enkel-molecuul FRET spectroscopie- en op internationale conferenties, zoals de Picoquant Single Molecule Spectroscopy workshop, Berlijn 2007, en de Biophysical Society Meeting, Baltimore 2007 en Long Beach 2008. Tevens heeft het onderzoek van Wiepke geleid tot diverse publicaties in de internationale vakliteratuur.

Nawoord

Ik kon dit onderzoekstraject tot een goed einde brengen door de zichtbare en onzichtbare steun van een groot aantal helpende handen. Met een dankbaar hart spreek ik daarom mijn waardering uit voor de volgende mensen:

Jesper Donsmark en Florian Kulzer onderwezen mij in de beginfase van mijn onderzoek in de praktische aspecten van de optica. John van Egmond leverde een onmisbare bijdrage aan de bouw van mijn microscoop-opstellingen door diverse fijn-mechanische componenten op maat te maken. Ineke de Boer maakte grote hoeveelheden fluorescent DNA voor mij. Raymond Koehler stelde mij in staat om alle elektronische componenten netjes aan elkaar te knopen. Fred Kranenburg stond steeds paraat om venijnige hardware- en softwareproblemen de wereld uit te helpen. Riet Nieuwenhuizen voerde achter de schermen belangrijk secretarieel werk uit.

Andrew Flaus, Maik Engelholm, en Andrew Routh hielpen met het opstarten van de nucleosoomreconstituties. Vooral door de samenwerking met Alexander Brehm en Colin Logie wierp dit uiteindelijk zijn vruchten af. Zhuangxiong Huang en Cees Dekker stonden mij toe om een kijkje in hun biochemische keuken te nemen, zodat ik mijn PEGylatie protocol kon toetsen. Gerda Lamers en Ralf Schmauder hielpen me op weg met Fluorescence Correlation Spectroscopy. Eyal Nir toonde me in Los Angeles alle details van zijn ALEX-FRET microscoop en hielp me daarna op afstand om een soortgelijke opstelling ook in Leiden te realiseren.

Veel dank ben ik verschuldigd aan mijn sympathieke collega's in de vakgroep biofysica. Allereerst aan John van Noort en Thomas Schmidt, voor hun dagelijkse begeleiding, betrokkenheid en coaching. De leden van de chromatine groep - Maarten, Martijn, Fan-Tso, Ruth, Thijn, Joke en Bram - bedank ik voor het delen van hun grote kennis en kunde, en voor het warme informele contact. Ook Anna, Freek, Jante, Laurent, Marcel, Paige, Stefan en Sylvie bedank ik voor de vriendelijke en ontspannen sfeer die zij maakten op de 10^{e} en 11^{e} verdieping van het Huygens lab.

Ik ben dankbaar voor de morele steun en interesse van mijn vrienden en familie. Een aantal mensen wil ik daarbij in het bijzonder noemen: Anne en Johan, Mirjam en Job (die ook de voorkant van het proefschrift heeft ontworpen), Tjerk, Janneke, Helma en Jan. Daarnaast heb ik veel gehad aan Charlotte, Irene, Jaap-Jan, Jessica, Pieter en Roelinka - muzikanten van

de Open Kerk band in Den Haag Mariahoeve.

Lieve papa en mama, bedankt voor alle kansen die jullie me hebben gegeven om de door God gegeven talenten te koesteren en ontwikkelen. Tot slot, Marieke: jij bent deze hele weg met me meegegaan en hebt me altijd op handen gedragen, juist wanneer dat nodig was. Wat een prachtig vooruitzicht dat jij er bij zal zijn als er nieuwe bergen aan de horizon liggen!